

Lab Book – Candidate 8277T

Contents

Meetings Summary	3
Chapter Introduction	3
Expression of Interest - 7th Oct	3
Start of Project Meeting - 13th Oct.....	6
LAMMPS Installation - 19/20th Oct	8
LAMMPS Running - 27th Oct.....	10
LAMMPS Fixes - 3rd Nov	11
LAMMPS Simulation - 13th Nov.....	12
Rigid Rod Thermodynamics - 24th Nov.....	13
Initial Report - 1st Dec.....	15
Phase Formation - 26th Jan.....	17
Nematic Phase Transition - 2nd Feb.....	22
Oblong Simulation Region - 10th Feb	23
Reverse Simulations - 16th Feb	24
Smectic Phase Formation - 23rd Feb	26
Nunchuck Phase Formation - 4th March	27
Orientational Correlation Func - 9th Mar	29
Final Simulations - 19th Mar	30
Particle Diffusion -23rd March.....	31
Diffusion Coefficients - 30th March.....	33
Report Draft - 13th April	34
Report Presentation - 7th May	36
Biaxial Phase Developments - 13th May.....	37
Project Records	40
Chapter Introduction	40
Initial Work	40
Phase Detection - Method 1	40
Phase Detection - Method 2	41
Oblong Detection Region	46
Order Parameter Calculation.....	48
Longtime records	50
Running in Parallel	52
Extended Rod Aspect Ratio	52

Crystalline Rigid Rods.....	55
Hysteresis Confirmation	57
Nunchucks - Initialisation.....	58
Nunchucks - A New Phase?.....	59
Orientational Order Parameter - T	62
Orientational Order Parameter - C.....	67
Altered Correlation Functions.....	74
Biaxial Phase Search.....	77
Dynamics - Diffusion Coefficient.....	79
Dynamics - Sampling Time	82
Dynamics - Further Analysis	84
Dynamics - David's Prediction	89
Daily Logs.....	90
Chapter Introduction	90
October.....	90
November.....	92
December	94
January	96
February - 1	97
February - 2.....	99
March - 1	101
March - 2	103
April	105
May	106
Literature Review.....	107
Chapter Introduction	107
Xing 2009 - Y-shaped Nanoparticles)	108
Gleeson 2016 - Nunchucks	109
Biliter 1998 - LC Simulations	112
Paolini (1993) - Soft Core Model	113
Dussi 2018 - Columnar Phase.....	114
Banana Colloids	116
Cholesteric Phases in DNA (T/E).....	119
LC Chevron Phases.....	121
Biaxial LC Phases	124
Gay-Berne Simulations	128
Other Theory Papers	130

Other Experimental Papers	138
Computation Resources	143
Other Resources	145
LAMMPS.....	146
Chapter Introduction	146
Software Introduction	146
Software Summary.....	149
How to Run LAMMPS	151
How to Write LAMMPS scripts	152
Record of Installation & Testing.....	153
Python Integration.....	157
LAMMPS Units.....	158
Implementing Fixes	160
Code Structure	160
Running in Parallel	161
Miscellaneous	162
Chapter Introduction	162
Useful Links.....	162
Deadlines.....	162
Using Ovito.....	163
Write-Up Lecture	164

Meetings Summary

Chapter Introduction

13 October 2020

19:30

This Chapter is written to act as a record of the weekly meetings with my project supervisor (Prof Erika Eiser), and my day-to-day supervisor (Mr Jiaming Yu), and I am very grateful for continual teaching, advice and support that they provided. These meetings were also attended upon occasion (particularly nearing the end of the project) by Prof Daan Frenkel, and I am indebted to him for the insights he offered.

Expression of Interest - 7th Oct

13 October 2020

20:16

Project Listing:

Abstract:

The programmability of DNA allows us to design anisotropic nano-particles such as rods, triangles and many other shapes. Such anisotropy is a pre-requisite to form liquid crystalline structures. The exciting part is that because we can now make new shapes we expect to obtain completely new liquid crystalline symmetries. Based on oxDNA, a semi-coarse-grained, freely available simulation package that can provide the topological and stability criteria of any DNA nano-particle [1], the Eiser group developed a more coarse-grained model to simulate large numbers of these mesogens such that their phase-behaviour can be studied.

In his project the student will use a course-grained model, based on LAMMPS [2,3], to study the phase behaviour of 'nunchuks', which are two hard rods connected via a flexible linker, such that they can vary their configuration from fully stretched to folded. Such systems are expected to form smectic (layered) phases at high volume fractions.

[1] https://dna.physics.ox.ac.uk/index.php/Main_Page

[2] Z Xing, C Ness, D Frenkel, E Eiser *Macromolecules* **52**(2), 504-512 (2019)

[3] <https://lammps.sandia.gov>

There are no safety hazards associated with this project.

From <<https://www-teach.phy.cam.ac.uk/students/courses/projects/100/projects>>

Background

Liquid Crystal Structures

Liquid crystals (LCs) are a state of matter which has properties between those of conventional liquids and those of solid crystals. For instance, a liquid crystal may flow like a liquid, but its molecules may be oriented in a crystal-like way. There are many different types of liquid-crystal phases, which can be distinguished by their different optical properties (such as textures). The contrasting areas in the textures correspond to domains where the liquid-crystal molecules are oriented in different directions. Within a domain, however, the molecules are well ordered.

Liquid Crystal Phases

The various liquid-crystal phases (called mesophases) can be characterized by the type of ordering. One can distinguish positional order (whether molecules are arranged in any sort of ordered lattice) and orientational order (whether molecules are mostly pointing in the same direction), and moreover order can be either short-range (only between molecules close to each other) or long-range (extending to larger, sometimes macroscopic, dimensions). Most thermotropic LCs will have an isotropic phase at high temperature. That is that heating will eventually drive them into a conventional liquid phase characterized by random and isotropic molecular ordering (little to no long-range order), and fluid-like flow behaviour. Under other conditions (for instance, lower temperature), a LC might inhabit one or more phases with significant anisotropic orientational structure and short-range orientational order while still having an ability to flow.

The ordering of liquid crystalline phases is extensive on the molecular scale. This order extends up to the entire domain size, which may be on the order of micrometres, but usually does not extend to the macroscopic scale as often occurs in classical crystalline solids. However, some techniques, such as the use of boundaries or an applied electric field, can be used to enforce a single ordered domain

in a macroscopic liquid crystal sample. The orientational ordering in a liquid crystal might extend along only one dimension, with the material being essentially disordered in the other two directions.

Smectic Phase

The smectic phases, which are found at lower temperatures than the nematic, form well-defined layers that can slide over one another in a manner similar to that of soap (whereas in nematic phases, the molecules are aligned but not in distinct layers). The smectics are thus positionally ordered along one direction. In the Smectic A phase, the molecules are oriented along the layer normal, while in the Smectic C phase they are tilted away from it. These phases are liquid-like within the layers. There are many different smectic phases, all characterized by different types and degrees of positional and orientational order.[18][19] Beyond organic molecules, Smectic ordering has also been reported to occur within colloidal suspensions of 2-D materials or nanosheets.

Mesogen

A mesogen is a compound that displays liquid crystal properties. Mesogens can be described as disordered solids or ordered liquids because they arise from a unique state of matter that exhibits both solid- and liquid-like properties called the liquid crystalline state. This liquid crystalline state (LC) is called the mesophase and occurs between the crystalline solid (Cr) state and the isotropic liquid (Iso) state at distinct temperature ranges.

The liquid crystal properties arise because mesogenic compounds are composed of rigid and flexible parts, which help characterize the order and mobility of its structure. The rigid components align mesogen moieties in one direction and have distinctive shapes that are typically found in the form of rod or disk shapes. The flexible segments provide mesogens with mobility because they are usually made up of alkyl chains, which hinder crystallization to a certain degree. The combination of rigid and flexible chains induce structural alignment and fluidity between liquid crystal moieties.

Lyotropic Liquid Crystals

A lyotropic liquid crystal consists of two or more components that exhibit liquid-crystalline properties in certain concentration ranges. In the lyotropic phases, solvent molecules fill the space around the compounds to provide fluidity to the system.[40] In contrast to thermotropic liquid crystals, these lyotropics have another degree of freedom of concentration that enables them to induce a variety of different phases.

A compound that has two immiscible hydrophilic and hydrophobic parts within the same molecule is called an amphiphilic molecule. Many amphiphilic molecules show lyotropic liquid-crystalline phase sequences depending on the volume balances between the hydrophilic part and hydrophobic part. These structures are formed through the micro-phase segregation of two incompatible components on a nanometre scale. Soap is an everyday example of a lyotropic liquid crystal, and these are common in soft matter (hence the inclusion here).

Techniques

xDNA

xDNA is a simulation code originally developed to implement the coarse-grained DNA model introduced by T. E. Ouldridge, J. P. K. Doye and A. A. Louis. It has been since reworked and it is now an extensible simulation and analysis framework. The code implements Monte Carlo and Molecular Dynamics.

The oxDNA and oRNA models are intended to provide a physical representation of the thermodynamic and mechanical properties of single- and double-stranded DNA and RNA, as well as the transition between the two. At the same time, the representation of DNA and RNA is sufficiently

simple to allow access to assembly processes which occur on long timescales, beyond the reach of atomistic simulations. Basic examples include duplex formation from single strands, and the folding of a self-complementary single strand into a hairpin. These are the underlying processes of the fast-growing field of DNA nanotechnology and RNA nanotechnology, as well as many biophysical uses of DNA/RNA, allowing the model to be used to understand these fascinating systems.

LAMMPS

LAMMPS is a classical molecular dynamics code with a focus on materials modelling. It is an acronym for Large-scale Atomic/Molecular Massively Parallel Simulator.

LAMMPS has potentials for solid-state materials (metals, semiconductors) and soft matter (biomolecules, polymers) and coarse-grained or mesoscopic systems. It can be used to model atoms or, more generically, as a parallel particle simulator at the atomic, meso, or continuum scale.

LAMMPS runs on single processors or in parallel using message-passing techniques and a spatial-decomposition of the simulation domain. Many of its models have versions that provide accelerated performance on CPUs, GPUs, and Intel Xeon Phis. The code is designed to be easy to modify or extend with new functionality.

Meeting Summary

The oxDNA simulation work has already been done, with an effective coarse-grained model of the structure developed. This is primarily in the form of an effective potential between the two arms of the nun-chuck, which accurately replicates the mechanical behaviour observed in the OxDNA model.

The project is them to implement this into LAAMPS, to consider a system of these nanoparticles in bulk. Play around with concentration, temperature etc to identify which phases form, and why they form.

Initial simulations have shown that a single strand section of ~10 base pairs is sufficient to give maximal (almost complete) flexibility, and the maximal angle range between the two arms increases with the number of base pairs up to this value.

Start of Project Meeting - 13th Oct

13 October 2020

20:14

Project Direction

Aim to replicate swirl phase observed in high concentration, completely flexible, nun-chucks; and then test whether this is observed in partially flexible nun-chucks as well (with a shorter single-strand connector).

The ultimate aim of the Eiser Group is to develop techniques to design new DNA origami, with new liquid crystal phase behaviour.

Initial Steps

Initially I will focus on very simple test systems with known behaviour, in order to ensure the accuracy of my approach, and develop my knowledge and experience using the LAMMPS software. In order of hierarchy:

- 2D hard spheres
- Stiff rods (while varying the aspect ratio to reproduce known phase transitions)
- Completely flexible nun-chucks (~20 base pairs in single stranded connector)
- Partially flexible nun-chucks (4-6 base pairs in single stranded connector)

It is important to consider how to quantise phase transitions, and aim to replicate known behaviour here.

Programming Notes

High Concentrations

- We are modelling lyotropic liquid crystals, which change phase based on temperature (whereas thermotropic liquid crystals change phase based on concentration).
- Many of the phase transitions relevant here occur at high concentrations, which are trickier to model
- In particular, anisotropic LC (i.e. non spherical molecules) cannot be modelled in a spatially isotropic region; we must adjust the aspect ratio of the modelling region to suit the aspect ratio of the molecule, so that many sequential molecules can fit adjacently in any given direction.
- Additionally, the equilibration time is particularly long in high concentration systems.
- Prof. Eiser has suggested that longer arms to the nun-chucks may reduce the time needed to reach equilibrium; this is also worth testing
- To achieve the concentrations required here, it is typical to initially form a high volume, dilute system. The volume is then decreased incrementally, while keeping pressure and temperature constant, to increase the concentration.
- This method avoids biases in the initial configuration of the liquid crystal molecules, and decreases the sensitivity to the initial molecule configurations.

Other Issues

- It is worth noting that the DNA nano-molecules are highly negatively charged (as are all DNA molecules, due to the phosphate groups in the backbone). Therefore, almost all experimental work is done in NaCl solution, as these ions form a Debye screening layer around the negatively charged regions.
- We also use soft interactions to minimise molecule overlap through repulsion. This is more effective than hard overlap (where there is no repulsion, but a step is rejected if it causes two molecules to overlap), due to the frequency of 'collisions' between molecules at high concentration, where two molecules come into contact in almost all time steps

To do List

- Start literature review on current papers, and relevant textbooks
- Read LAMMPS manual and documentation, to understand the motivation and approach behind the software
- Download LAMMPS and try to set up basic systems within this. (Use Windows initially, but revert to linux if you experience bugs/have difficulty here).

LAMMPS Installation - 19/20th Oct

19 October 2020

14:47

This is a summary of meetings in Week 2 (starting 19th Oct)

The first meeting was arranged with Jiaming to discuss issues regarding the installation process, and the template nun-chucks code

The second was the scheduled weekly meeting with Erika and Jiaming to discuss the wider first points of testing.

First Meeting

Nun-chucks code

In.run (executive file)

`read_data input_data_nunchucks_${N}_${box}.file` # inputs the file below, with initial position and attributes of all particles.

Define bond and angle style (i.e. harmonic), and properties (such as rigidity) for each bond type

Notation: `angle_coeff * 500.0 180` is of the form: property/bond type/rigidity/startng angle

(where * is a wildcard to denote all bond types

`dump 1 all custom 1000 output.dump id mol type x y z vx vy vz` defines data for dump.

input_data_nunchucks_\${N}_\${box} (input data file)

Variables in the name define particle number and box size (in unit lengths)

First we define the number of objects:

10 atoms - there are 10 atoms in each nun-chuck molecule

9 bonds - each bond is formed between two atoms

8 angles - each angle is defined between two bonds

0 dihedrals - these face-to-face angles may be relevant later for more complex structures

Then we define the number of types (ie different objects in each class). In this code, each object has its own type, to allow for flexibility later on. For example all bonds in the rigid nun-chuck ends are the same, but if we want to make nun-chucks of unequal length then we will have to change some of these characteristics.

`-5.000000 5.000000 xLo xhi` etc then defines the x_min and x_max of the box dimensions (initially)

The rest of the file initialises objects in the following forms:

Masses: ID/Mass

Atoms: ID/Associated Molecule ID/Atom Type/ x,y,z position/ x,y,z velocity

Bonds: ID/Bond Type/Atom₁ID - Atom₂ID

Angles: ID/Angle Type/Atom₁ ID - Atom₂ ID - Atom₃ ID

Note: the x,y,z positions are determined by nun-chucks.py file. Primarily, these locations must all be in the box defined above. Furthermore, all atoms in the same molecule should be adjacent, with the origin of the molecule randomly selected. However, if there is overlap with another molecule, this random origin is rejected, and another chosen. (In the code, this is implemented as a proposed ghost position, which is then implemented subject to validity)

Python Integration

Used to generate the input file, which defined the simulation size and particle number & attributes. This allows the initial properties and positions of the each particle to be generated automatically; handy when there are many particles.

Should be possible without specific build parameters

Useful Software

- **Sublime Text** - useful for displaying all textfiles (code and output dumps) for this project in a readable way
- **Ovito** - Used for visual processing afterwards, very little setup needed for ball-stick models. Basic version is sufficient.
- **VMD** - A Visualiser for Molecular Dynamics simulations, it is more targeted at biological models, but could be handy for more complex models. Freeware, and easy to install.
- **R** - Jiaming uses R for data processing, so this may be considered as an alternative to python if necessary

Second Meeting

Literature

- Research of Prof. Marjolein Dijkstra, available through <https://colloid.nl/people/marjolein-dijkstra/>
- Massimiliano Chiappini – "Of Twist, Bend and Other Deformations"
- Frenkel - Understanding Molecular Simulation (p~67 depicts how phase transition is observed in pressure/density plot)

Initial Simulations

Will start on model of hard spheres, then work up to rigid rods and flexible rods.

A good test of stability in these systems is energy conservation (as while pressure etc are controlled explicitly, this is not. I may have to sum over kinetic and potential energy here. LAMMPS can directly read out the energy of a system, in *thermo_style custom step time pe ke*", from *single_nunchuck_test*, to output the PE and KE at each time step.

Phase Measurement

A discontinuity in pressure or density may be a good indicator of a change here.

More formally, we would want to consider a change in the director for rigid rods. There is no directly analogous property for flexible rods, but considering the local correlation of opening angle is a good start. This can be calculated easily by forming a vector along each end segment (as the difference between particle positions), and taking the opening angle between these vectors in python.

LAMMPS Running - 27th Oct

27 October 2020

16:34

Motivation behind this Research

One of the key aims for this research is to attempt to detect phases in DNA beyond the traditional nematic and smectic phases that have been previously observed. Previous research has only considered rigid rods in this respect.

We can also apply these techniques to more complex DNA origami to find the phase behaviour of such structures. We tend to work backwards here, first considering what simple DNA structures (among which there is great variation) may give rise to Liquid Crystal behaviour, before then considering how these may be implemented in DNA origami. These techniques are ultimately key for developing self-assembly techniques.

This technology can be applied to displays, with new phases being applicable for different colour development/better colour control. Very little is known about the potential of DNA here, however its tunability and controllability at the nano-level suggests it could be significant. (For example we can consistently make DNA stands of the same length to within a base pair, whereas carbon nanotubes (for example) have a much variable length in manufacture).

This is also relevant for light harvesting; conventional solar cells are limited by their well-defined, narrow band gap, which only absorbs from a small part of the black body spectrum. For example there are efforts being developed to down/upconvert the incoming light here to improve the efficiency.

Running the 2D Spheres Test Case

- Fix cannot be used to define and end volume, but can control how long you shrink the box for. (The resultant volume can then be determined from the output, i.e. via Ovito.)
- You can then run 'get frame' after this to set the frame to stay at this volume
- You may also use 'write_restart' here too, which outputs a restart file to start the simulation from. This can be especially useful when running long simulations, so you can save along the way in case of computer failure.
- The Shell can be used to write commands directly into command line (i.e. to make a copy of the output file with a more useful name!)

Evaluating Output Data

- Log files contain the thermodynamic variables output the the command line (determined with thermo_style)
- Dump files contain particle wise data, such as kinematic variables, for visualisation software such as Ovito

These can be read using python, i.e. by searching for 'step' and reading lines after that (or even just line counting)

Other Literature

<https://www.uu.nl/en/news/researchers-discover-a-novel-liquid-crystal-phase-of-banana-shaped-particles>

Researchers discover a novel liquid crystal phase of banana-shaped particles - Dijkstra and Chiappini

A team of researchers from Oxford and Utrecht has developed a new system of micrometre-sized banana-shaped particles. With these bananas they experimentally confirm the existence of the so-called ‘splay-bend nematic’ liquid crystal phase, which was predicted forty years ago, but had remained elusive until now.

This paper has useful context of the scale and importance of current research, although the findings themselves may be limited. The primary issue here is that the scale of the mesogens is too large, so the system may be granular rather than truly thermodynamic. This means they may be forming equilibrium phases as a result of mechanical shear rather than thermodynamic forces.

Pierre de Gennes (Physics Nobel Prize 1991) wrote a detailed book on the theory of these systems, however it is possibly unnecessarily mathematical, with a focus on the exact forms of the large stress tensors etc.

LAMMPS Fixes - 3rd Nov

03 November 2020

15:53

Fixes

In LAMMPS, a “fix” is any operation that is applied to the system during time-stepping or minimization. Examples include updating of atom positions and velocities due to time integration, controlling temperature, applying constraint forces to atoms, enforcing boundary conditions, computing diagnostics, etc.

- I have used an npt fix (constant number of particles, constant pressure and constant temperature) for my 2D spheres simulation. However, despite temperature being fixed, energy drifts over time during this process.
- Jiaming advises using an nph fix (combined with a Langevin fix), during the shrinking process which seems to work better
- For volume conservation when reaching equilibrium, nve is used instead (typically with the Langevin fix in case).
- A recentre command stops all particles being continually offset, by fixing the centre of mass of the system

Parameter Values

I wasn't sure how to choose these values (i.e. what the basis for the parameter values chosen).

In LAMMPS, temperature is relative, and expressed by a relative value, with only relative changes being relevant. Conversion to physical values may only be through experiment - i.e. matching values at a known phase transition. Variation in temperature parameters tends to have minimal effect on the simulation output.

There are also complications of step to time conversion. It is worth noting here that the step values tend to correspond to very small times, although this is dependent on the level of coarse graining in the simulation.

We may also consider the volume fraction here, as this is more easily comparable to external physical quantities, being dimensionless. This will be the limiting factor in many compression fixes, where the volume cannot be compressed so that the volume fraction exceeds the maximum packing efficiency. This is easily obtained theoretically for hard spheres (N.B for DNA rods, i.e. connected balls, a diameter of 2nm can be used).

LAMMPS Simulation - 13th Nov

03 November 2020

20:56

Initial Questions

- Do we use point particles for simulations (as part of the molecular class in atom_style, in comparison to the finite size particles (in the spherical class for example)).
- Do I have the most up to date version of nunchucks.py? (Some of the documentation says it is yet to be added)

Other goals - try to get nunchuck sim working and fully document code

Run of 1000 particles in 100 size box for 50000 steps takes 4 minutes. How many particles are we looking at simulating here?

Overview of Project Direction

Phase Change Detection

Initially, I will write code to analyse the phase change within the rigid rod test case. We expect a discontinuity in the final pressure and density relation (i.e. achieved at equilibrium, not during the NPT fix when density varies due to the box shrinking). This is a time consuming process, as each point requires a separate run to change the density and then reach equilibrium.

Daan Frenkel has suggested plotting pressure and internal energy (as the two most easily obtained thermodynamic variables here).

I may also consider measuring the self diffusion coefficient (and the translational diffusion coefficient of the CoM of each molecule) to quantify the phase change.

N.B Note to self: is it possible to plot density over time here? (based on box size attributes, and volume of particles is conserved)

Limited Flexibility

Consider the two cases where the nunchucks have very limited flexibility. If theta is the deviation from linear rods:

1. Theta = 15 deg (I.e. the angle is completely fixed, rigid rods with a kink in them)*
2. Theta < 15 deg (I.e. the nunchucks have limited flexibility and can bend up to the angle theta)

Here it is worth also considering the effects on varying theta, or the aspect ratio (by increasing the rod length)

*This should correspond to 1-2 base pairs, with rigidity 3.5-10 in arbitrary units.

Full Flexibility

After this, we will look at the fully flexible case, where there is no restrictions on the angle between the two arms of the nunchuck molecule. Jiaming has not yet observed a phase change in this system, however the concentration may not have been sufficiently high.

Simulation Details

- 500 particles should be sufficient. HOWEVER the final results must not be dependant on the size of the box; so tests must be done at a different number of particles (and hence different box size for the same number density) to ensure this is not the case.
- It would be interesting to vary the length of the arms of the nunchucks as well. Onsager predicts that LC phases will not be observed for aspect ratios less than 4. However, they will occur more readily for greater aspect ratios; this is worth comparing.
- The nunchucks file is indeed up to date. It is not fully documented, and requires intensive user input (ie there is no variable for the number of atoms in the molecule, so this must be changed by hand), however Jiaming advises this is feasible and is available to assist.

Rigid Rod Thermodynamics - 24th Nov

23 November 2020

19:10

Questions for the Meeting

Phase Detection - Technical Issues

- Pressure plot; pressure is negligible for these simulations (and centred about zero) - *This is the pressure difference from the initial value, and so is not useful for tracking phase changes. In general, the physical pressure is not easily represented here; there is an ideal gas based calculation at "compute pressure", but it is not a particularly relevant representation of this system. Internal energy would be more representative, although calculating the order parameter is probably best.*
- Nunchucks.py file does not generate output script - *These issues have now been resolved. The key problems lay in the 'import quaternion' line, which was incorrect and should have read 'from pyquaternion import Quaternion', meaning that the incorrect*

module was uploaded. Furthermore, the script must be ran from the command line with the statement "py nunchuck.py -g 100 10", for 100 Molecules in a box size 10.

- How do I generate oblong simulation region (including initial positions in nunchucks). Note that simply changing the ylow and yhigh in the input file is insufficient; particles are still confined in box

How should I vary density? Should this be done through different box sizes or different shrinking times? - *Particle number may indeed be varied to change volume fraction, however it is much more efficient to vary the final box size through the shrinking time, so that the same input script (detailing initial positions of particles) may be used each time*

And is there an effective particle radius I can use to work out a numerical value for the density fraction/packing efficiency? - *This is defined within LAMMPS as approx 0.56 distance units in the nunchuck.py file. However 0.5 would be a more accurate representation, as the balls overlap within the molecule; the bond length is 0.98 which is closer to reality.*

Project Submission (3rd Dec)

- What is required here?
- Elements of project to focus on?
- Balance of theoretical background and project plan?

Also discuss holiday expectations.

Literature Review

Physics of Liquid Crystals - Chapters 1 & 2

Unsure of symmetry notation used here (Schoenflies and crystallographic notation mentioned) DNA is a chiral molecule, so it cannot strictly form nematic phases? (These would be cholesteric phases?) - *Strictly speaking this is the case, however the varying size of the base pairs (minor groups) disrupts the chirality here; there is experimental evidence to show that any chiral effects are insufficient to disrupt the nematic phase behaviour*

Meeting Summary - General

Progress Report Summary

Abstract

Explanation of the science behind this project, explaining the aims of the project and the processes involved. Include a description of the physical system being considered.

Background

Include the history of liquid crystals and their applications. Also detail the development into DNA, and previous simulation research in this area.

My Progress

Detail the literature review I have completed and the work developing familiarity with LAMMPS. This would be best set in the context of its importance, with explanations of the mechanisms within LAMMPS as well, such as how to prepare the system and how to plot phase diagrams from the output data.

Future Work

- Vary aspect ratio of rods
- Introduce flexible bend in the rods to replicate nunchuck behaviour
- Vary the rigidity of this bend

Initial Report - 1st Dec

30 November 2020

18:16

Notes on Initial Report

The nve integration is the microcanonical ensemble (*note to self*)

Overall the tone is good and appropriate for the report

Meeting Summary

Short meeting this week; mainly put in place to catch any issues on the initial report, but this is signed and ready for submission.

I have made progress this week on the phase plots, particularly through the implementation of a loop over mixing time, to allow plotting of phase plots in pressure and internal energy. These plots are reproduced in the progress presentation below.

Code Restructure

The fundamental issue with my simulations here was insufficient time to equilibrate, and too fast compression to achieve the high density phases.

This will be rectified in a second directory with a new coding approach:

- Compress a short way to achieve a new volume fraction
- Allow sufficient time to equilibrate at this value
- Record thermodynamic properties here
- Repeat (continuing from this system state) to achieve a new volume fraction

By avoiding recompression over the same regions, this should be more efficient, while giving more accurate results. However, it is a very different structure to my previous work, and so will be attempted in a new directory ("Rigis_Rods2") to preserve the previous method.

Phase Hysteresis

Thermodynamic theory suggests that no phases should undergo hysteresis; i.e. that every phase transformation should occur at the same concentration (for lyotropic phase transformations) whether the concentration is being increased or decreased (i.e. whether the transformation is being approached in either direction).

Daan Frenkel has therefore suggested that simulations also be carried out increasing the simulation volume, so that the volume fraction is decreasing. This may be initiated from a crystal lattice structure, with maximal packing efficiency.

I had concerns that this artificially introduced order into the system, and so any smectic phases observed could be artificial. While this may be the case, the purpose of this test is to confirm whether the smectic to nematic transition occurs at the same volume fraction in this direction, which would validate the existence of this transition.

Relevant Literature

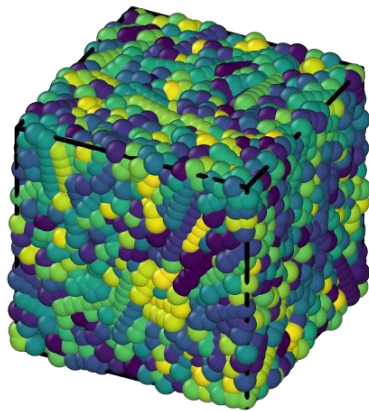
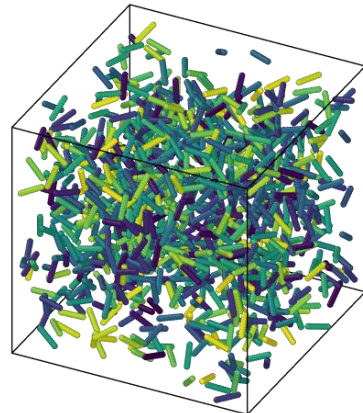
Daan Frenkel has published much of note in this area, searchable from his google scholar account. Specifically relevant are:

- Simulation of Liquid Crystals
- Computer Simulation of hard core models for liquid crystals
- Influence of polydispersivity on the phase behaviour of colloidal liquid crystals

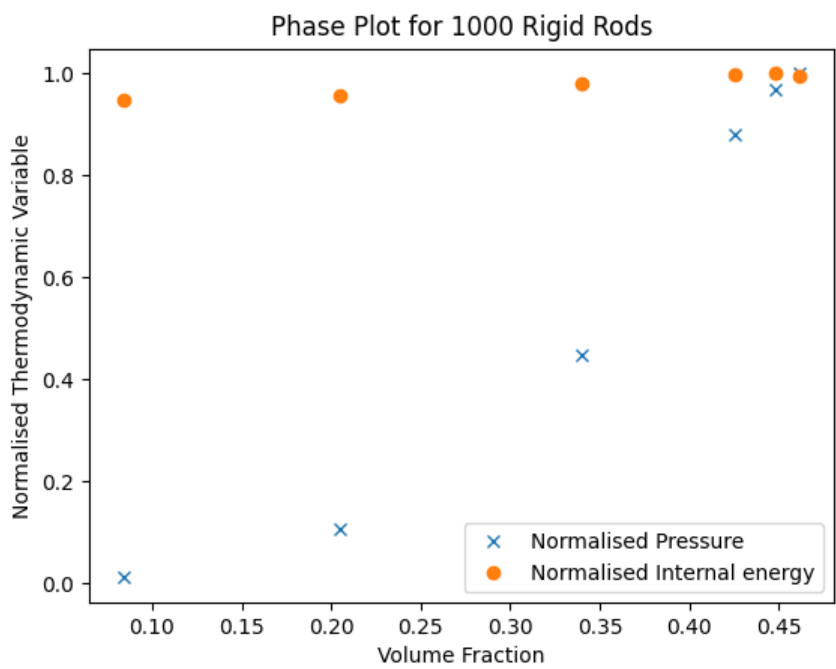
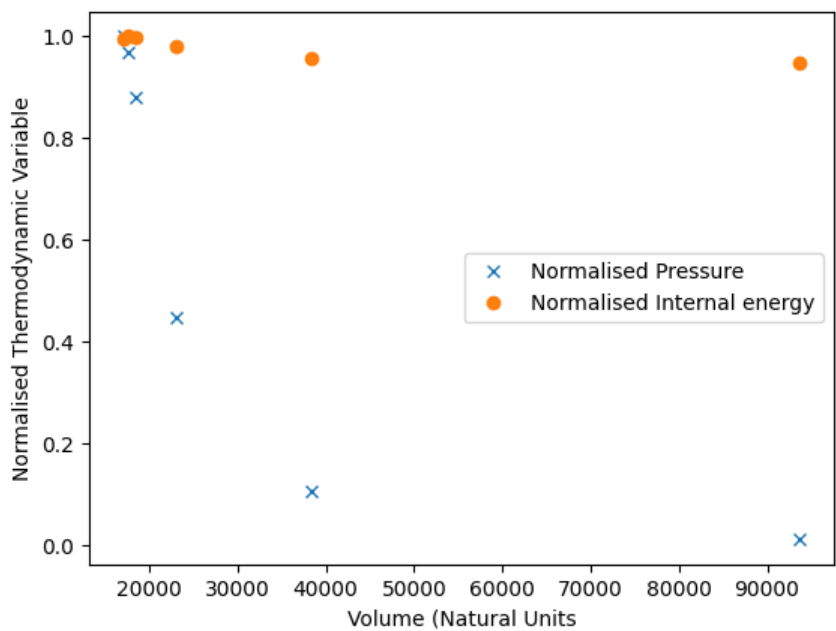
This Week's Results

First time I had results to present, just to give an idea of how the project is progressing.

These first two images show the simulation region of 1000 nanoparticles, before and after compression. The volume fraction in the second image is approximately 46%, not far off the maximal value of 74% for spherical packing, and this did not account for the spheres being joined into molecules. However, it does not display a clear nematic phase ordering; likely a result of insufficient equilibration time.



I went on to plot phase diagrams over volume and concentration anyway, displayed below. As expected, pressure increases with volume fraction, in a quasi-inverse relation.



Phase Formation - 26th Jan

24 January 2021

21:55

Erika was unable to attend, so this was with Jiaming alone.

Progress Report

Sadly I haven't made significant progress since the previous meeting (i.e. over the Christmas vacation). This was a result of a number of competing commitments over this period, primarily major exams preparation and PhD applications/interviews, as well as personal challenges.

While this lack of progress is certainly regrettable, I was aware of these commitments in advance of the vacation and so anticipated that any significant progress here would be unlikely. While I had hoped to have phase plot results of the rigid rod system before the New Year, I am not worried by the extent of progress so far.

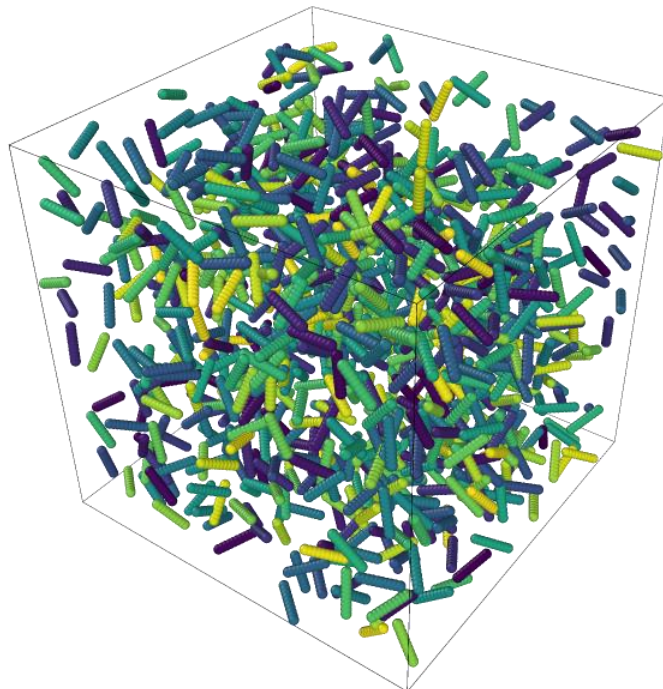
I have however been able to implement the new looping method on 25/01/21. This was successful in providing a more efficient way to achieve higher concentrations required for nematic phase observation.

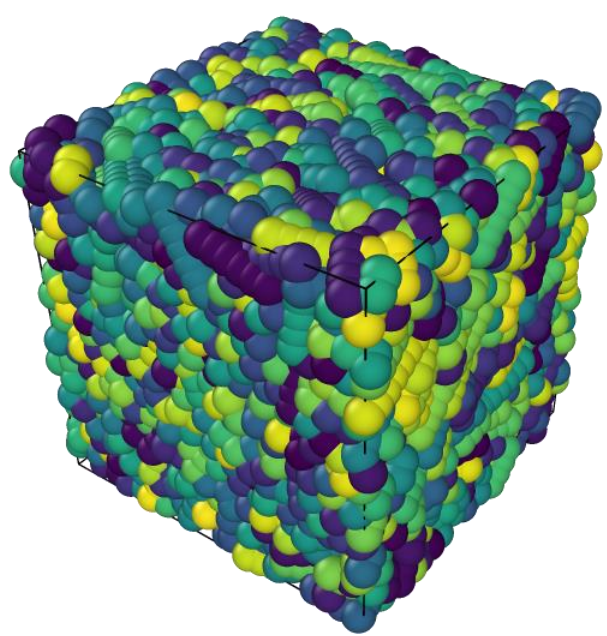
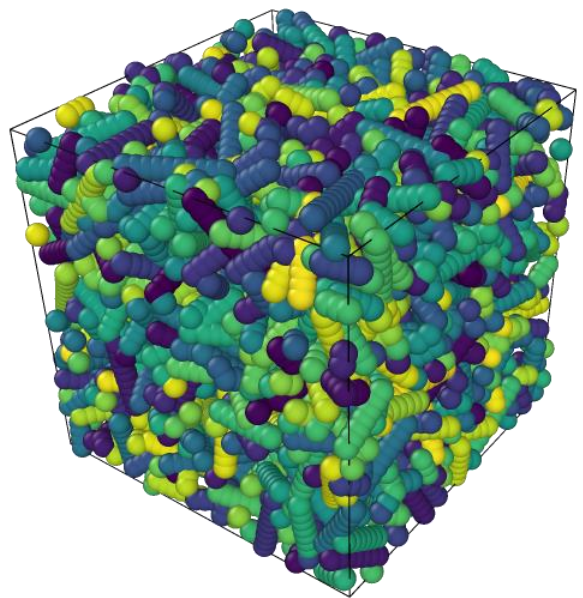
Extended Phase Detection Run

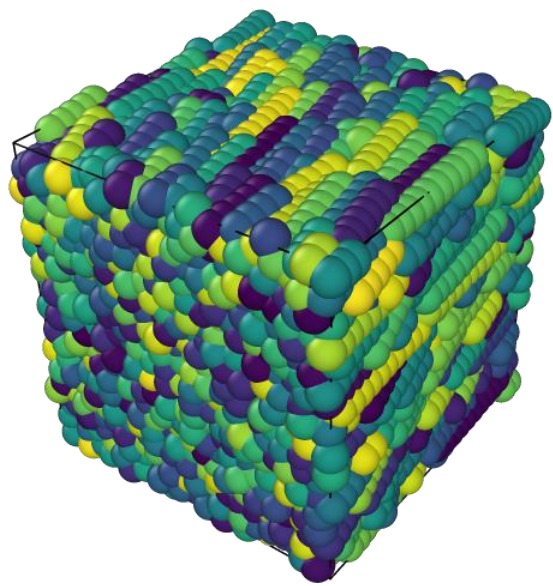
On the 26th Jan, I ran an extended simulation with approximately 5 times the length of the previous simulation, to endeavour to add sufficient time for equilibration. I have included the important parameter values below for reference:

```
variable N      equal 1000
variable box    equal 100 # cubic box of length scale 'box'
variable T      equal 0.5
variable t_step  equal 0.005 #originally 0.005
variable mix_steps index 50000 50000 50000 50000 50000 50000 #6 reps of shrinking
variable run_steps equal 1000000 # steps to run simulation in order to reach steady state
```

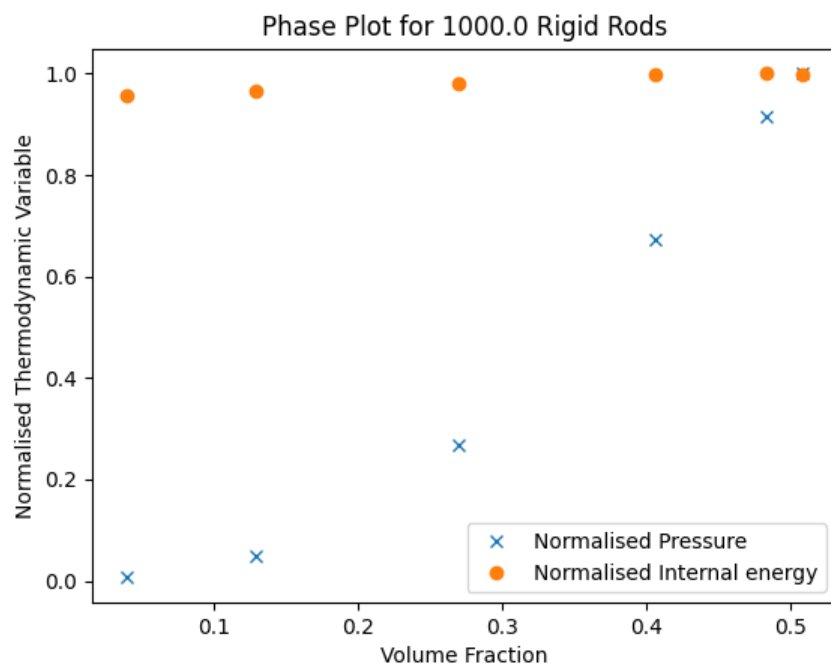
The runtime for this was 3 hours. The box simulations at various points are depicted below:

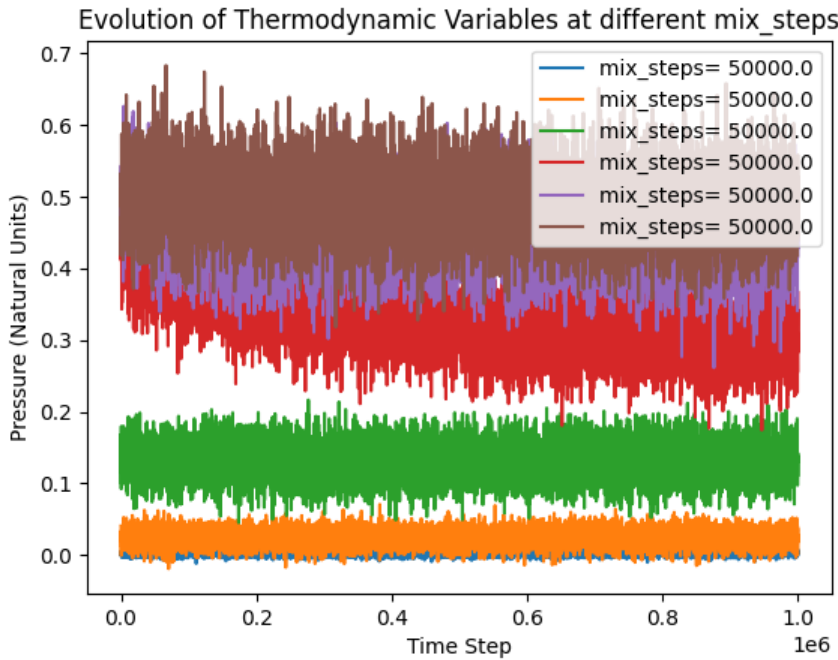






The phase transition here is clear between the final pair of images. This is also observed in the phase plot below, with a significant difference between the pressure of the third and fourth points. This is where the phase transition occurred, as observed by the shifting pressure in the pressure plot (which recorded the pressure change over the equilibration period). The shift in the red line demonstrates the phase change here.





Future work here however needs a number of adjustments:

Quick changes involve considering more points to isolate the phase transition, and plotting a smoothed version of the pressure (ie a running average) to better visualise the pressure change here. Furthermore, the pressure in the phase plot is currently the mean value across the entire equilibration time, whereas a mean from the last 10% (when the system has reached equilibrium) would be more accurate (as currently the fourth point corresponds to the mean of the red line, including the period where the system is undergoing a phase change and has not yet reached equilibrium).

Longer term, it would also be beneficial to move to an oblong simulation region. To observe a smectic phase, we really need a box with a long axis 5/6 times greater than the length of the particles (currently the final side length of the box is 2.5 times the particle length). To minimise the particles required, it is easier to simulate this in an oblong region, so the volume of the box is not increased significantly. This may be adjusted in line 147 of nunchucks.py.

I had raised concerns that it would be hard to also ensure that the final box dimensions are equal to an integer number of particles, as I believed this may be necessary for the smectic phase, however Jiaming believes this is not required; we will check with Erika upon our next meeting. This will be difficult to do, as LAMMPS cannot shrink to a given volume, only over a given time period. It was suggested we could take our final configuration here (in a 25.3x25.3x25.3 box) and place it into a 30x30x30 box, however this would reduce the volume fraction. There is no easy solution here, but it may prove that an extended long axis solves this issue.

I also want to look into measuring the director for the final state at equilibrium, however this will be a challenging prospect and take time to code up. Subsequent to this, I will introduce a bend in the particles.

Computation time

The simulation above took 3 hours. While this was not unreasonable (and is in fact very much on par for this type of simulation on a personal laptop), it is also becoming limiting in terms of what is

computationally possible. I will not be able to increase the particle number or equilibration time significant, while continuing to run such simulations. Therefore it may be necessary to use other computational resources; Jiaming has suggested the Cambridge High Performance Computing centre, as well as Erika's GPU. However this can be tricky to set up, not helped by the remote nature of all work at the moment, and so I will continue to use my personal laptop when possible.

Nematic Phase Transition - 2nd Feb

01 February 2021
21:05

Discussion Points

Current Progress

- Implemented oblong box as well as square box
- Have observed phase transition in both cases, both visually and in pressure change
- Steeps change in order parameter as well.
- Plotted order parameter and volume fraction simultaneously to view changes in both over time

Issues

- Dual director system formed in oblong case? Two different regions of nematic phase formed with different directors
 - Negative order parameter observed. This results from a $\langle \cos^2(\theta) \rangle$ value between 0.3 and 0.33, so this is not significantly less than the theoretical value for a random case, and may just be a sampling error? Worrying though, so not sure where to go from here?
 - But gets down to 0.12 in more ordered region; what is going on here??

Meeting Summary

Erika was unable to attend, so this was with Jiaming alone.

New Order Parameter

In this system we do not know the nematic phase vector, so I have approximated this as the mean director, however this is not ideal (particularly when multiple nematic regions are present).

Eppenga and Frenkel detail an alternative method to approximate the order parameter which I will implement instead:

R. Eppenga & D. Frenkel (1984) Monte Carlo study of the isotropic and nematic phases of infinitely thin hard platelets, Molecular Physics, 52:6, 1303-1334, DOI: 10.1080/00268978400101951

This relates the eigenvalues of Q (ie the true order parameter) with the eigenvalues of M (which approximate to this in ordered systems.) Strictly speaking, the most positive eigenvalue here is the conventional order parameter.

Highly ordered phases

Even after long equilibrium runs, I am unable to achieve highly ordered states, with a uniform nematic vector. Jiaming has no ideas why this may be occurring, but suggests that there is a significant random element to the nature of the phase formed, and whether the nematic phase director lies along the long axis of the simulation region (which has not been occurring up to this point).

The most ordered phases are typically obtained from expanding from the lattice configuration of a perfectly ordered system. In fact in the phase diagram he produced, these points were not obtained from a simulation run, but rather added by eye.

Oblong Simulation Region - 10th Feb

06 February 2021

16:42

Pre-Meeting Discussion Points

Details of experimental analogue of this experiment? Are the nunchucks suspended in a liquid? What concentration etc are they able to achieve? (how does this compare to lammps which has no solute/liquid (and how is pressure etc measured in LAMMPS, does it assume gaseous phase?)

Have filled in tick-box form, but also plan presentation date?

Have achieved half length simulations but not expecting a phase transition here

Meeting Summary

This is the first time I have met with Erika since the end of last term, however I was able to share significant progress since then, including nematic phase formation. She was able to suggest that the 'mixed nematic' phase I observed in longrun2, with a non-uniform director orientation across the simulation box, was a common unphysical artifact of simulations not accounting for boundary effects, which provide a uniform orientation for phase formation.

We discussed how this nematic phase transition increases the translation diffusion coefficient of the system, increasing entropy due to this additional translational freedom, and hence resulting in an entropically driven phase transition.

Reverse Simulation

Erika highlighted the importance of comparison with simulation results from an expanding system (starting from a crystalline phase). As well as verifying the nematic \rightarrow isotropic phase transition (and ensuring there is no hysteresis here with the phase transition occurring at the same volume fraction, it would also allow observation of the smectic \rightarrow nematic phase transition in theory).

Nunchuck Simulations

I highlighted the need to progress from rigid rod simulations, which the others agreed with. Initially I will consider small bending in the rods, through two methods:

- Fixed Angle - All rods may be defined to have a 150 deg bend at the centre
- Fixed Rigidity - All rods may have a central bond with a specified rigidity that allows rotation about this point. This means the bond may open up to about 150 deg, but may take values anywhere from 180 to 150.

In previous simulations, it has been difficult to identify whether equilibrium has been reached here, and also to quantify any phases that do form (such as the elusive 'swirl' phase). I also have concerns that such phases (having a much larger length-scale than the rigid rod nematic phase) may required

a larger box size, and hence more simulation complexity. In particular, it may also be helpful to run multiple simulations over different box sizes, to ensure that any phase formed is not dependant on the box size (and so being affected by the periodic boundary conditions).

N.B If necessary, we can use Erika's GPU for this; may run 5-10 times faster as it is designed for such mathematical calculations. Has 4 cores, but can be run in series or parallel, and accessed via ssh. I want to try to configure parallel simulations on my laptop first however.

Initially, introducing an arbitrary angle/ bond rigidity is sufficient here, as well simply want to justify the existence of such phases. Further work would then be required later to validate that the DNA system would be able to form these, through comparison of the mechanical properties of DNA in the OxDNA model to the LAMMPS parameters here.

Experimental Details

All experiments are done in aqueous solutions. However, it is worth noting that in a pure aqueous solution, the phosphate backbone tends to dissociate. To decrease the Debye screening length we may replicate a physiological solution by increasing the salt concentration (even 0.12M of NaCl is sufficient), to allow hydrogen bond formation.

We also must avoid G-heavy regions, having 3-4 Guanine bases in a row tends to be unstable and can form G-quadruplexes instead of the normal duplexes, with four strands bound together.

Such systems with undergo lyotropic phase transitions, as there is a solvent present, so the phase transition is entropically driven by changes in concentration and mixing free energy . This is replicated in LAMMPS without a solvent, but the driving force for the phase transition remains unchanged. Typically the concentration is varied through evaporation and subsequent filtration, however more experimental details are available in papers sent through by Jiaming.

Reverse Simulations - 16th Feb

15 February 2021
21:41

Simulation Fixes

The expanding simulation region is controlled by the nph (isentropic) fix. This specifies a target pressure, and a damping term, and then the system evolves isentropically to achieve this. The target pressure must be lower than the system pressure for expansion to occur (and the rate of expansion is controlled by the damping term, however this has not been changed from previously).

It is also worth noting that the Langevin fix is there to ensure the temperature of the system is also conserved during this process.

Concerns of simulations thermostat usage is particularly dangerous when you have internal degrees of freedom in the molecule (i.e. vibrational/rotational modes). The thermostat can 'freeze out' these degrees of freedom in the colloid molecules while not affecting the temperature of solvent particles, and so you don't get a uniform effect across the system. However this is not relevant for our simulations (as there are no solvent particles so a uniform effect across the system).

Supposed Swirl Phase

This week I have ran simulations with a range of nunchuck flexibilities. For low flexibilities (or large angles between rods), we can easily observe similar nematic phases to those previously seen in the completely rigid rod systems. However, with greater flexibility I do not observe any long range order (positional or orientational).

We looked in more detail at Jiaming's swirl phase, however it turns out this was composed of multiple images stitched together, and it is much harder to see any pattern in a single image. Daan also suggests this is unlikely to form anyway, as this restriction of translational entropy would be unlikely to be entropically favourable. The image itself may show short range order due to local restriction of molecular orientation (two particles next to each other will probably have some alignment), but no long range order (which would indicate a new phase).

Such systems could be investigated further by introducing a $\sin^2(\theta)$ potential to form an initial 'swirl' phase, and then probing the stability under temperature or concentration changes. However, there is unlikely to be much mileage in this, for the reasons stated above!

Other Potential Phases

It is highly likely that semi-flexible nunchucks (or those with a fixed large angle) will form nematic phases analogous to those in the rigid body systems; and indeed I have found evidence for this already, although this would be worth consolidating.

It is possible molecules with an appreciable (fixed) bend would form nematic phases similar to this, but possibly with other features too, such as:

- Orientation symmetry about the axis of the particle
- Formation of a biaxial nematic
- Some kind of 'zig-zig' phase structure
- Chiral nematic (due to kink in molecule), but this may happen over long length-scales!

It has also been suggested that molecules with very small angles could potentially form disks/rosettes, which might stack in a columnar structure! While I am skeptical about the possibility of this, I will attempt to identify these phases as well.

Order Parameter Calculation

Daan published a lot of work on this (in liquid crystals systems) in the 1980s; one example is:
[Phys. Rev. A 31, 1776 \(1985\) - Evidence for algebraic orientational order in a two-dimensional hard-core nematic \(aps.org\)](https://doi.org/10.1103/PhysRevA.31.1776)

Long range orientational order is computed by the orientational correlation function, expressed through an averaged Legendre polynomial on the director compared with adjacent values. Typically the second order Legendre polynomial is used, as I have previously done to quantify the phase transition. He has suggested that it may be instructive to consider a Legendre polynomial as a function of length (ie by only averaging over the set of particles a given length away) to determine the extent and lengthscale of order within the system. This would be helpful in identifying whether there is any long range order in the nunchuck systems we observe (i.e. being able to conclusively confirm/deny the existence of this 'swirl' phase).

He also mentioned that, when using the Q matrix, I may need more care when choosing which eigenvalues to take. Taking the largest eigenvalue is more accurate in ordered phases, but when considering a non-ordered phase it may be better to consider the middle eigenvalue (or -2 * central

eigenvalue) which can truly fluctuate above zero (whereas the maximum value is bound above zero and so is forced to have a finite size).

I have also realised I need to correct my current work here, as it does not account for particles crossing over the boundary of the simulation region (their director is no longer properly represented by a vector between the two end particles). This error is minimised by choosing adjacent particles (which are much less likely to be separated by the simulation boundary) however ideally this would be fixed fully. This would require transforming end particle positions across the simulation region if the particle crosses the box boundary (or simply rejecting data from particles with an end-to-end 'distance' greater than expected (i.e. on the order of the size of the simulation region)

Other Literature

Mike Allen has a very interesting review article

Daan also published a review article in the Advances of Chemical Physics, as well as papers in 1983/1984 in Molecular Physics.

Paolini did work in the 1980s on rigid rods, showing that a rod constructed out of spheres had to be at least 8 units long to display a nematic phase transition.

Work with Dijkstra: [Phys. Rev. E 50, 349 \(1994\) - Simulation study of a two-dimensional system of semiflexible polymers \(aps.org\)](#)

For interest: [Interview with Daan Frenkel, Boltzmann Medallist 2016 | SpringerLink](#)

Dark side of simulations: [\[1211.4440\] Simulations: the dark side \(arxiv.org\)](#)

Smectic Phase Formation - 23rd Feb

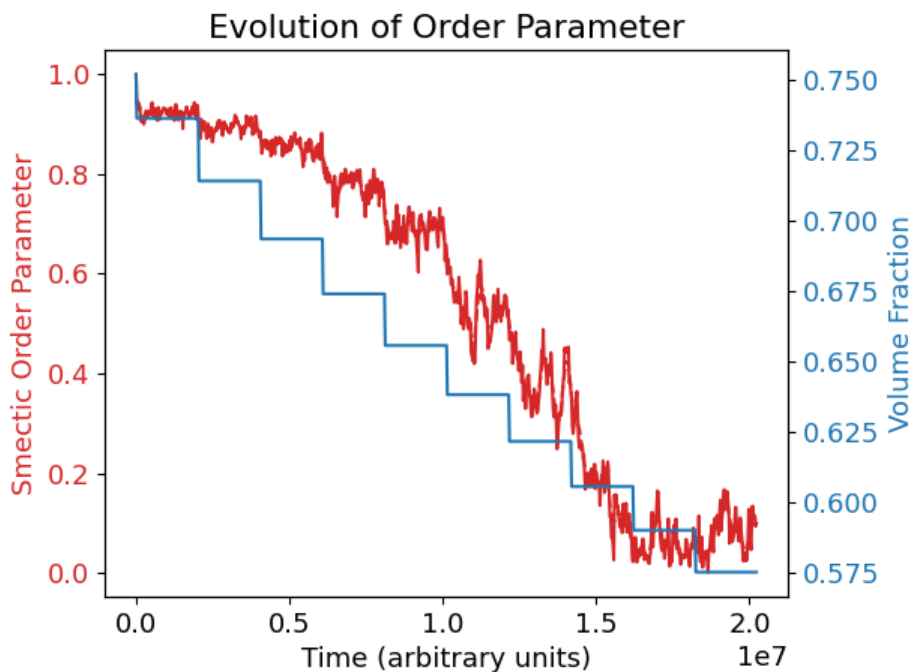
23 February 2021

18:31

Potential Smectic Phase

This is a result of extended high volume fraction simulations from the initial crystalline phase of the initial rigid rods system. I have implemented the Smectic order parameter, from Polson and Frenkels paper.

This clearly displayed a decrease in smectic order, however this does not occur discretely at a single volume fraction:



Daan has suggested that, while Landau Theory does predict the smectic \rightarrow nematic phase transition to be discrete, there is other evidence for a continuous phase transition here. However, this may not be conclusive evidence for it; ideally we would observe the same effect 'in reverse' - i.e. upon shrinking. It is hard to achieve sufficient volume fractions for this, however it may be possible to increase the volume fraction somewhat to demonstrate the beginning of this trend.

Further work might vary the aspect ratio of the box, while conserving the volume fraction, however this is not essential and would be difficult to implement in LAMMPS, so will not be a current priority.

Nunchuck Phase Behaviour

I have observed ordered phase formation in both the fixed angle and fixed rigidity system, for longer nunchucks with a flexible central angle. Most notably, in the fixed rigidity case, there is evidence for a 'preferred' angle, and reduction in configurational entropy. The phase dependence of this will be investigate further (i.e. by plotting the angle distribution at different phases; potentially with a colourmap key?), and the Legendre Polynomials will be investigated further a method of characterising the new phases observed.

Nunchuck Phase Formation - 4th March

27 February 2021
14:45

General Questions

I have been looking through some of the experimental literature, and wondered how accurate a representation of DNA this model is? I am aware of the chiral nature of DNA, and many of the experimental studies seem to observe the formation of cholesteric rather than nematic phases as a result of this.

In real experiments, this is very dependant on the sequence used. It can be hard to identify the minor and major grooves on short strand DNA, as the pitch of these grooves undergoes short-scale variation (dependant on local base pair distributions). We may also observe quadruplex formation with short strands, which may form columnar phases. This is also dependant on high salt concentrations, to reduce the Debye screening length (i.e. reduce the effective size of the DNA) so other particles can get close enough to experience the effects of the differing grooves.

Also, is the interaction potential dependant on the base-pair sequence? And what sequence was used for the OxDNA simulations (and did changing this sequence have any impacts)?

Not a significant effect; a few different sequences have been tested but they potential was not significantly affected; the main factor of this was the length of the arms/linker. Initial cases were coded for 'T only' sequences. OxDNA accounts for different bases by changing the strength (not the shape) of the potential.

The effect of different sequences can be observed through: "A Numerical Study of Three-Armed DNA Hydrogel Structures YA Gutierrez Fosado, Z Xing, E Eiser, M Hudek, O Henrich arXiv e-prints, arXiv: 1903.04186"

Ouldrich mentions data from the 1970s comparing the persistence length of pure A and pure G chains, but this should not affect our simulations here.

On a different note, I have been reading Paolini's paper; what is the difference of the soft-core potential he uses here?

Soft core tends to zero slowly (ie Yukawa potential etc). This is beneficial in Monte Carlo simulations, as small overlap is allowed (with an associated energy cost), rather than having to reject that trial move. It is also a more accurate representation of reality (rather than having a discrete potential change). My simulations would be classed as soft core as well, through the cut-off LJ potential, which includes this soft-core repulsion.

Pair-wise Angle Correlation Function

My way it likely valid, but very inefficient! Hopefully Daan will have more memory of the approach he used with Mulder in 1984/1985; Erika will feed back on this! May be possible to use more of a 'continuous window' approach.

I am concerned that the box size may be insufficient to observe periodicity in the phase structure; ie if there is a twisted-nematic or swirled phase that has a repeating pattern, then the length-scale of this may be greater than the box itself. This would mean that $g(r)$ would not extend to great enough radii to observe secondary peaks.

Sofia Kanterovich (Univ. Vienna) has a cluster (ESPResSo) and may be able to simulate this system with much large particle numbers to observe this. This system is compatible with LAMMPS and so could be a promising avenue for further work.

Report Writing

Will discuss this in more detail near the end of next work, but helpful to start working on this. Model details/simulation approach is a good place to start, then filling out the results and background (come back to the introduction and abstract etc last).

Orientational Correlation Func - 9th Mar

08 March 2021

11:08

Mention SCM summer school/IOP conference; I was thinking of attending but how do these work/ what level is it etc?

[Advanced School in Soft Condensed Matter - Solutions in the Summer 2021 \(iopconfs.org\)](https://iopconfs.org)

Pair-Wise Orientational Correlation Function

Daan helping gave a presentation on how to calculate this using spherical harmonics; the details are in the notes which have been saved separately. He explains that we want to measure a correlation function that is invariant under a global rotation of the system; the simplest of these is $\cos(\theta)$. However it is worth noting we tend to use the second order Legendre polynomial, instead of simply the first order $\cos(\theta)$, as that averages to zero for molecules with no dipole.

This is best expressed using spherical harmonics! It is worthwhile looking up the spherical harmonic addition theorem here, which describes spherical harmonics form a complete basis for any orthogonal function on a unit sphere. It is important to note that, due to the global rotation invariance, we may be in any coordinate system for this; we tend to arbitrarily align ourselves with that of the simulation region.

This approach allows us to sum terms over all molecules j for one molecule i . $\gamma_{lm}(\omega_j)$ is a function of a single molecule!

There may be approaches to this in Fourier space; even just to reduce the computational load. It is possible to use an analogous approach to the standard correlation function, where $g(r)$ is the F.T of the structure factor (itself calculated as the mean squared density correlation).

I mentioned an approach I had seen combining this step with the spherical harmonics to use the Fourier-Bessel transform, however this could only be valid for a simulation region with spherical symmetry. In a cubic box, it leaves out particles in the corners - ie those at large distances. It is therefore better to simply F.T with wavevectors compatible with the box size.

TO DO: Implement spherical harmonic approach to calculate the orientational correlation function. I would also like to consider implementing a rolling window here, instead of discrete bins, if it is necessary to smooth the function.

During/after this discussion it occurred to me that it may be worth investigating the FT of the pair-wise orientational order correlation. We expect oscillatory behaviour on the length-scale of swirl phase, however this may be longer than our box itself, and so hard to identify. I wondered whether such oscillations could be identified as a peak in the Fourier spectrum, however the sampling required for this might require a longer length-scale anyway; we can't get information for free!

Phase Categorisation

Erika has suggested to correlate between the orientation of individual arms, which should help elucidate zig-zag/herringbone structure (which my current method of a director between ends of the molecule will not do). Apparently some literature exists already on so-called "Cheveron phases" so this would be worth seeking, it may mostly be focused on structures formed at lipid membranes however. Mike Allen's review is particularly worth revisiting, as well as the mathematical phase analysis within the banana colloids studies (splay/bend nematic phases?).

It would also be interesting to run a simulation of smaller angles, to see what (if any) structure is formed here.

Finally, Daan suggested two new ways to characterise the herringbone structure. Firstly, consider correlation between the normal vector to the plane of each molecule. This should be expressed best in the second order correlation function g_2 . Additionally, take the vector along the bisector of each molecule, and calculate g_1 . I suspect this last method may be successful in giving an oscillating pattern for the zigzag phase, so would be very interested to see what it turns out.

Final Simulations - 19th Mar

17 March 2021

12:26

Orientational Correlation Function

We discussed the simulation method, and established that the calculation inevitably scales an $O(N^2)$ even if spherical harmonics are used to evaluate the angular components, as the pair-wise separation calculations must scale with the square of the number of particles. While the use of a Fourier transform may reduce this to $M \log(M)$, where M is the number of Fourier components, M is not necessarily smaller than N , and this process is not well documented. For the (relatively) small values of N used in this project, the time spent implementing stuff methods would likely be greater than the ultimate time saved from them, so we shall not dwell on this method further.

Further Simulations

The phase transition with bend rigid rods can be hard to pin down, and so it is worth completing further simulations here, both varying the rods length (5 molecules per arm etc) and the separation angle (135 deg, 105 deg).

It is not worth trying to identify whether the phase transitions I have observed are first order (i.e. have a discontinuous change in the order parameter over a infinitesimal change in volume fraction) or continuous; as this is very challenging and requires higher resolution simulations than are possible for this (fairly complex) system. The isotropic to nematic transition is expected to be first order, however the nematic to smectic phase transition is much less certain and still an active research problem (in all liquid crystals).

Further simulations may be conducted on Erika's GPU. I have tried to get remote access to this, but we will likely need to use a root account to set up a separate account for me on here. In the meantime, it may be simpler to use Erika's/ Jiaming's accounts on this. Such simulations may only be done later in term, after the project deadline as part of our ongoing research.

There has been some suggestion of considering the phase behaviour in the simpler 2D system. This has its advantages; larger systems may be simulated with ease, and so we may observe phase behaviour over a larger length scale. However this only really allows us to test the correlation functions used, which we have already done on the smectic system, as there is no reason to believe that phase behaviour observed in 2D would be extended to 3D (and extended simulation evidence that it in fact does not!).

Dynamics

While some research of the static phase behaviour of this system has already been conducted, very little is known about the dynamics of the system. There are many interesting questions here, particularly with regards to the viscosity parameters and shear wave behaviour in the system, or even elastic coefficients of the crystalline phase. However, to start with, the diffusion constants in the three cartesian directions (particularly in the crystalline phase) would be particularly interesting to investigate!

It is worth noting that my simulations do not include hydrodynamic interactions (i.e. there is no explicit consideration of the solvent interactions). But over the timescales we expect such effects to decay very quickly, and so have minimal effect. Therefore, it is perfectly fine to use Langevin dynamics here.

Particle Diffusion -23rd March

21 March 2021

17:03

Report Writing

Graph Conventions:

Enclosed 'box' or just two axes - I prefer encased I think!

Major and minor tick marks?

No title right? - *No title here, but detailed caption! Figure should be stand alone (explains what you see but don't include the ; but also referred to in order in the text.*

Font for text? - *Font size should be same as report!*

Do you have a recommended style guide for this? - *It is up to your preference, but be consistent!*
Look at papers/ masters project report provided

Some ideas at [An Introduction to Making Scientific Publication Plots with Python | by Naveen Venkatesan | Towards Data Science](#)

Pack as much info into one graph as possible, particularly when comparing between datasets! Don't just rely on colour coding - change marker style between points

Appendices

Reasonable to include mathematical derivation that are relevant to the project, i.e. the order parameter calculation or Onsager theory? - *yes this would be great*

How much code should be included? —*can have snippets in text but don't have it all in the appendix. Or even specific modules/ functions - ie where I implement the order param calc*

LAMMPS Mechanics

How much should be included on the mechanics of LAMMPS (or MD in general) simulations? Or just give info on how to set them up in the same way I did (so my results can be replicated)? - just enough info to replicate, and explain why I made the decisions I did. I.e. lammps has built in MD calculations that account for thermal fluctuations - but don't need detail of how this is done

Natural units - defined by sigma and epsilon. Can I use room temperature for the energy (gives 4.1 E-21)*, or should it be the characteristic energy of the interactions (i.e. the characteristic strength of the Coulomb interactions?)

Strictly speaking sigma is the cut-off not the size of the particle - there is a small difference there. 1ms for the total simulation sounds reasonable though.

As done in the LJ potential here ([\(PDF\) Dissipative particle dynamics simulation of entropic trapping for DNA separation \(researchgate.net\)](#))

Numerical values for magnitude of LJ potential from individual atoms are given here: [1989_03_257.pdf \(sav.sk\)](#) - but focused on base stacking whereas phosphate backbone will be primary driving force here.

[Accurate Representation of B-DNA Double Helical Structure with Implicit Solvent and Counterions \(core.ac.uk\)](#) suggests 1.3 kcal/mol (9.0 E-21) for the LJ interaction. This is remarkably similar to the thermal energy of the system.

Would also be good to know the time taken to diffuse over its own lengthscale (for given mass)

Other

How much simulation theory to include? I.e. do I explain the motivations behind natural units/periodic boundary conditions (like a textbook would) or do I just say I used them? (Like a journal paper would?) - *info on the choices you made, and your expectations are useful!*

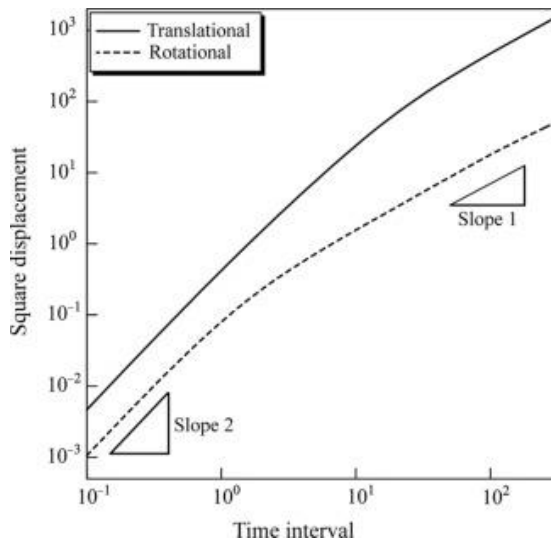
Single column rather than double? - *single would likely be best, double is unnecessary here.*

Additionally, the advantage of using Overleaf here is that I can share it with Erika! Revtek is a common package used for such papers.

Particle Diffusion

In my plot of D over volume, it would be worth plotting over volume fraction instead. If I can also include the order parameter on the top x axis, or shade regions of the graph I believe to be in different phases, this would be most useful! This requires identifying the phase present at each order parameter via separate analysis.

It would be extremely useful to plot the mean squared displacement over time, on a log-log plot; this describes the nature of the motion extremely well (as below):



I would need to account for periodic boundaries here; which is non-trivial but worth spending time on! It is particularly useful for identifying whether there is any impact of confinement effects.

I would also like to compare these results to the rigid rods!

Erika would also like me to look at the dilute and semidilute diffusion fractions. - ie if the overlap of effective sphere around each particle overlaps or not.

Dilute: Should be $1+2.5*\text{vol_frac}$

Semidilute: Strong reduction in diffusion coefficient

(This would build on theoretical work by her current student David)

Diffusion Coefficients - 30th March

24 March 2021

15:11

Misc Questions from Report Writing

How accurate is the LJ potential? What would be the magnitude of coulombic interactions in this system?

LJ accounts for excluded volume here. The molecules are likely to be completely repulsive in sufficient salt due to the coulombic repulsion. Primary difference between simulation and experiment here is just the ability of really short rods to stack together in columnar phases. Salt concentration also reduced Debye screening length, effectively increasing aspect ratio as the rod is thinner. More info on interactions in DNA: [DNA model introduction - OxDNA](#)

Check required knowledge on phase transition theory (universality classes etc)

Really shouldn't require this; stat mech etc is much more relevant! Useful recapping free energy and link to order parameter (there might be an old examples sheet question on this, and maybe basics on universality classes. Basically just remember Gibbs free energy has a global minimum, corresponding to location of phase. But phase separation occurs when there are two minima here, chemical potential formed by tangent rule).

Diffusion Coefficients

Dilute Regime

Building on the work of your student David, I tried simulating the diffusion coefficients in the dilute and semidilute regimes.

Check the calculation for the semidilute limit

Check expected results for dilute region (as gradient would be 1 for diffusive behaviour, higher values seem to indicate super-diffusive behaviour?) Should it be 1-2.5vol_frac in the dilute limit?

For vol frac = 0.7090, slope = 0.2176

For vol frac = 0.4046, slope = 0.3353

For vol frac = 0.2488, slope = 0.4201

For vol frac = 0.1293, slope = 0.4424

For vol frac = 0.0546, slope = 0.4429

For vol frac = 0.0131, slope = 0.4684

For vol frac = 0.0044, slope = 0.4704

This is not correct - the true expression is $\eta = \eta_0(1 + 2.5\phi)$, where we may relate viscosity diffusion coefficient. We may therefore measure D at different values of volume fraction to v only valid for volume fractions less than 0.1

Report Draft - 13th April

01 April 2021

14:55

Having issues with rendering some graphs - ie the combined nematic/smectic order plot for crystalline rigid rods (legend in savefig doesn't match the one shown by python).

- What is best file format to use to maintain quality?
- How to plots look? (Box around legend? Font type/size? Do I need different markers arbitrarily placed on lines for colourblind? - *Format is fine, although add angle label to figure 2 (using inkscape) and volume fractions to figure 6 caption. Origin, Mathematica, Igor and Gnuplot are all useful options for plotting if needed.*

What code to include (in appendix or otherwise?) - *putting it on github is fine. Chat with charles on how much is needed here and anonymity requirements.*

Include this in appendix:

RANDOM WALK IN 1 & 3D

- For translational diffusion, after a walk of N steps taking a time $t = N \Delta t$...

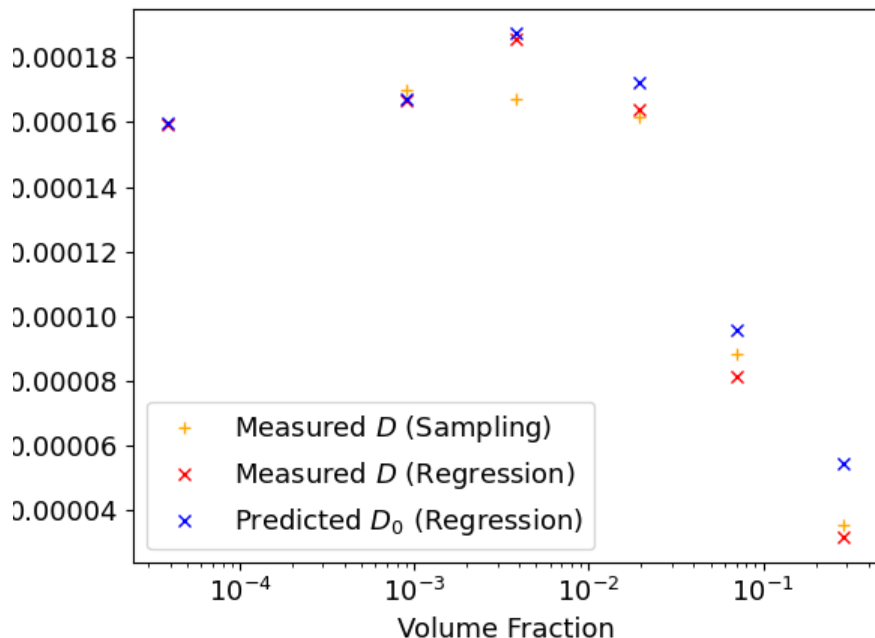
★ We can define a diffusion coefficient $D = \frac{b^2}{2\Delta t}$

or $\langle(x_N)^2\rangle = 2Dt$ in 1D.

- Of course, motions in x , y , and z -directions are independent, hence

$$\langle(r_N)^2\rangle = \langle(x_N)^2\rangle + \langle(y_N)^2\rangle + \langle(z_N)^2\rangle = 6Dt$$

Diffusion - David's Work



This graph depicts the observed diffusion values, through both sampling (total displacement/time over each equilibration phase), and by linear regression (for total displacement against time). The diffusion clearly decreases as volume fraction is increased, and the use of a $(1+2.5/\phi)$ factor does not offset this to give a constant estimate for D_0 . The variability in diffusion coefficient is also much greater than the magnitude of this adjustment in the dilute regime; it may be beneficial to increase the sampling size here (to reduce this variation so any trends in the dilute regime may be observed) but this is not an imminent priority.

Summary - Statistics insufficient as there is too much noise in the dilute region; will investigate greater sample sizes here at a later date.

Further Work

Biaxial phase!! And maybe characterise cheverons too?

Also do we need to account for particles crossing the boundaries in our nematic order parameter (if there is time?)

<https://advances.sciencemag.org/content/advances/4/5/eaas8829.full.pdf> - bent core phases
<https://pubs.acs.org/doi/pdf/10.1021/jacs.5b11546>

Further diffusion work could consider different diffusion coefficients or rotational diffusion

Report Presentation - 7th May

07 May 2021

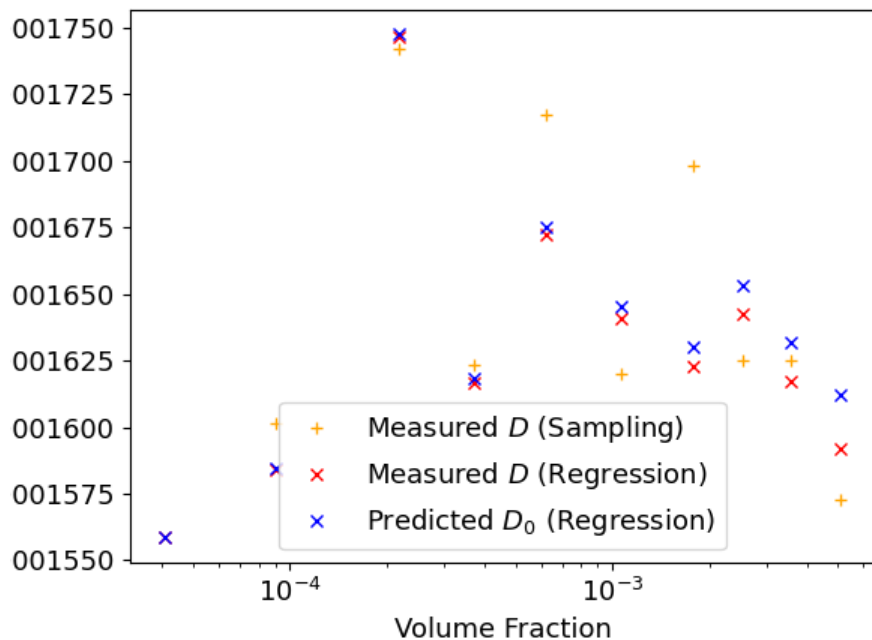
10:14

The primary focus of this meeting was to discuss the applications and motivations of this study. Primarily we care about anisotropic liquid crystals as they may lead to the formation of new phases. This are of direct interest in liquid crystal technology; for example there is already some evidence that anisotropic liquid crystals gives rise to phases that offer wider viewing angles for display screens. Such phases are much easier to test and identify in silico, and so such simulation approaches demonstrate what might be possible (along with the associated molecule parameters most likely to be successful), without using costly experimental resources (especially with expensive custom-made DNA molecules!).

There are many wider applications, such as light harvesting technology in solar cells, or thermotropic liquid crystals in colour changing temperature sensors. The techniques in modelling DNA here may also be applied to DNA origami and other nano-machine self assembly techniques.

Diffusion Dataset

I repeated the previous analysis over longer sampling periods with 500 particles (running for about 12 hours), to identify whether we were able to obtain the statistics required to test this hypothesis (put forward by David).



The difference between the red and blue points shows the affect of David's predictions on finding D_0 by including the volume fraction correction factor. However this difference is much less than the overall spread observed, and so we have insufficient statistics to be able to give concrete identification of any trends there.

Biaxial Phase Developments - 13th May

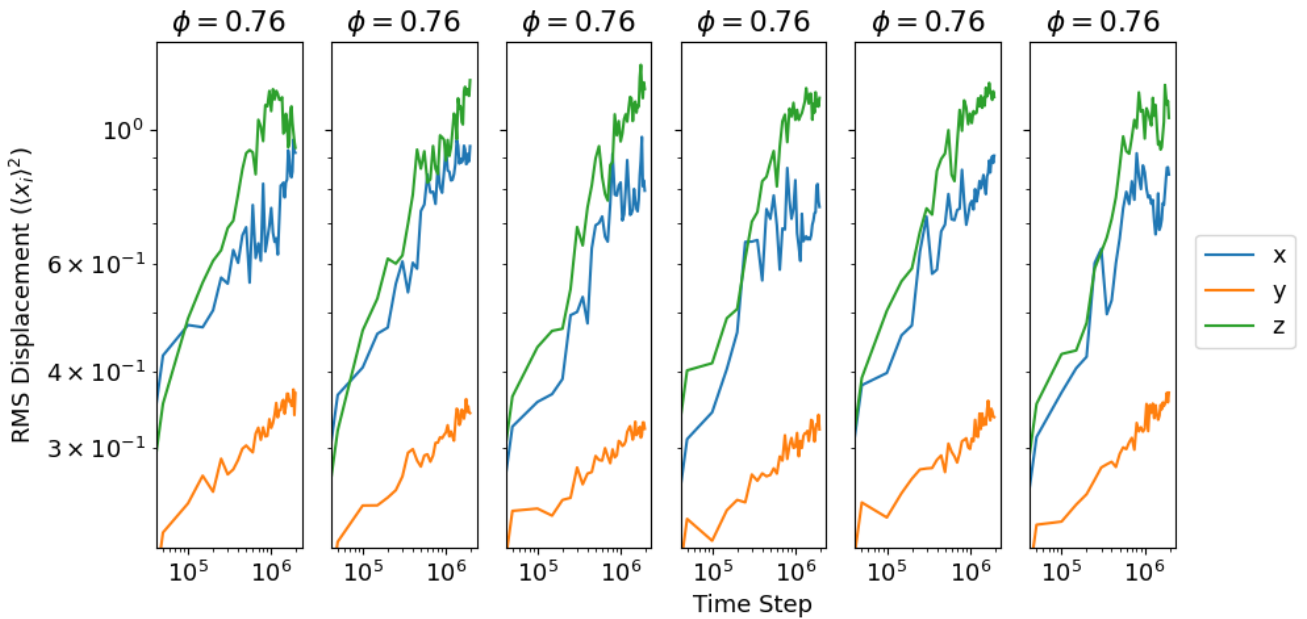
13 May 2021

14:04

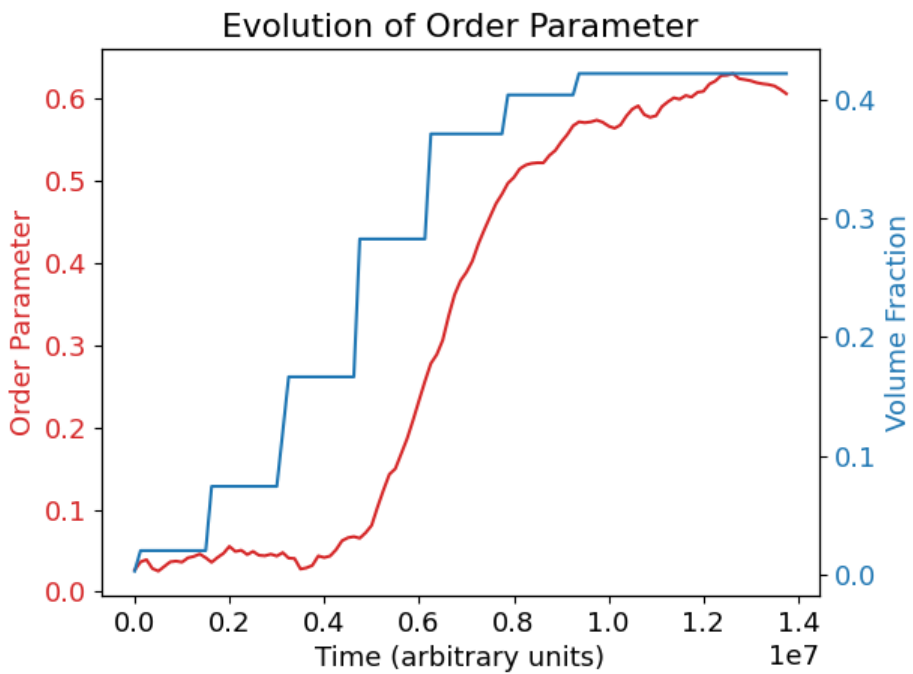
Here we discussed a few recent findings on the biaxial phase, which seems to be becoming more conclusive! I do not think I have enough evidence to present a full picture in my report (nor enough space to do it, more pertinently!) but Erika has suggested providing a reference to future work on this (particularly as we hope to publish these results over the summer).

I initially ran extended equilibration simulations at a constant volume fraction from an unordered smectic phase. This was generated by relaxing a crystalline configuration of rigid rods, while introducing a bend in the rods to give the fixed opening angle of 150 deg used here.

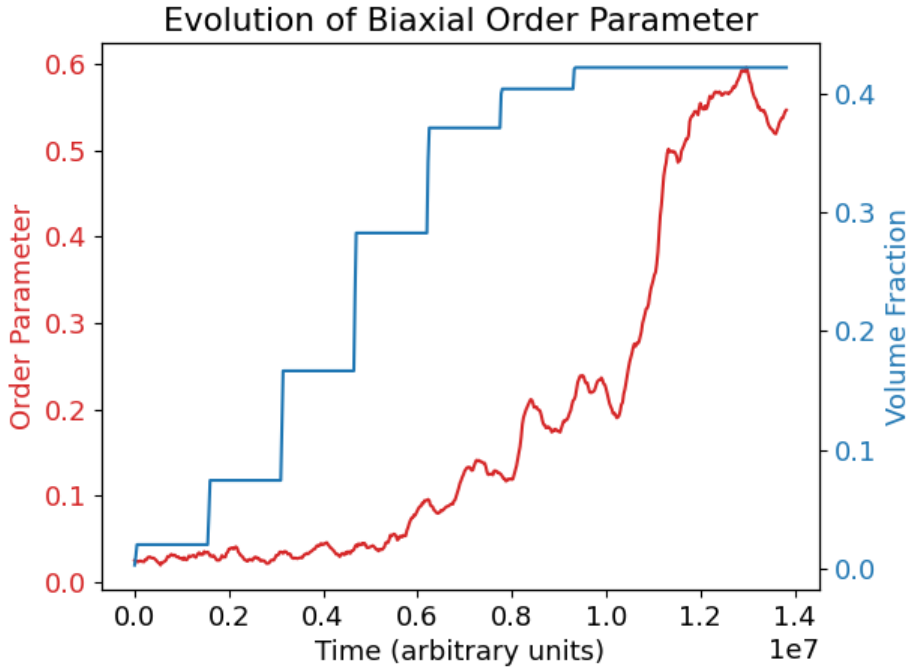
The smectic layers are oriented in the x-z planes, and so anisotropy in the y axis is expected for the smectic phase. However, anisotropy within the x,z plane suggests a degree of biaxiality to the simulation, otherwise these components would be expected to be equal (as observed in the rigid rods case). Six simulations at this volume fraction compound evidence for a slight anisotropy between these axes, with consistently high mobility in the z direction in this case:



Further simulation revealed this biaxiality may even be detected in contracting simulations from an initially dilute system. Here we observe the nematic order parameter for the particle director along the molecular axis (a vector connecting the ends of the particle):



In addition to this, we notice a subsequent formation of order for particle directors oriented along the bisector of the molecule (ie perpendicular to the molecular axis) below. This suggests biaxial order, which is not observed in nunchucks with wider opening angles (and certainly not in the rigid rod simulations).



Further work is necessary to consider this transition however. In particular, the nematic/smectic division is rather important. My dilute simulation (which I had assumed was nematic) may have an offset smectic structure, and the smectic layers are not fully formed in the crystalline simulation. I believe the degradation here is a result of the length of the box; it is not an integer multiple of the layer width and so the periodic boundary conditions lead to destructive interference, resulting in some of the layers expanding and breaking down.

Daan has suggested that the Parrinello-Rahma method for MD simulations may be most appropriate; it adjusts the simulation region to ensure a constant stress in all directions. I am not sure how this should be best implemented into LAMMPS, while ensuring the oblong geometry of the box is maintained as the aspect ratio varies (ie keeping the right angles of the box!)

Project Records

Chapter Introduction

13 October 2020

18:50

This chapter is intended to provide a record of the progress of the project, collected thematically (as opposed the Daily Logs, which are strictly chronological). This record allowed me to consider multiple aspects of my system concurrently, while documenting each separately. I found this invaluable when working on simulations with long run-times, as this allowed me to make progress on separate aspects of my project, and test different aspects of this system simultaneously.

This section records all major milestones/significant results obtained within the project, as well as the (approximate) date upon which they were obtained. It should be regarded as the primary source for such developments, although elements will also be replicated within the Meeting Summary chapter (for graphs etc discussed within the supervisor meetings), and also within the Daily Logs. All entries are dated automatically by the OneNote software, below the title.

Initial Work

13 October 2020

20:14

Much of the initial work for this project is detailed in the LAMMPS section; for setting up LAMMPS and running test cases. The results obtained each week are detailed within the meeting summaries

Initial Steps

Initially I will focus on very simple test systems with known behaviour, in order to ensure the accuracy of my approach, and develop my knowledge and experience using the LAMMPS software. In order of hierarchy:

- 2D hard spheres
- Stiff rods (while varying the aspect ratio to reproduce known phase transitions)
- Completely flexible nun-chucks (~20 base pairs in single stranded connector)
- Partially flexible nun-chucks (4-6 base pairs in single stranded connector)

It is important to consider how to quantise phase transitions, and aim to replicate known behaviour here.

Phase Detection - Method 1

23 November 2020

21:55

Methodology

Loop variable

Each simulation run corresponds to a single point on the phase diagram (i.e. a single thermodynamic variable at equilibrium). For testing purposes, this was set to the temperature to iterate over.

However this is adapted for formal plotting on 30/11/20, looping over a set number of mixing steps instead.

Problems

Reading thermodynamic variables from output

A program was written to read through the entire output file, and list line numbers which began with "Step" (the line before the thermodynamic output) and "Loop" (the line after the thermodynamic output). These could then be used to determine the header and footer (ie the extra lines to ignore) when extracting the data in a numpy array.

This was particularly tricky when iterating over multiple parameter values (so the output file contains multiple runs), as these result in many blank lines. The genfromtext function in numpy does not include blank lines in its skip_footer argument (although it does in the skip_header), so these had to be calculated separately. This process was done iteratively when reading the document, so the number of blank lines encountered by every 'Loop' line was recorded. This allowed me to find the number of blank lines still to come, which was added to the 'adjusted' end line value. Therefore, the skip_footer function would skip fewer lines to account for the extra blank lines it skipped 'without being asked to'. Lines with comments in them (i.e. pre-faced with a hashtag) are automatically read as blank by the genfromtext function, and so this behaviour must also be suppressed when calling the function.

Reaching equilibrium

Fundamentally this approach is inefficient, and this will be prohibitive when running over sufficiently long times to reach true equilibrium (see notes on 1st Dec meeting). A second approach is therefore required...

Phase Detection - Method 2

24 January 2021

22:26

Motivation

Reaching Equilibrium

The fundamental issue with my first class of simulations was insufficient time to equilibrate, and too fast compression to achieve the high density phases.

This will be rectified in a second directory with a new coding approach:

- Compress a short way to achieve a new volume fraction
- Allow sufficient time to equilibrate at this value
- Record thermodynamic properties here
- Repeat (continuing from this system state) to achieve a new volume fraction

By avoiding recompression over the same regions, this should be more efficient, while giving more accurate results. However, it is a very different structure to my previous work, and so will be attempted in a new directory to preserve the previous method. This is the reason for the rigid_rod2 directory (a simple name!).

Methodology

Loop variable

On 11/12/20, this method is adapted to avoiding resetting the particle configuration after each run, but rather record the equilibrium positions and then compress further from this state. This method cannot use the 'jump' command, as it closes the current file, and (re-)opens the named file. Even if these files are the same, the current configuration is lost. The label command (which determines where LAMMPS should begin executing in the new file) does not avoid this issue, as the old configuration is still not preserved. While it is possible to save and reload this, it is easier to keep the current file open.

A simplistic approach of simply setting another fix and running again is possible if all previous fixes are removed as necessary. This gives a satisfactory result (see "*in.run_simple*"), but hopefully there is a better way to loop over this, particularly when plotting a phase diagram with -10/20 points, and potentially variable mix_step values.

A loop is in fact possible (25/01/2021), but cannot avoid closing the file after each run. The commands 'write_restart' and 'read_restart' allow the current configuration to be saved and reloaded at each point. The full methodology for this approach is given in the next section.

Code Structure

In.run_setup

This file imports the input_data file (which is generated by nunchucks.py and contains the initial positions of each particle within the simulation box). It sets up the potential interactions, bond properties and general simulation parameters, then writes the initial positions to a restart file.

In.run_loop

Initially, all previous restart files are deleted, and then *in.run_setup* is run.

This file then loops over the mix_steps given at the start of the file. It loads the restart file, contracts over the given number of mix steps and then lets equilibrate over the given number of run steps. Thermodynamic variables are output to the command line, and saved in the log file, while an output file can save the particle trajectories at each timestep to be visualised in Ovito.

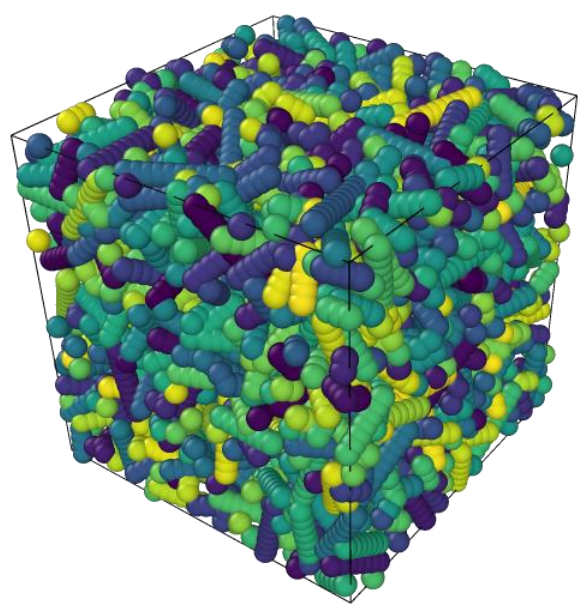
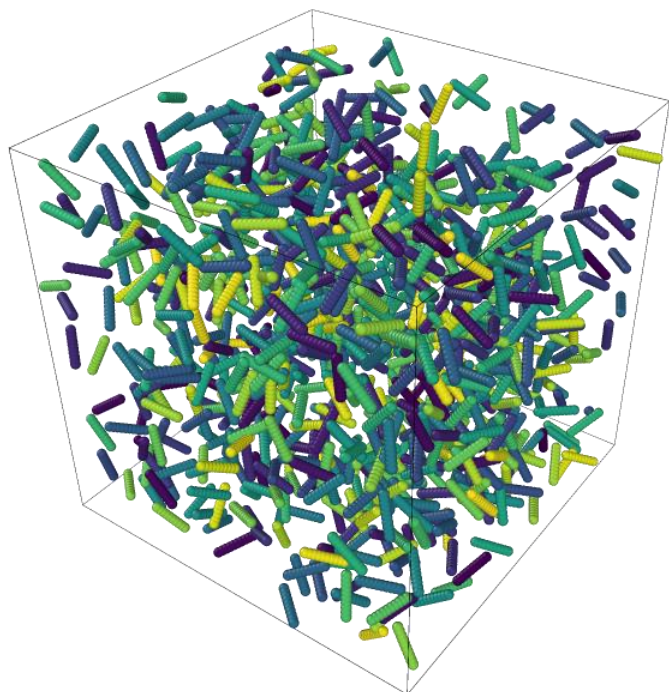
Results

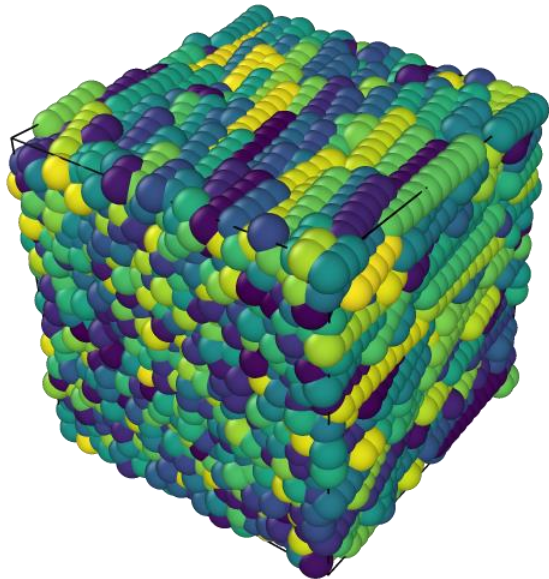
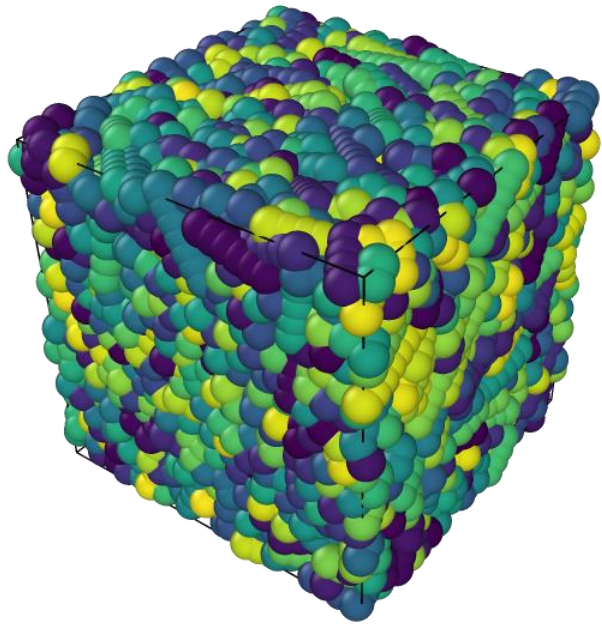
Extended Phase Detection Run - *longrun1*

On the 26th Jan, I ran an extended simulation with approximately 5 times the length of the previous simulation, to endeavour to add sufficient time for equilibration. I have included the important parameter values below for reference:

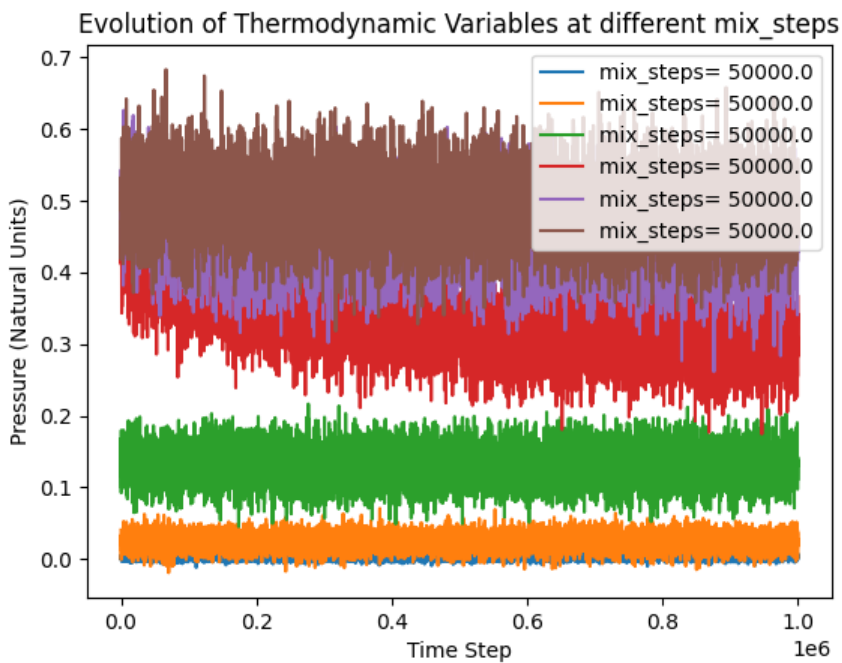
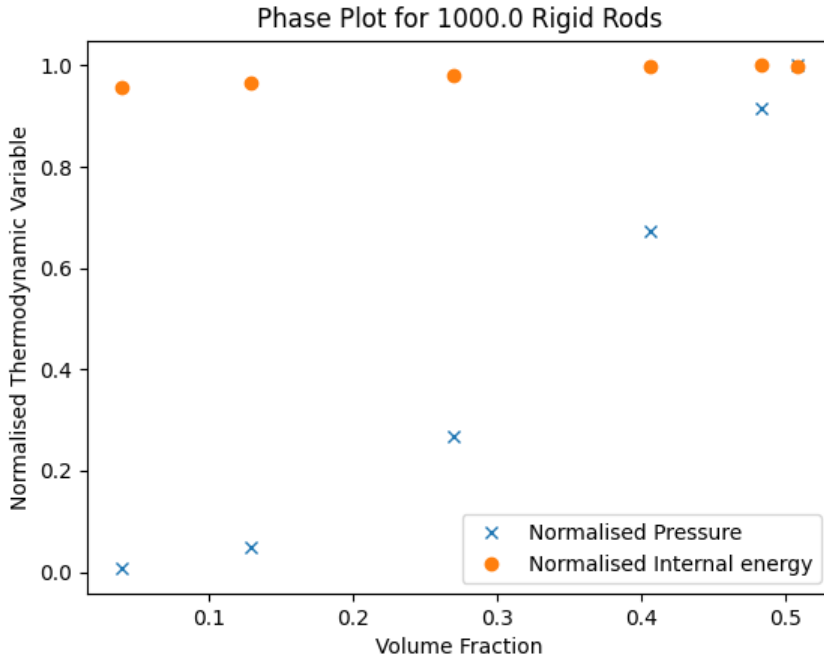
```
variable N      equal 1000
variable box    equal 100 # cubic box of length scale 'box'
variable T      equal 0.5
variable t_step  equal 0.005 #originally 0.005
variable mix_steps index 50000 50000 50000 50000 50000 50000 #6 reps of shrinking
variable run_steps equal 1000000 # steps to run simulation in order to reach steady state
```

The runtime for this was 3 hours. The box simulations at various points are depicted below:





The phase transition here is clear between the final pair of images. This is also observed in the phase plot below, with a significant difference between the pressure of the third and fourth points. This is where the phase transition occurred, as observed by the shifting pressure in the pressure plot (which recorded the pressure change over the equilibration period). The shift in the red line demonstrates the phase change here.



For future work, quick changes involve considering more points to isolate the phase transition, and plotting a smoothed version of the pressure (ie a running average) to better visualise the pressure change here. Furthermore, the pressure in the phase plot is currently the mean value across the entire equilibration time, whereas a mean from the last 10% (when the system has reached equilibrium) would be more accurate (as currently the fourth point corresponds to the mean of the red line, including the period where the system is undergoing a phase change and has not yet reached equilibrium).

Longer term, it would also be beneficial to move to an oblong simulation region. To observe a smectic phase, we really need a box with a long axis 5/6 times greater than the length of the

particles (currently the final side length of the box is 2.5 times the particle length). To minimise the particles required, it is easier to simulate this in an oblong region, so the volume of the box is not increased significantly. This may be adjusted in line 147 of nunchucks.py.

Oblong Detection Region

31 January 2021

14:58

Motivation

Typically, the formation of ordered phase structures such as nematic or smectic phases is impeded by the edge effects of the box; the periodic boundary conditions here can destabilise the formation of ordered phases if the simulation dimensions are not an integer multiple of the molecule dimensions. (For example, when forming a smectic phase the molecules cannot line up fully in columns and must overlap at the edges of the box.)

This effect is mitigated by increasing the volume of the simulation box, as the overlapping regions form a smaller proportion of the overall structure (and this overlap may be distributed further to reduce the energy cost). We typically aim for a simulation region 5/6 larger than the molecular dimension. However, a larger simulation regions comes with associated computational costs, as a greater number of molecules are required to achieve the same volume fraction.

These costs can be reduced by breaking the symmetry of the system; we may be introduce a long axis in our simulation region to generate an oblong box. Ordered phases will preferentially form along this long axis, as the energy costs associated with the boundaries are reduced. In this way the number of particles required to 'fill' the box (i.e. achieve the desired volume fraction) is minimised, while retaining the longer simulation axis for ordered phase formation.

Implementation

I defined an 'elongation' factor in the nunchucks.py file, which acts as a scaling factor along one axis (chosen arbitrarily to be the y axis within the code). This is implemented as a vector, with each value giving the scaling factor on the corresponding axis.

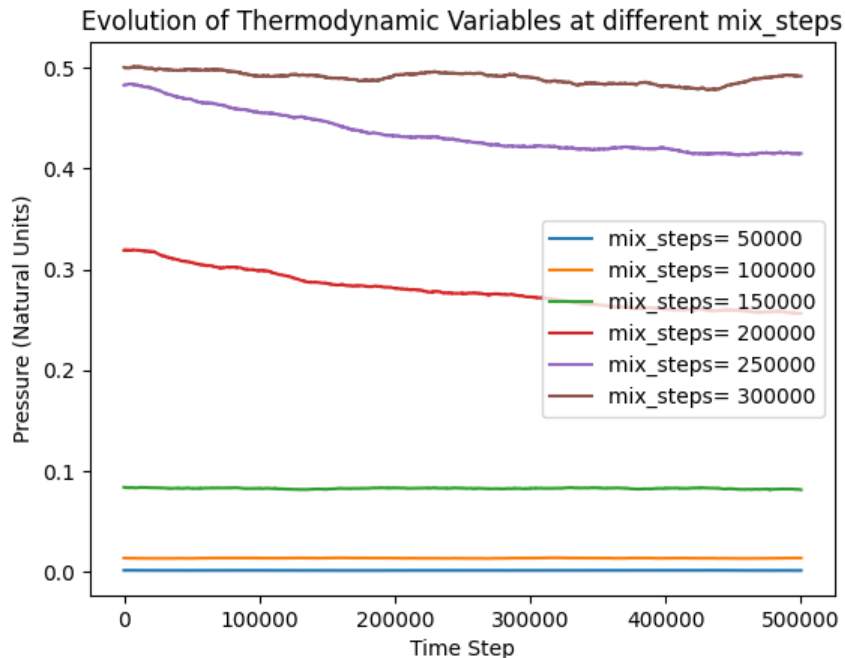
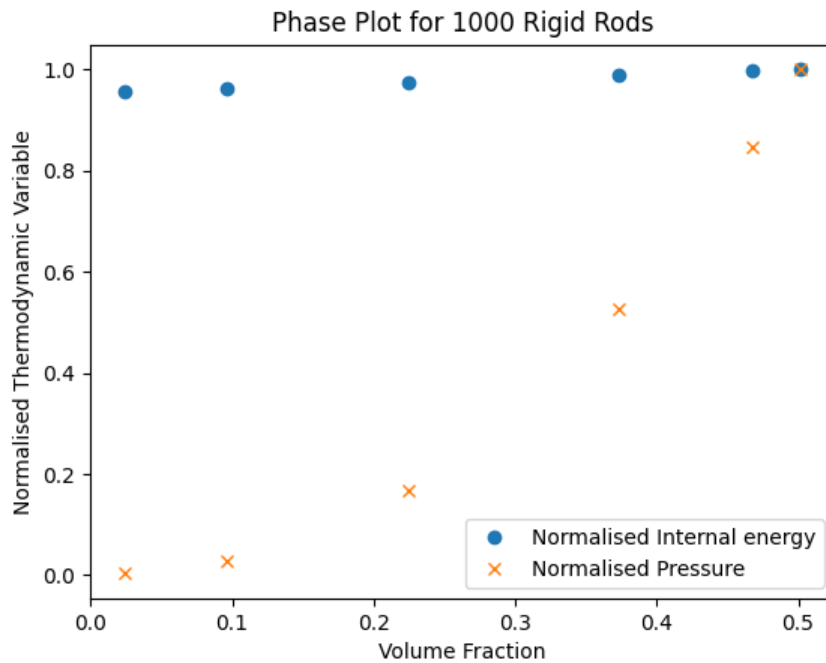
This is then added into the 'within_box' function, to check whether the newly placed molecule lies within the new extended box region. It is also added (as a scalar for simplicity as this code will only be used to rescale one box dimension) into the random displacement generated in the 'gen_ghost' function. Finally, the plotting axes in 'plot_all' are also updated to reflect this change.

Results (longrun2)

These include simultaneous implementation of a running average in the pressure measurements.

```
variable N      equal 1000
variable T      equal 0.5
variable t_step  equal 0.005 #originally 0.005
variable mix_steps index 50000 50000 50000 50000 50000 50000
variable mix_tau equal ${t_step}*${mix_steps}
```

```
variable run_steps equal 500000 # steps to run simulation in order to reach steady state
```



The phase formation is visualised in an animation, also produced, and the following images from this file.

Order Parameter Calculation

06 February 2021
12:11

Current Method

In general, the orientational order parameter is usually defined based on the average of the second Legendre polynomial:

$$S = \langle P_2(\cos \theta) \rangle = \left\langle \frac{3 \cos^2(\theta) - 1}{2} \right\rangle$$

where theta is the angle between the liquid-crystal molecular axis and the local director (which is the 'preferred direction' in a volume element of a liquid crystal sample, also representing its local optical axis).

However, in our case the local director is not known, and so I have approximated it as the mean director averaged across all particles.

Issues

This method is not particularly valid, and particularly struggles when there are multiple phase regions present, and so can lead to a negative order parameter.

Volume Fraction Calculation

The volume fraction is clearly defined as the ratio of summed volume of all molecules in the system to the overall volume of the simulation region. How we define the volume of a simulation molecule is harder however; I have simply summed the volume of ten balls with radius 0.5. However Jiaming suggests he has drawn a cubic box around the molecule, leading to significantly higher volume fractions than I have achieved.

It is also worth noting that the particles strictly have a radius greater than 0.5, to ensure overlap between adjacent spheres in the same molecule. The area of this is slightly tricky to compute, but outlined below:

$$V = \frac{1}{12} \pi (4R + d)(2R - d)^2.$$

(for overlap between two spheres of radius R, with separation d).

For R = 0.56, d = 0.98 we find the overlap volume is V = 0.0156 (2% of the atom volume 0.736). There will be 9 overlaps per atoms in a molecule, so the percentage error is slightly less than this. It should also be noted that the volume of a sphere of R = 0.5 is V = 0.534, significantly less than the per-atom volume for R = 0.56. Therefore this approximation should not be used.

Finally it is worth considering an alternative approach of using a cylindrical volume encasing the particle, when in comparison with Onsager's rigid rod theory. This is significantly easier to compute than the overlapping volumes case, and should be used for comparison with Onsager's limit of stability (0.4 volume fraction in this case).

Summary of Volume Fraction Options

Unit Volume Formulation	Exact Form	Numerical Form
Sphere ($R = 0.5$)	$\pi/6$	0.524
Sphere ($R = 0.56$)	$\frac{4}{3}\pi R^3$	0.736
Sphere with overlap* ($R = 0.56$)	$\frac{4}{3}\pi R^3 - \frac{1}{12}\pi(4R - d)(2R - d)^2$	0.719
Cylinder ($R = 0.5$)	$\pi/4$	0.785
Cylinder ($R = 0.56$)	$\pi R^2 d$	0.966

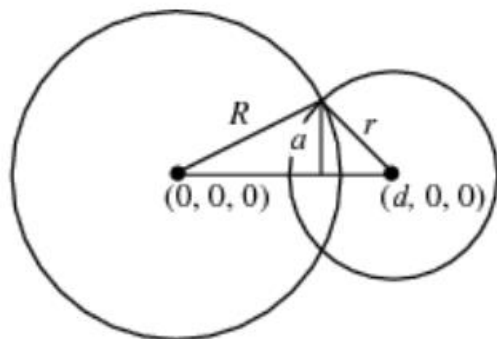
*This accounts for one atom, with one overlap volume subtracted. Strictly speaking, the molecule has 10 atoms with 9 overlap volumes subtracted, however we don't account for this here. Distance between sphere centres (d) is 0.98

New methods

Eppenga and Frenkel detail an alternative method to approximate the order parameter which I will implement instead:

R. Eppenga & D. Frenkel (1984) Monte Carlo study of the isotropic and nematic phases of infinitely thin hard platelets, Molecular Physics, 52:6, 1303-1334, DOI: 10.1080/00268978400101951

This relates the eigenvalues of Q (ie the true order parameter) with the eigenvalues of M (which approximate to this in ordered systems.) Strictly speaking, the most positive eigenvalue here is the conventional order parameter.



Taken from: [Sphere-Sphere Intersection -- from Wolfram MathWorld](#)

Longtime records

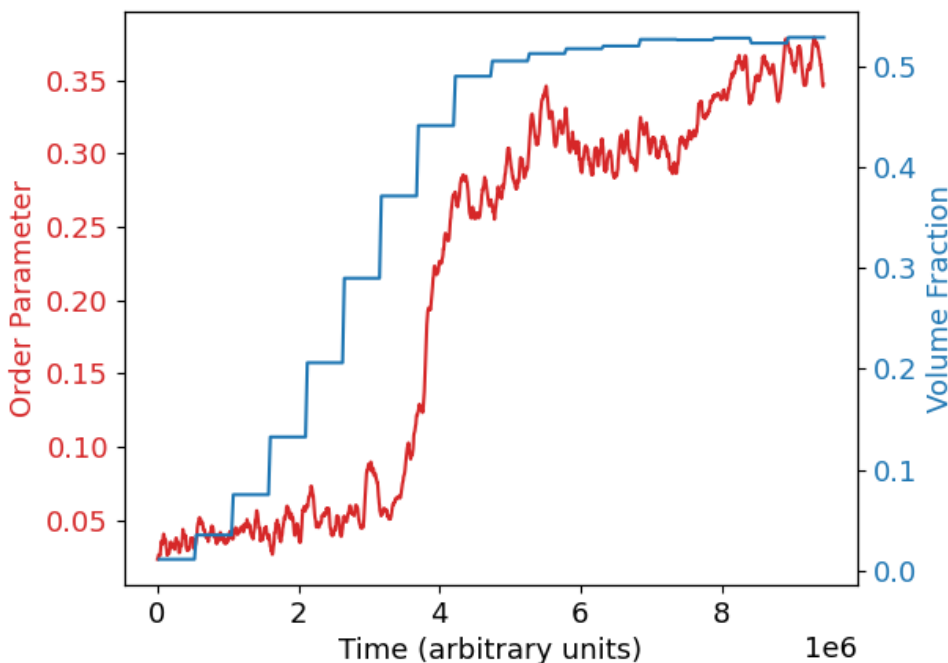
08 February 2021
09:08

This gives the phase plots of various rigid rod systems, ran over long periods of time. The average runtime for these simulations was 8 hours. The aim of these simulations was to identify the critical volume fraction where the phase transition occurs. The timestep where the order parameter increases most steeply is indicated below in bold, within the record of all steps ran. Note that in all cases, the rate of shrinking is the same between simulation runs (determined by the damping of the thermostat in LAMMPS), although it may be dependent on the volume fraction of the system.

Longrun2

```
variable mix_steps index 25000 25000 25000 25000 25000 25000 25000 25000 25000 25000 25000 25000  
25000 25000 25000 25000 25000 25000 25000 25000 25000 25000  
variable run_steps equal 500000 # steps to run simulation in order to reach steady state
```

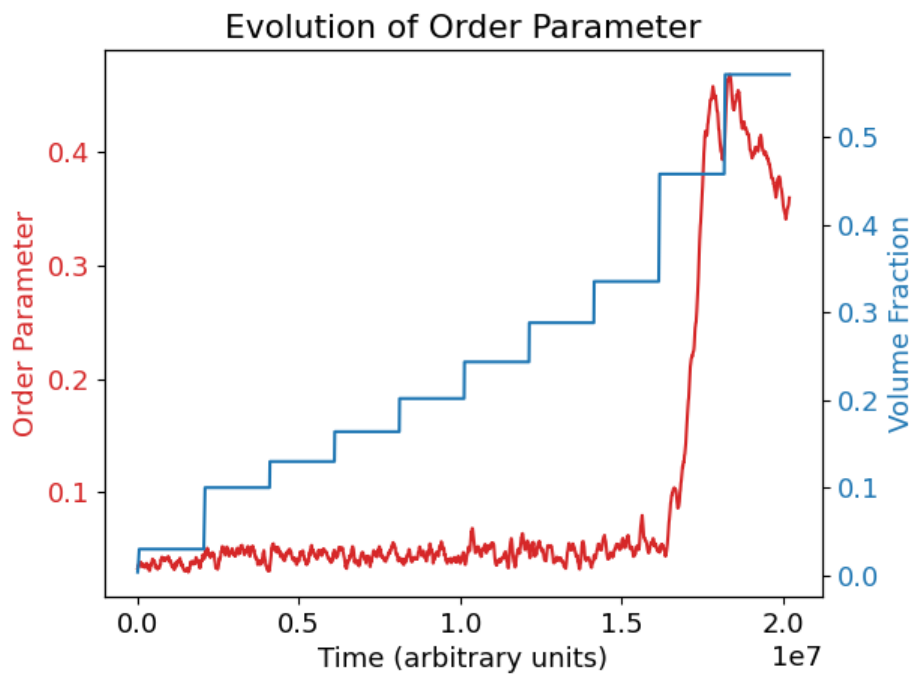
Phase transition after 175000 steps of mixing.



Longrun3

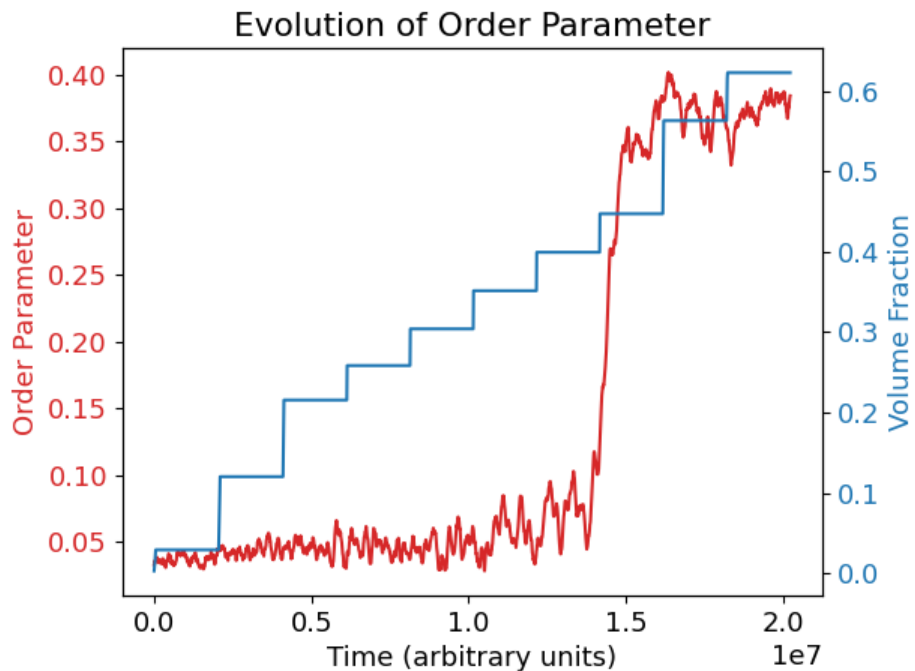
```
variable mix_steps index 50000 40000 10000 10000 10000 10000 10000 10000 30000 30000  
variable run_steps equal 2000000 # steps to run simulation in order to reach steady state
```

Transition after 150000 steps of mixing



Longrun4

```
variable mix_steps index 50000 50000 30000 10000 10000 10000 10000 10000 10000 10000 10000 30000 30000
variable run_steps equal 2000000 # steps to run simulation in order to reach steady state
```



Running in Parallel

12 February 2021
22:29

Put simply, this is complicated, and I don't understand all of it! In short, the `lmp_mpi` executable would likely be ideal. However this is difficult to setup on windows, and not compatible with `lmp_serial`. `lmp_serial` does however support multi-threading, which speeds up the computation times slightly.

MPI Running

"Only the `lmp_mpi` executable supports parallel execution via MPI (which can be combined with OpenMPI multi-threading). For that you also need to install a specific version of MPICH2 from Argonne lab linked above. The installer does not contain it and does not check for it. Please note, that you need to download a very specific (and rather old) version of the MPICH package, as this is what LAMMPS was compiled with and the latest available Windows binary version compatible with the GNU compilers used to compile LAMMPS."

Multi_Threading

"All LAMMPS binaries from this repository support multi-threading via OpenMP, however by default only one thread is enabled. To enable more threads, e.g. four, you need to either set it at the command line prompt via set `OMP_NUM_THREADS=4`, via the `-pk omp 4` command line flag, or via the package `omp 4` command in your input script."

`lmp_serial -pk omp 8 -sf omp -in in.run_loop` - Run in command line - uses 8 threads

Also added the line 'package omp 8' at the start of the setup file, which may(?) be necessary.

This enables us to set 8 (max) OpenMP thread(s) per MPI task (which remain limited to 1), and use multi-threaded neighbor list subroutines (speeding up specific sections of the code).

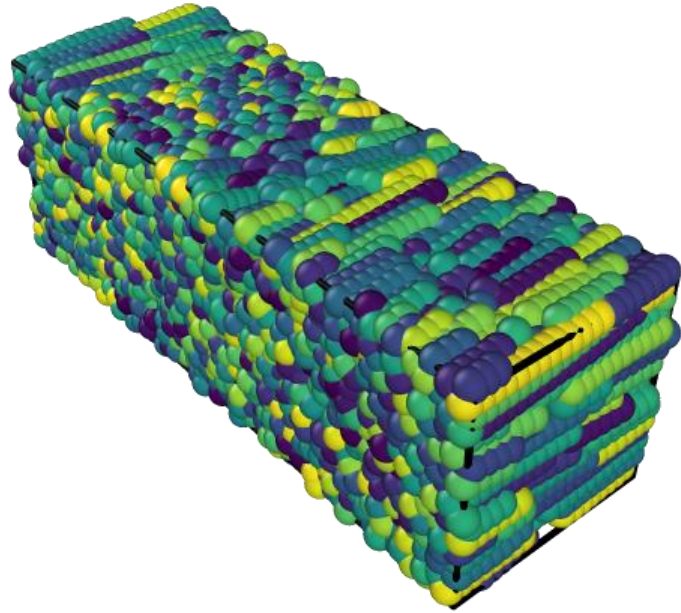
Extended Rod Aspect Ratio

14 February 2021
17:42

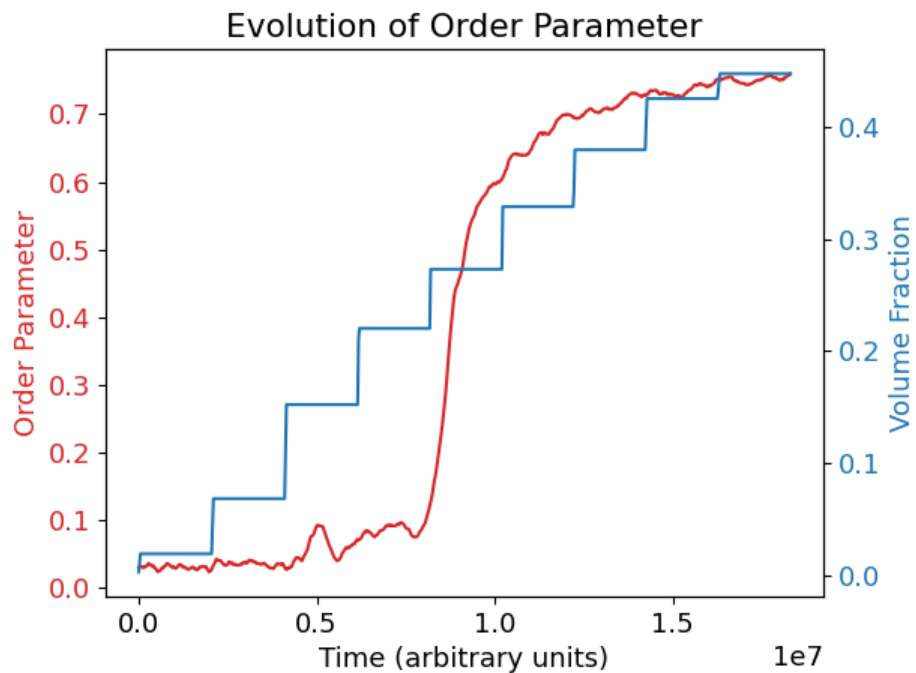
We consider here a rigid rod system of extended aspect ratio; with particles comprised of 16 sequential balls instead of 10 (and hence having an aspect ratio of 16 instead of 10, as previously used). According to Onsager theory, this should reduce the critical volume fraction for the nematic phase transition to $4D/L$, where D and L are the diameter and length of the particles respectively; in this case this evaluates to 0.25 .

This was achieved through adapting the `nunchucks.py` script to produce particles of 16 balls, instead of 10. It would be possible to have adjusted the `nunchucks.py` file to take an arbitrary initial particle size, however this would have been a more significant time investment. Being rather pressed for time at the moment, and as this script is no longer used actively within the group's research (nor do I plan to consider alternative length rigid rods), I decided this was not an effective use of time.

The nematic phase formed here is displayed below:

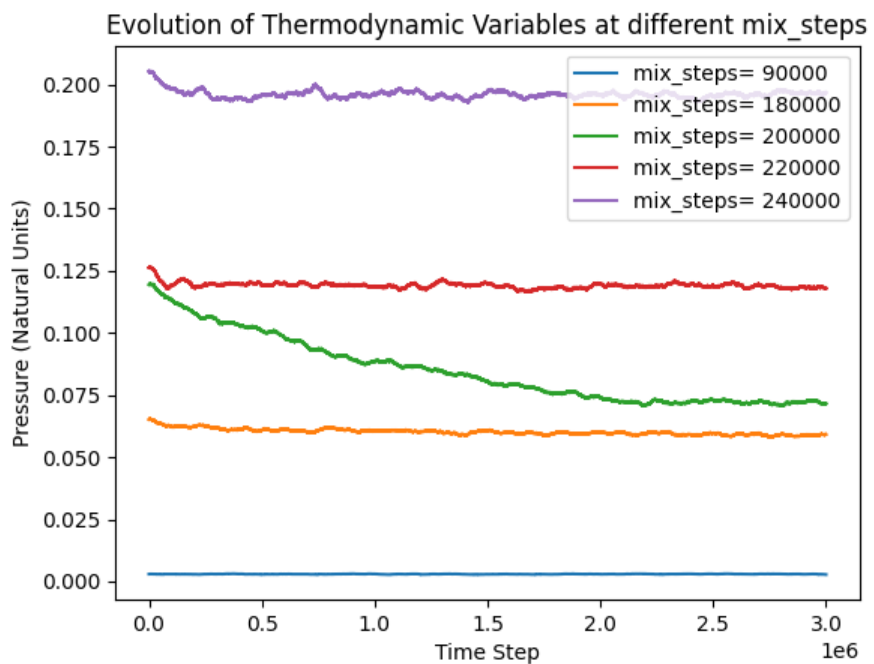
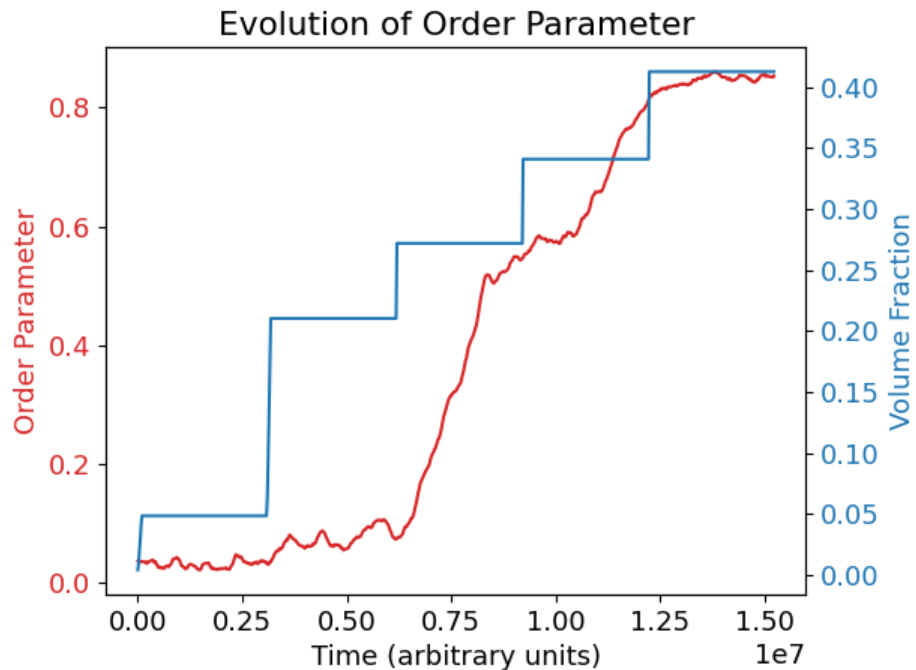


While it displayed the same separated nematic regions observed in the oblong simulation region for aspect-ratio 10 particles (longrun2), the same phase analysis may still be applied (the only difference being that the same magnitude of order parameter may not be achieved. The evolution of order parameter (calculated using the method suggested by Eppenga et al.) is given below, and clearly occurs between 0.2 and 0.3 as predicted.



Further simulation work is completed on this system, confining the phase transition very close to the expected critical volume fraction of 0.25. This is done in the longrun3 directory, and required

reconsideration of the volume fraction calculation under Onsager's theory. This also provides a nice example of the pressure evolution over time, with a clear shift when the phase transition occurs:



Crystalline Rigid Rods

14 February 2021

18:22

It has long been an aim to run my simulations 'in reverse' - i.e. start from a perfectly ordered (crystalline) phase, and expand the system to observe the introduction of disorder. This is particularly important to demonstrate the validity of the nematic phase transition we have previously observed when shrinking the simulation region, and particularly that it was observed at equilibrium. This is because non-equilibrium effects will manifest themselves as hysteresis here; i.e. the 'backwards' phase transition will not occur at the same critical volume fraction as the 'forwards' (i.e. reducing volume fraction) transition.

However I have not yet attempted it due to the magnitude of changes required to the nunchucks script to initialise these initial conditions; it will effectively require rewriting. The results of this change are given in the new directory 'crystalline' within the 'Rigid_Rods2' directory.

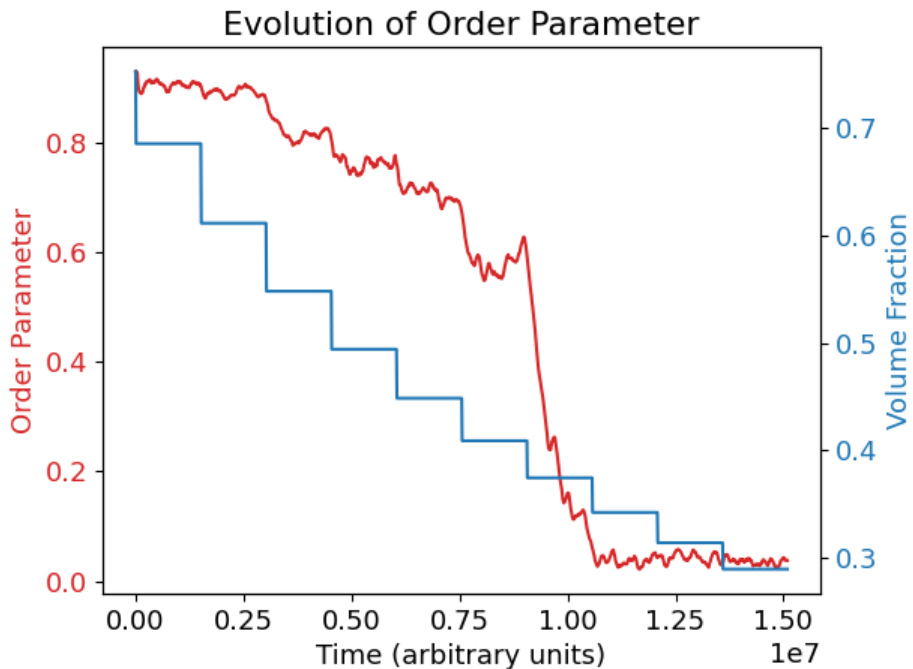
Box Expansion

The expanding simulation region is controlled by the nph (isentropic) fix. This specifies a target pressure, and a damping term, and then the system evolves isentropically to achieve this. The target pressure must be lower than the system pressure for expansion to occur (and the rate of expansion is controlled by the damping term, however this has not been changed from previously).

It is also worth noting that the langevin fix is there to ensure the temperature of the system is also conserved during this process.

Nematic Phase Transition

We see clear formation of an isotropic phase from the nematic phase when the simulation region is expanded, as was anticipated. Most crucially, this is indeed observed at a volume fraction of 0.4, ruling out the potential for hysteresis in this phase transition, and confirming that an equilibrium phase transition was indeed observed.

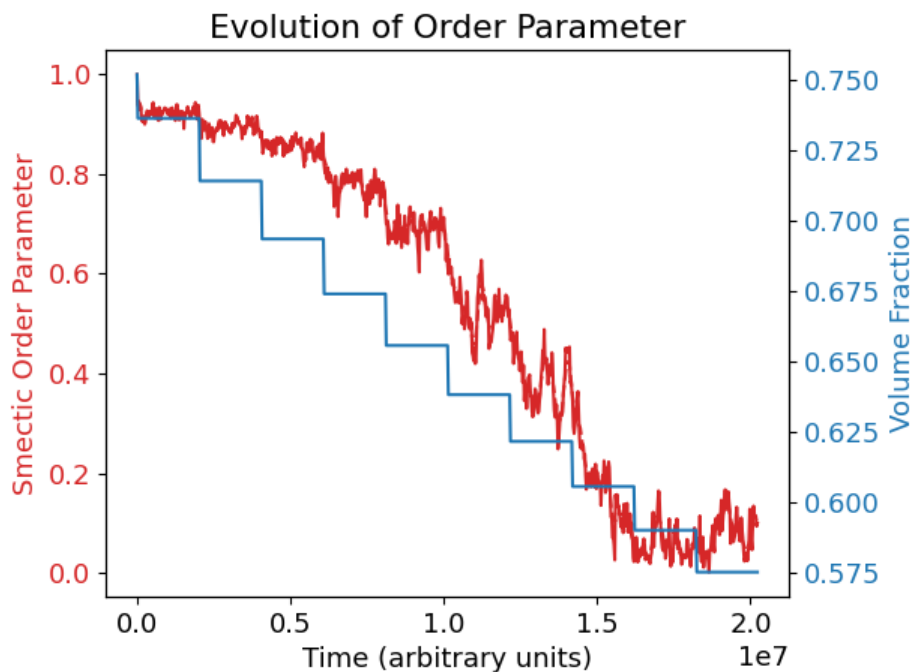


The gradual decrease in order parameter before this is explained below, due to the changing 'smectic' phase at this point.

Potential Smectic Phase

This is a result of extended high volume fraction simulations from the initial crystalline phase of the initial rigid rods system. I have implemented the Smectic order parameter, as described in:
"First-order nematic-smectic phase transition for hard spherocylinders in the limit of infinite aspect ratio" - by James M. Polson and Daan Frenkel, from Phys. Rev. E 56, R6260(R) – Published 1 December 1997.

This clearly displayed a decrease in smectic order, however this does not occur discretely at a single volume fraction:



Daan has suggested that, while Landau Theory does predict the smectic \rightarrow nematic phase transition to be discrete, there is other evidence for a continuous phase transition here. However, this may not be conclusive evidence for it; ideally we would observe the same effect 'in reverse' - i.e. upon shrinking. It is hard to achieve sufficient volume fractions for this, however it may be possible to increase the volume fraction somewhat to demonstrate the beginning of this trend.

I suspect however that the result of the smectic order degradation may be that the long axis of the box is no longer favourable for smectic phase formation as expansion occurs, as it is no longer an integer number of molecules long (and so the periodic boundary conditions cause interference in the phase formation. This may be simply reduced by expanding over two axes alone.

More formally, this should be done via the variation of the aspect ratio for a constant volume after each shrinking step, to determine the stability of the smectic phase over changing aspect ratio (and ensure continuation of favourable conditions at each box volume). This may be implemented ideally via a small Monte Carlo approach to vary the aspect ratio of the box at constant volume between each molecular dynamics simulation. However this is very difficult to achieve through LAMMPS, and so may have to be the subject of future work.

*Further, more convincing evidence for smectic phase found in
'Rigid_Rods2/Crystalline/Full_transition/smectic_only' directory when investigating diffusion -
30/03/2021.*

Hysteresis Confirmation

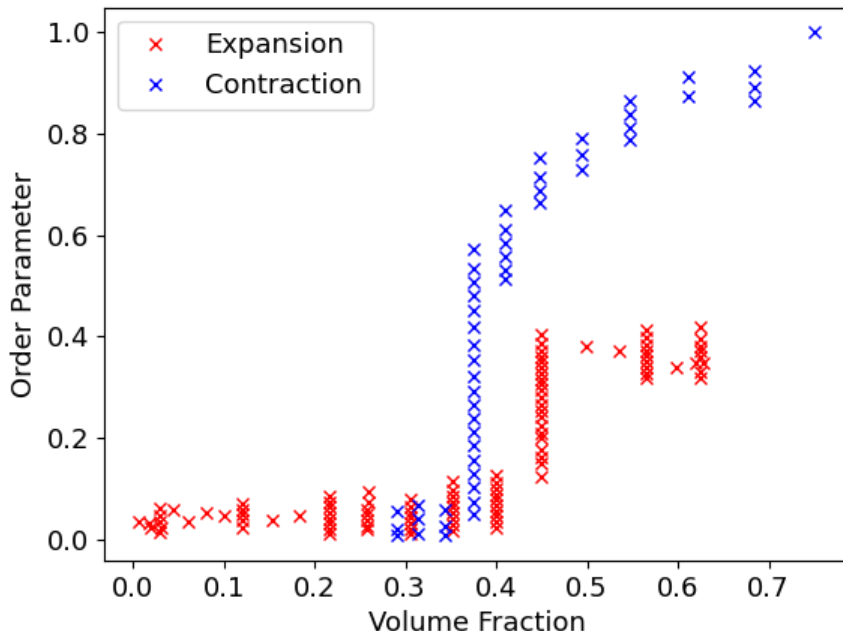
08 May 2021
15:45

This page is really just an appendix on the application of the reverse simulations detailed in previous sections

The aim of these is to confirm that the phase transition occurs at approximately the same volume fraction, whether the volume fraction is increased or decreased over the span of the simulation. In reality, there will be some gap between the volume fractions, as each method samples the system at discrete volume fractions. Therefore, the expanding simulation will find return a critical volume fraction (when the phase transition occurs) below the true value, whereas the contracting simulation will return a value above the true value.

Within this error (given by the sampling intervals of each processes) we observed good agreement. We cannot compare the evolution of order parameter over time for each process directly, as the rate of volume change is not constant. However, we may compare the order parameter over volume fraction, as below. Remember this is not a perfect method (and is not used more widely in this project) as it doesn't differentiate between noise in the order parameter at a particular volume fraction, and change in the order parameter over time.

Nevertheless, we can clearly see a change at approximately the same volume fraction (around 0.4 in both cases), as required.



It should also be noted that the maximal order parameter achieved is significantly higher in the contracting case, as it is initiated from a crystalline phase, with perfect orientational alignment. Effectively, the contracting case evolves over time left to right (starting in a disordered state), whereas the expanding case evolves over time right to left (starting from a perfectly ordered case).

Nunchucks - Initialisation

14 February 2021

23:26

I have initialised two new folders within the new nunchucks directory to represent the two cases I am considering here:

- Fixed Angle - All rods may be defined to have a 150 deg bend at the centre

- Fixed Rigidity - All rods may have a central bond with a specified rigidity that allows rotation about this point. This means the bond may open up to about 150 deg, but may take values anywhere from 180 to 150.

In previous simulations, it has been difficult to identify whether equilibrium has been reached here, and also to quantify any phases that do form (such as the elusive 'swirl' phase). I also have concerns that such phases (having a much larger length-scale than the rigid rod nematic phase) may require a larger box size, and hence more simulation complexity. In particular, it may also be helpful to run multiple simulations over different box sizes, to ensure that any phase formed is not dependant on the box size (and so being affected by the periodic boundary conditions).

Initially, introducing an arbitrary angle/ bond rigidity is sufficient here, as well simply want to justify the existence of such phases. Further work would then be required later to validate that the DNA system would be able to form these, through comparison of the mechanical properties of DNA in the OxDNA model to the LAMMPS parameters here.

Phase Detection Ideas:

- Place molecule director as the bisector of the rods. This doesn't uniquely specify the molecule position so consider two directors, or a projection onto a given plane
- Plot distribution of angles between rod arms (only works for fixed flexibility)

Fixed Angle

Jiaming's code for this case initially included two central angles about a even-numbered rod (ie a rod with ten spheres, and angles defined between spheres (4,5,6) and (5,6,7)). However the second angle adds an additional degree of freedom, as rotation is now possible in two places so that the angular separation between rods is not actually constant; it is therefore necessary to only define one angle here.

To achieve this, we must use an odd-numbered rod (i.e. a rod with an odd number of spheres), so that we may define an angle about the central atom while retaining equal length arms. I will adapt the nunchucks.py code to achieve this, implementing methods to generate an input file for an arbitrary number of atoms.

Nunchucks - A New Phase?

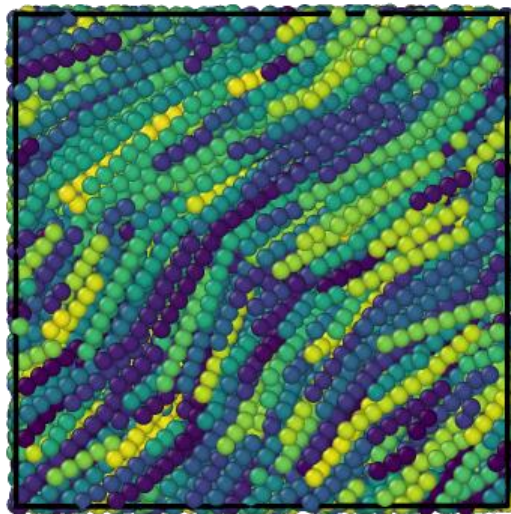
23 February 2021

18:17

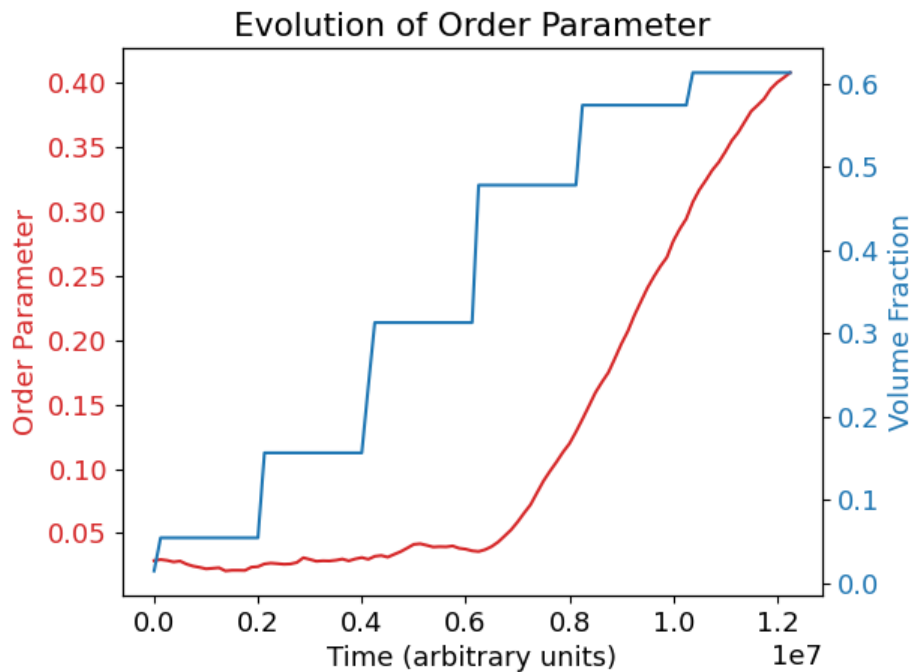
In this section, following on from the work of the previous section, we consider a nunchuck formed of 15 spheres, with a flexible join in the centre so that the angle about the central molecule may deviate from 180° - this is either set at 150° in the fixed angle case, or unrestricted in the fixed rigidity case. Note that this extended aspect ratio (from particles of 10 spheres) is used to increase the likelihood of phase formation.

Fixed Angle

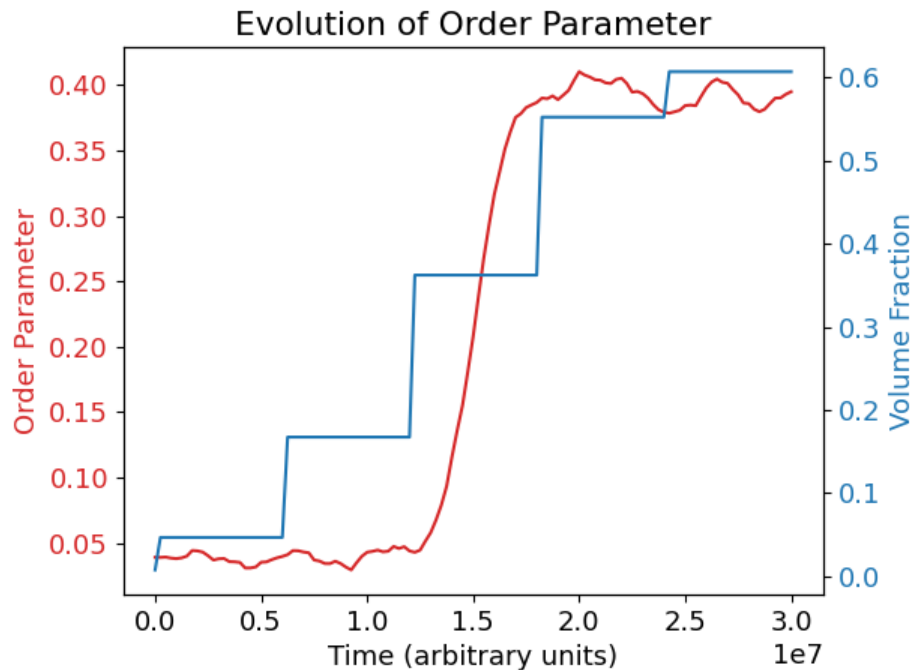
We have clear evidence for a new phase here, with strong alignment visible in the final state of the molecule. It remains to be shown whether this is a distorted nematic phase, or there is a true 'zig-zag' aspect to it (or other chiral/biaxial behaviour). This will be examined further with more detailed order parameter analysis, using position dependant averages of the Legendre polynomials.



However, simply using the nematic order parameter gives clear justification for the claim of a phase transition here, around a volume fraction of 40% (although this is a broad estimate due to the magnitude of the jump in volume fraction; this may be reduced in further targeted simulations).

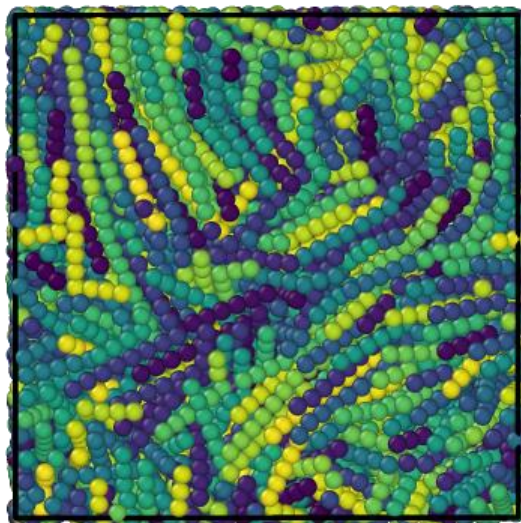


A further long time simulation here was ran to isolate this transition further, and verify that it did indeed occur at a fixed volume fraction:



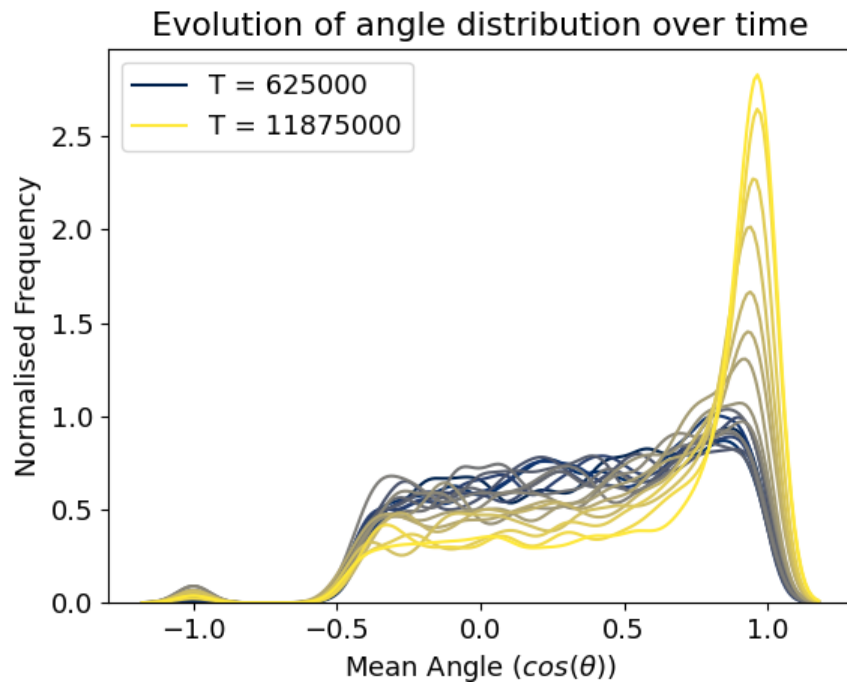
Fixed Rigidity

We again observe a similarly ordered phase formed in this case as well, possible with a slight 'swirled' characteristic; though of course I would be wary about claiming this in any wider settings without some justification for that!



Again, the formation of this phase results in an increase in the nematic order parameter (although it is less significant; as this new phase is less well described by the nematic phase description and does not have uniform director alignment across the system).

The distribution of intramolecular angles (between the two arms of the nunchuck) is very interesting however, and provides further evidence for the formation of order over time. This plot suggests that, as the simulation progresses (from blue to yellow curve), the angle distribution becomes less uniform, and sacrifices freedom in the molecule configuration to form a more ordered phase with a more uniform angle distribution.



Orientational Order Parameter - T

01 March 2021

18:44

As suggested by Daan, I will try to implement a position dependant orientational order parameter. I had not come across this before in the literature, and it turns out there was a good reason for this! Here I outline some of the previous work in this area.

Simulation of site-site soft-core liquid crystal models - Paolini

3.1. Collective orientational order parameters

In a computer simulation, the orientation of the nematic director is not known *a priori* and will generally fluctuate during the time evolution of the system. We choose the nematic director $\hat{\mathbf{n}}$ as the unit vector that maximizes the expression [3]

$$\begin{aligned}\epsilon(\hat{\mathbf{n}}') &= \frac{1}{N} \sum_{i=1}^N [\frac{3}{2}(\hat{\mathbf{n}}' \cdot \hat{\mathbf{u}}_i)^2 - \frac{1}{2}] \\ &= \hat{\mathbf{n}}' \cdot \mathbf{Q} \cdot \hat{\mathbf{n}}',\end{aligned}$$

with respect to $\hat{\mathbf{n}}'$. The maximum $\epsilon(\hat{\mathbf{n}})$ is the instantaneous *orientational order parameter*. Here $\hat{\mathbf{u}}_i$ are the unit vectors describing the orientations of molecular axes in the laboratory frame, and

$$\mathbf{Q} = \frac{1}{N} \sum_{i=1}^N (\frac{3}{2} \hat{\mathbf{u}}_i \hat{\mathbf{u}}_i - \frac{1}{2} \mathbf{I}),$$

is the tensor associated to the order parameter [3, 15]. The instantaneous orientational order parameter is then equal to λ_{\max} , the maximum eigenvalue of \mathbf{Q} , and $\hat{\mathbf{n}} = \hat{\mathbf{n}}'(\lambda_{\max})$ is the corresponding eigenvector. What we do in practice is compute \mathbf{Q} along a trajectory of the system, diagonalize it, and estimate the ensemble average $\langle P_2 \rangle$ with the average over time of λ_{\max} . We call this average $\bar{P}_2^{(a)}$. Thus

$$\bar{P}_2^{(a)} = \lim_{\tau \rightarrow \infty} \frac{1}{\tau} \int_0^\tau \lambda_{\max}(t) dt. \quad (4)$$

Orientational order between pairs of molecules can be monitored via the L th rank *orientational correlation functions* [3]

$$G_L(R) = \frac{\langle P_L(\hat{\mathbf{u}}_i \cdot \hat{\mathbf{u}}_j) \delta(R_{ij} - R) \rangle}{\langle \delta(R_{ij} - R) \rangle} \quad (5)$$

where the brackets denote an ensemble average and $R_{ij} = |\mathbf{R}_i - \mathbf{R}_j|$. The $G_L(R)$ expresses the correlation in orientation between two molecules at a given distance R . For small separations $G_L(R)$ defines the short-range order, while for large R it measures the long-range order. In the disordered phase, G_L decays to zero, while in the ordered phase it decays to the square of the orientational order parameter [3]

$$\lim_{R \rightarrow \infty} G_L(R) = \langle P_L \rangle^2, \quad (6)$$

thus giving an alternative way to estimate the nematic order parameter from simulation data. Hereafter we will call $\bar{P}_L^{(b)}$ the order parameters computed via equation (6).

This paper outlines the function I want to consider, however gives no details on how to compute it! I have considered simply averaging over bins of R , but would rather take a continuous approach (which I believe would require evaluation in Fourier space). Hence I have searched further to try to find some records of this. We first investigated reference [3] cited here:

In the Molecular Physics of Liquid Crystals - Zannoni

This gives a very theoretical treatment of the subject, of which I don't understand large portions.

Orientation Distribution Function

This is defined as so:

$$f(\Omega) = (1/N) \int d\mathbf{r} P^{(1)}(\mathbf{r}, \Omega),$$

which may be simplified for a translationally invariant fluid (such as in the nematic case we consider here). This may then be expanded in terms of the Wigner rotation matrices (D), which form a suitable basis for the problem. Multiplying by D^* and integrating over all angles, we find that:

$$f_{Lmn} = [(2L+1)/8\pi^2] \overline{D_{m,n}^L},$$

where this constant of proportionality will appear again later (for rank L in this case). There can be up to $(2L+1)^2$ order parameters of a given rank L, however this is simplified by symmetry; so example if a uniaxial phase has a symmetry plane perpendicular to the director (as we do in the rigid rod system), the only terms with even L need be considered.

Pair Distribution

We may also apply this method to the pair distribution function, to consider the pair-wise angle correlations.

In the previous section we have seen how symmetry can be used to limit the number of order parameters and hence the possible form of the singlet distribution function. Similar arguments can be applied to the pair distribution $G(X_1, X_2)$ or, rather, $G(r_{12}, \Omega_1, \Omega_2)$ since we shall confine our attention to translationally invariant liquid crystals and so ignore the smectic phases. We use the methods developed by Steele [8], Jepsen and Friedman[18] and Blum and Torruella [17] for ordinary fluids. Let us start by noticing that $G(r_{12}, \Omega_1, \Omega_2)$ when written in a laboratory frame has to depend on the intermolecular separation r_{12} as well as the orientations Ω_1, Ω_2 of molecules 1 and 2, together with the orientation of the intermolecular vector Ω_r . Therefore we can write down immediately

$$G(r_{12}, \Omega_1, \Omega_2) = \sum G_{L_1 L_2 L}^{m_1 m_2 m; n_1 n_2} (r_{12}) D_{m_1, n_1}^{L_1} (\Omega_1) D_{m_2, n_2}^{L_2} (\Omega_2) D_{m, o}^L (\Omega_r), \quad (94)$$

In general, it is possible to apply a symmetry of the system by projecting the distribution onto the group representation of this symmetry. In this case, the distribution should be invariant under any symmetry operations of the molecules, and under permutation of identical particles. A non-trivial simplification yields:

$$G(r_{12}, \Omega_1, \Omega_2) = \sum (-)^n ((2L+1)/64\pi^4) G_L^{n_1 n_2} (r_{12}) D_{-n_1, n_2}^L (\Omega_{12}), \quad (103)$$

where Ω_{12} is the angle of rotation from molecule 1 to molecule 2. This shows that for a rotationally invariant fluid the reduced pair distribution $G(r_{12}, \Omega_1, \Omega_2)$, which does not depend on the orientation of the intermolecular vector must be a function of relative orientations only. The same conclusion obviously applies to $G(r_{12}, \Omega_1, \Omega_2)$ for any fluid where the distribution of intermolecular vectors is spherically symmetric. For such a situation, if the molecules are cylindrically symmetric, $n_1 = n_2 = 0$ and

$$G(r_{12}, \Omega_1, \Omega_2) = G(r_{12}, \Omega_{12}), = \sum ((2L+1)/64\pi^4) G_L^{00} (r_{12}) D_{0,0}^L (\Omega_{12}). \quad (104)$$

As this is rotationally invariant, it can be used to describe the onset of the nematic phase from the isotropic. The coefficients of G^{00} may simply be interpreted as the centre of mass pair distribution:

$$G_0^{00} (r_{12}) = \int d\Omega_1 d\Omega_2 G(r_{12}, \Omega_{12}),$$

For a rotationally invariant phase, we have:

$$P\{f(\omega_1)f(\omega_2)\} = \sum \{(2L+1)/64\pi^4\} \overline{D_{n_1, n_2}^L(\omega_{12})} D_{n_1, n_2}^L(\omega_{12}), \quad (106)$$

with $n_1 = n_2 = 0$ for uniaxial molecules. Thus we find

$$G_L(r_{12}) = \sum_q \overline{D_{q, 0}^{L*}(\omega_1)} \overline{D_{q, 0}^L(\omega_2)}, \quad (107)$$

Determination of the orientational pair correlation function of a molecular liquid from diffraction data - Soper

The structure of a molecular liquid is defined by means of the orientational pair correlation function (OPCF), which determines the likelihood of a molecule being found at position r , with orientation ω_2 , given a molecule with orientation ω_1 at the origin. Diffraction experiments and most computer simulations of liquids however present only the site-site radial distribution functions, which by definition contain less information than the OPCF. By expanding the OPCF as a series of generalised spherical harmonic functions (SHARM), we may show that this series, even when truncated, contains important orientational information.

The problems of trying to describe or store $g(r, \omega_1, \omega_2)$ directly in histogram form are formidable: if it is assumed that 100 radius values are needed, that 0 values need to be specified in steps of say 5° from $0 - 180^\circ$ (37 values), while phi and xhi need to be specified in 5° steps from 0 to 360° (73 steps), the total number of pixels needed is of order $(100 \times 37 \times 73 \times 73 \times 37 \times 73) = 5.3 \times 10^{10}$, which is well outside any computer memory capability. The number becomes smaller when molecular symmetry is imposed, but it is still huge and not amenable to direct calculation and storage.

It has been shown that by exploiting the spherical harmonic expansion of the OPCF [2], and by truncating this series at a sensible point, the number of pixels required to define $g(r, \omega_1, \omega_2)$ approximately can be reduced drastically [3,4]. This expansion is written as :-

$$g(r, \omega_1, \omega_2) = \sum_{l_1 l_2 l} \sum_{m_1 m_2 m} \sum_{n_1 n_2} g(l_1 l_2 l; n_1 n_2; r) C(l_1 l_2 l; m_1 m_2 m) D_{m_1 n_1}^{l_1}(\omega_1) D_{m_2 n_2}^{l_2}(\omega_2) D_{m_0}^l(\omega) \quad (1)$$

where $D_{mn}^l(\omega)$ are the generalised rotation matrices, $C(l_1 l_2 l; m_1 m_2 m)$ are the Clebsch-Gordan coefficients and $g(l_1 l_2 l; n_1 n_2; r)$ are the coefficients of the series that need to be determined.

Orientational correlation function for molecular liquids: The case of liquid water - Soper

Cited as [4] above, this paper expands upon the spherical harmonic expansion. Requires calculation of Clebsch-Gordan coefficients etc

Computational Methods

Within the 'freud' module, there is 'freud.density.CorrelationFunction', which purports to evaluate this, but only in a 2D case. No other simple computational methods could be found.

Radial Distribution Functions

The structure of a liquid can be characterized by a radial distribution function (RDF) $g(r_i, r_j)$. This gives the probability of finding a molecule, i , at a position r_i and a molecule, j , at a position r_j . For a simple liquid this becomes $g(r_{ij})$ where r_{ij} is the intermolecular separation. $g(r_{ij})$ is defined to be

$$g(r_{ij}) = \frac{V}{N^2} \langle \delta(r - r_{ij}) \rangle \quad (3.49)$$

where $\delta(r)$ is the Dirac delta function. The $\frac{V}{N^2}$ prefactor normalizes the RDF relative to an ideal gas of the same density. For use in a simulation, the delta function is replaced by a function that is equal to one when the separation is in the range $r - \delta r, r + \delta r$ and equal to zero otherwise. An example RDF is shown in Fig. 3.7.

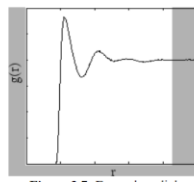


Figure 3.7: Example radial distribution function

Jiaming has also recommended a few sources:

Simulation of Molecular Liquids - Allen & Tildesley (Section 11.5)

Has a very complete (and new perspective on the) history of the field, as well as interesting musings on how to formally identify a phase transition:

How can we be sure that we are really simulating a nematic-isotropic transition? To be as convincing as the simulation of melting, it would be necessary to determine the free energies of isotropic and nematic phases close to the transition, and to locate the liquid crystal transition in relation to the normal melting point, so as to ensure against simulating a metastable state of some kind. In other words we would need to map out the complete phase diagram of the system. Ideally, spontaneous ordering from isotropic to nematic phases should be seen. In addition, it might be possible to observe a specific heat anomaly consistent with the predictions of finite size scaling for first order transitions [Mouritsen 1984].

The relevant discussion here is given below:

An alternative approach is to look at pair correlations of orientation, as measured by

$$g_2(r) = \langle P_2(\cos \gamma_{ij}) \rangle_{\text{shell}}. \quad (11.20)$$

The average in eqn (11.20) is calculated by considering molecule i at the origin and calculating the average of $P_2(\cos \gamma_{ij})$ over all molecules j in a spherical shell of width δr a distance r from molecule i . In the nematic phase, at large distances (but below the range of spatial director fluctuations) $g_2(r)$ will approach a constant value equal to $\langle P_2 \rangle^2$. Thus, measuring $g_2(r)$ and observing a plateau for $r < L/2$ is a route to $\langle P_2 \rangle$ [Frenkel *et al.* 1984, 1985; Frenkel and Mulder 1985]. In the isotropic phase, $g_2(r)$ should tend to zero at large r , but is subject to the same sorts of fluctuation as discussed above for $\langle P_2 \rangle$.

The hard ellipsoid-of-revolution fluid I. Monte Carlo simulations - Frenkel & Mulder (1985)

Going through the papers referenced above, Frenkel and Mulder detail their use of this correlation function, but do not expand on how they calculated it:

solid branches. This nematic branch is more clearly visible in figure 3. The onset of orientational order was studied by monitoring the behaviour of the orientational correlation function $g_2(\mathbf{r}_1 - \mathbf{r}_2) \equiv \langle P_2(\mathbf{l}(\mathbf{r}_1) \cdot \mathbf{l}(\mathbf{r}_2)) \rangle$, where P_2 stands for the second Legendre polynomial and $\mathbf{l}(\mathbf{r})$ is the unit vector characterizing the orientation of a molecule at a position \mathbf{r} . In the isotropic phase $g_2(r)$ decays to zero within approximately one molecular diameter. In the nematic phase $g_2(r)$ approaches a constant value at large r

$$g_2(r) \xrightarrow[r \rightarrow \infty]{} \langle P_2 \rangle^2, \quad (3.1)$$

where $\langle P_2 \rangle$ is the average value of the nematic order parameter. In our simulations we observe that $g_2(r)$, which is initially short ranged, becomes long ranged as the density is increased. Upon reducing the density, $g_2(r)$ once more becomes short ranged. This behaviour is illustrated in figure 4. It is important to note that the isotropic–nematic transition exhibits hysteresis. The isotropic fluid can be overcompressed and the nematic fluid can be overexpanded. This effect is more pronounced for prolate than for oblate ellipsoids. Hysteresis effects are clearly

Phase Diagram of a System of Hard Ellipsoids - Frenkel et al. (1984) - gave no more details than this either. Similarly, the 1985 paper by Frenkel et al. (Phase Diagram of Hard Ellipsoids of Revolution) referenced here also refers to the correlation function g^* , but gives no details on the method of calculation:

fluid was compressed. There are several ways to monitor the onset of nematic order; in the present simulation we monitored the behavior of the correlation function $g_2(r) \equiv \langle P_2(\mathbf{l}(0) \cdot \mathbf{l}(\mathbf{r})) \rangle$. In the isotropic phase $g_2(r)$ decays rapidly to zero while in the nematic phase $g_2(r)$ tends to $\langle P_2 \rangle^2$ as $r \rightarrow \infty$. Of course, as the systems studied in the simulations are finite we can only probe the behavior of $g_2(r)$ at distances smaller than half the diameter, D , of the periodic box. However, this is no real drawback as we observe that once nematic ordering takes place $g_2(r)$ reaches its limiting value within a few particle diameters. Hence the value of $g_2(r)$ at $r = D/2$ is a good measure for $\langle P_2 \rangle^2$.

Spherical Harmonics Method - 13/03

Frenkel describes the spherical harmonics approach in more detail, described in the meeting summary for 9/3. This uses the spherical addition theorem ([Spherical Harmonic Addition Theorem -- from Wolfram MathWorld](#)) as well, to ensure that $O(N^2)$ angles do not need to be calculated. However, this still seems to require calculation of $O(N^2)$ separation distances, which has the same computational cost - I have asked about this.

Orientational Order Parameter - C

05 March 2021
19:52

This details the computational implementation and results for a basic pair-wise orientational order parameter.

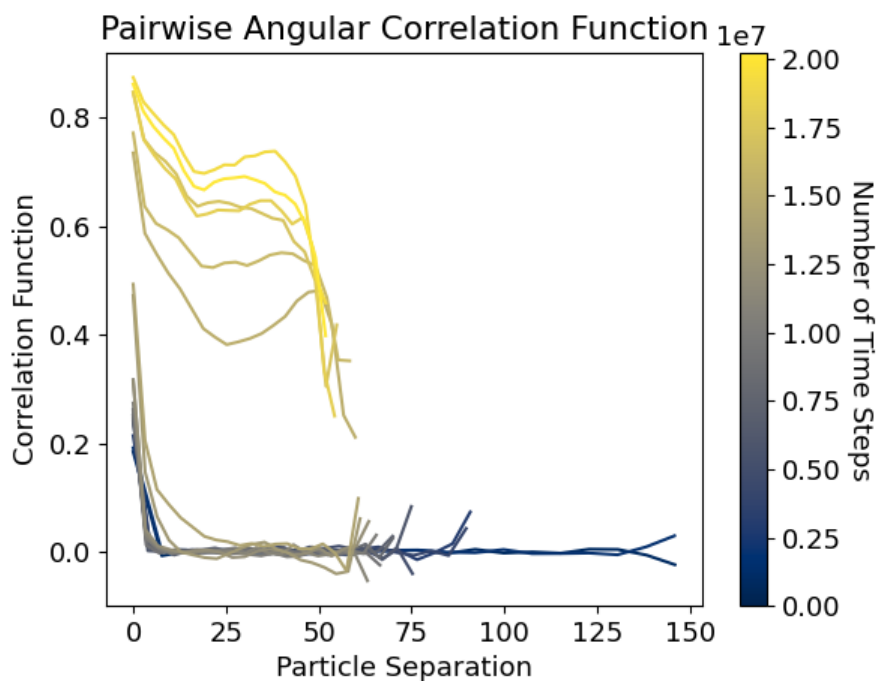
Method

Initially this is simply calculated by finding the maximum separation, and splitting the range of r values into N 'bins'. The average Legendre polynomial is calculated for all pairs which have a separation in the given bin, identifying using a numpy mask to reduce running time.

I have also implemented a method to cut-off points that have an insufficient sample size (i.e. are based on too few angles) This may reduce data at the extremes of the simulation region.

Results

Rigid Rods



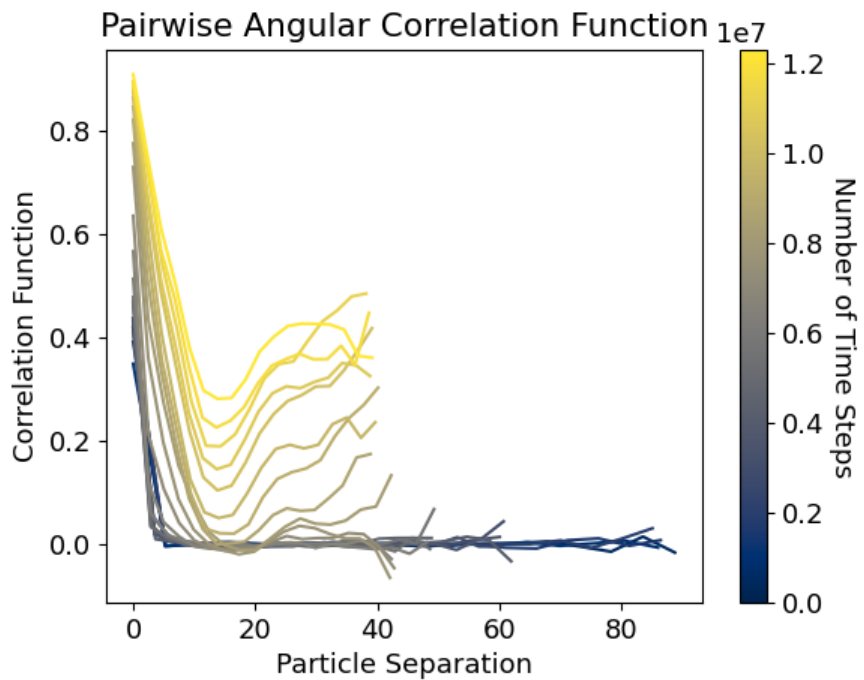
For the rigid_rods2 directory (where formation of a nematic phase across the span of the simulation region was observed), the orientational correlation function is depicted above. It is worth noting the discrete nature of the phase change observed here, where there is a clear difference between the curves for the isotropic and nematic phases. Note that no minimum sample size was used here, so there is noise in the data at the higher particle separations for each curve. (Naturally this maximal value changes over time as the box shrinks).

Fixed Angle

Note that this is based on an opening angle of 150 degrees, a separate simulation with a narrower opening angle of 120 deg showed no formation of long-range order.

Here there is a clear secondary maximum, although no clear separation where a new phase might be formed.

I was initially very excited by this secondary maxima, as it might suggest the presence of a new phase, however I have since realised that it likely an artifact of the periodic boundary conditions; so the correlation function increases nearer the boundary where the program actually overestimates the 'true' separation between the pair of particles.



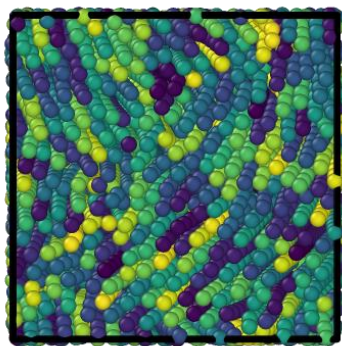
No such order is observed in the 'fixed rigidity' case.

Further Tests

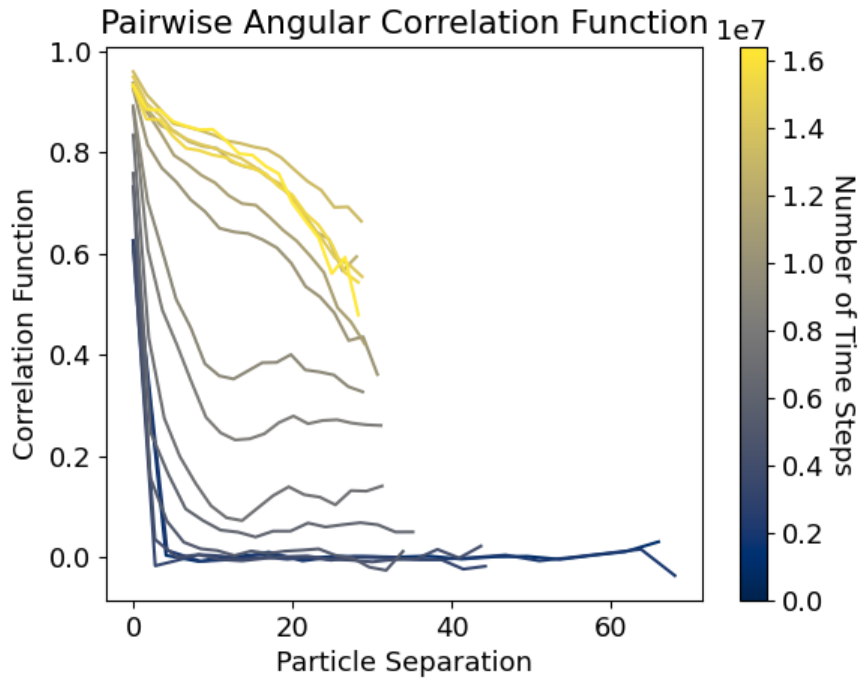
500 Particles

A test was implemented on a smaller system (with half as many particles), to test whether the minimum in correlation function is dependent on system size (which would confirm it is likely an effect of the box size/periodic boundary conditions, instead of being a true artifact of a new phase).

Clear orientational order is depicted here again, in the perspective view left. There is some suggestion of a 'swirled' structure in the left view-field, however with a repeating length scale greater than the size of the box, so it will not be represented by a secondary maximum in the pairwise correlation function.



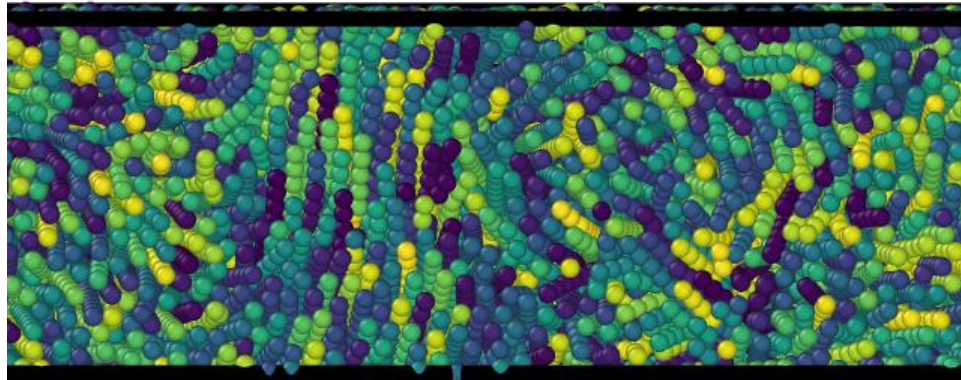
The director-based order parameter depicts a clear phase transition around a volume fraction of 0.3/0.4 (this could be narrowed down with further simulation). The pair-wise orientational order parameter is depicted below:



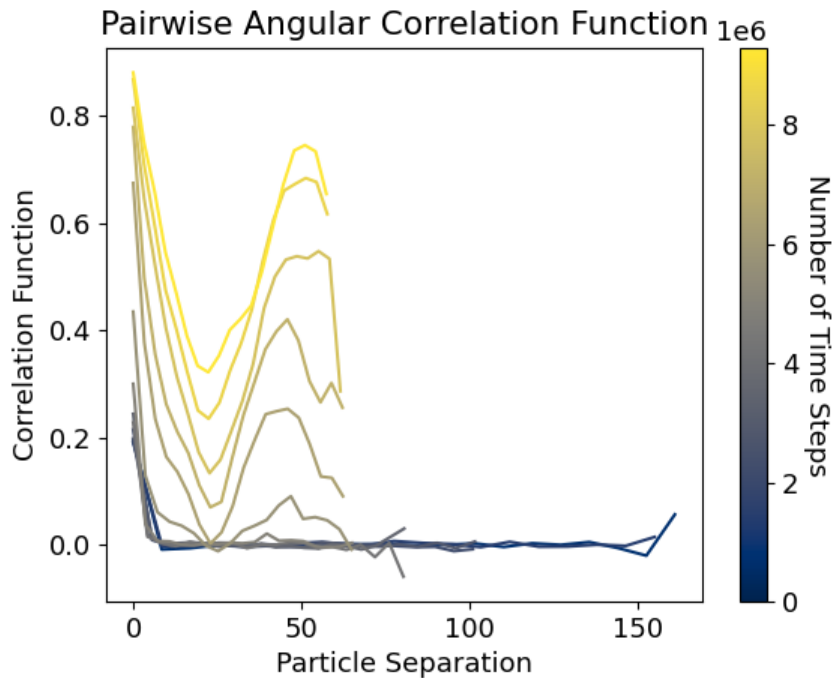
This is confusing, is there a second transition where this intermediary maximum disappears? I think this will be best resolved by accounting for 'shadow' reflected particles in the distance calculation.

Elongated Simulation Region

Again an ordered structure is observed in the perspective view (left). There is potentially a periodic structure visible in the orthonormal view-field below, however this may simply be the combination of multiple phases, as has been observed previously in the elongated simulation regions.



Again, there is sufficient evidence for a nematic phase in the director-based order parameter. As in the above case, this takes longer to form than in the shorter rigid-rod case; it may be worth running one of these simulations over longer equilibration times to ensure the phase transition occurs completely at a single volume fraction. The orientational correlation function repeats the previous secondary maximum observed, with some suggestion of a secondary decay! It might just be toying with me at this point; the only way to resolve this is clearly to improve my measurement of particle separation to include shadows, as previously mentioned.



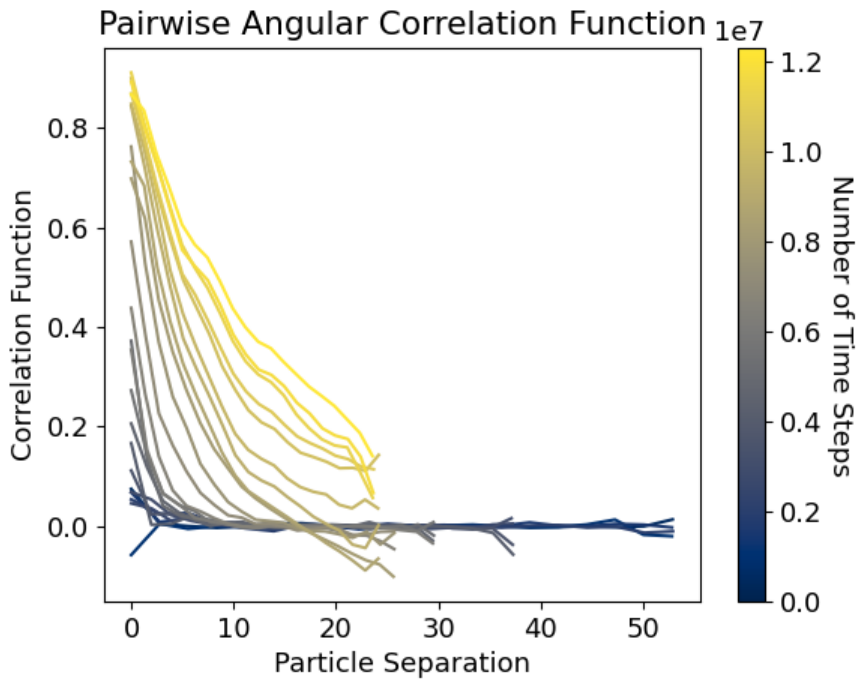
Accounting for Particle Ghosts

It can be shown simply in one dimension that, if the separation between two particles $|x_2 - x_1| > \frac{L}{2}$, then the distance to the nearest ghosts must be used instead, which is given by $\Delta x = L - |x_2 - x_1|$.

For multiple dimensions, the smallest total separation between particles may be measured by minimising the separation in each dimension separately, and applying the analysis above.

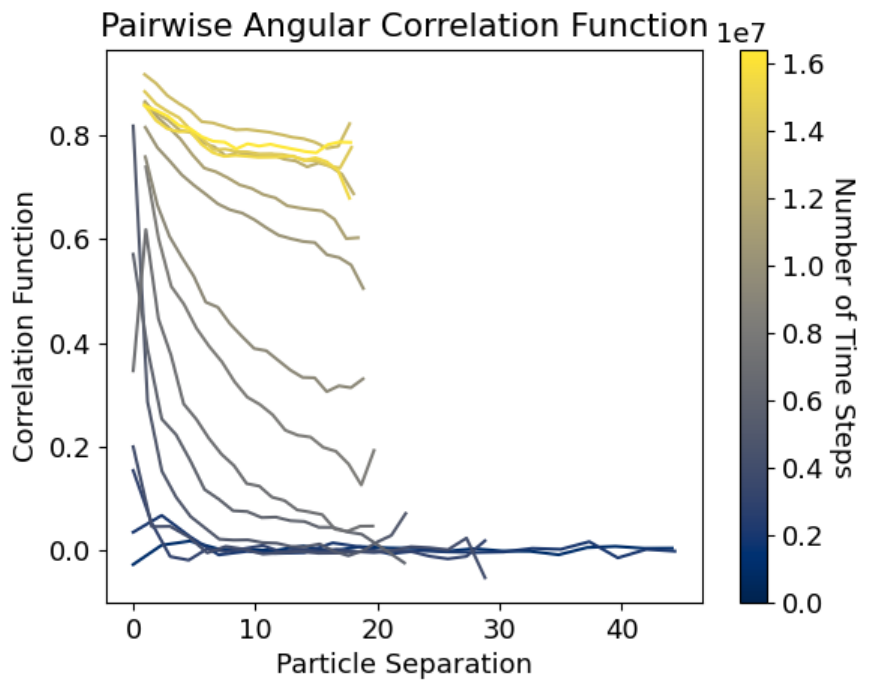
Fixed Angle

This does indeed remove the secondary maxima previously observed in this case, as depicted below:

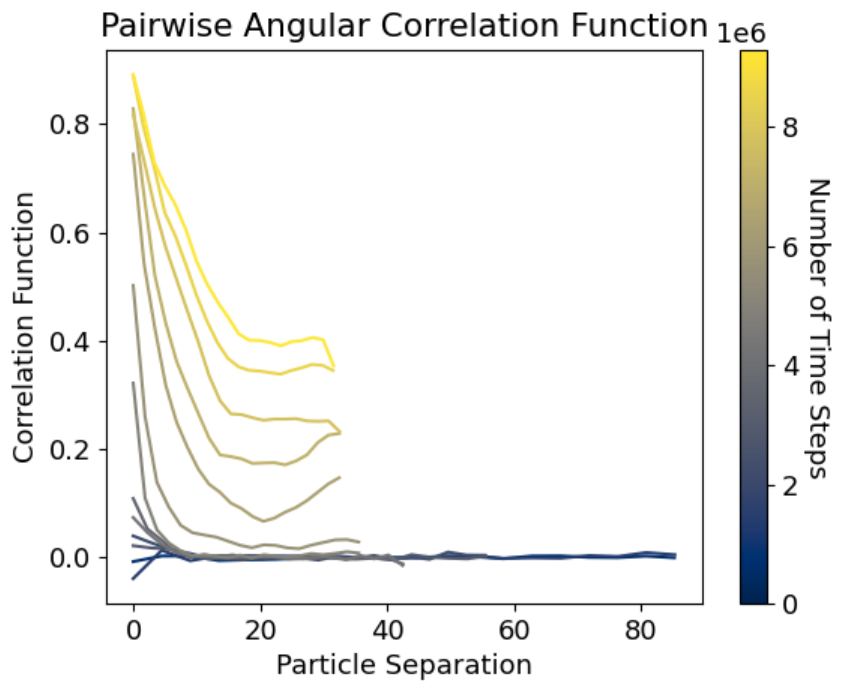


Regardless, there is still clear evidence for long-ranged order. This is accentuated in the supplementary cases of the oblong region and 500 particles, as shown below: (***particularly well in elongated simulation region***)

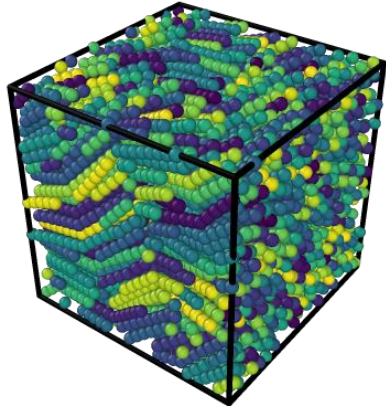
500 Particles



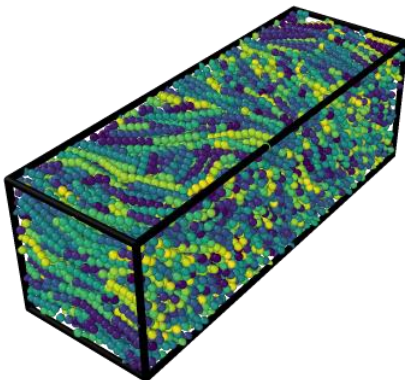
Oblong Region



We simply find the angle between the directors (given by the long axis) of each pair of particles. Then $g(r)$ is given by the mean Legendre polynomial for all pairs of particles separated by r , which in reality is found by averaging over all r' which satisfy $r - \delta r < r' < r + \delta r$.



Perspective view



Perspective

Altered Correlation Functions

13 March 2021

13:32

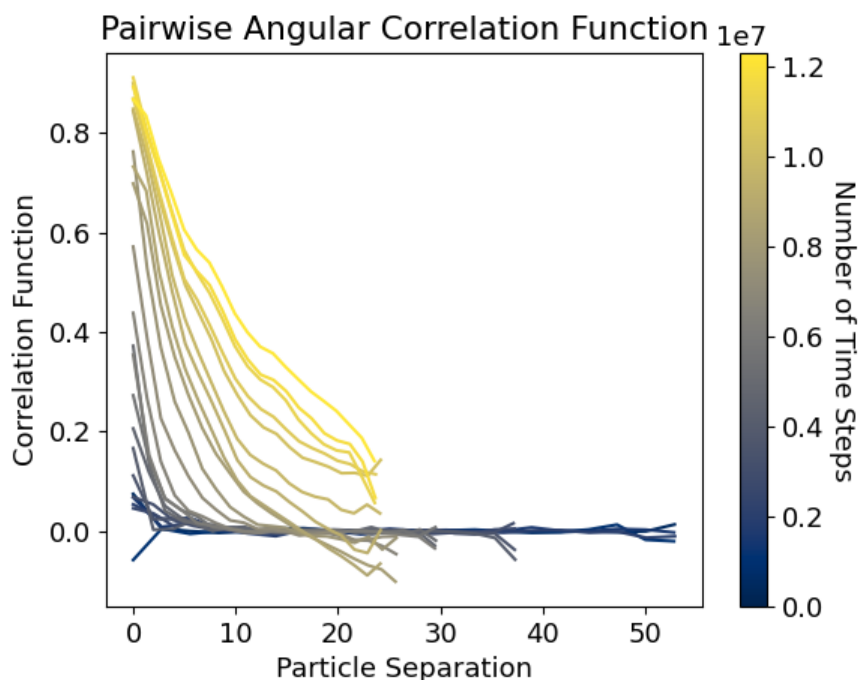
The previous logs detail the implementation and use of the pair-wise orientational correlation function. Here, we consider a few alternative implementations/approaches here that may better represent the system.

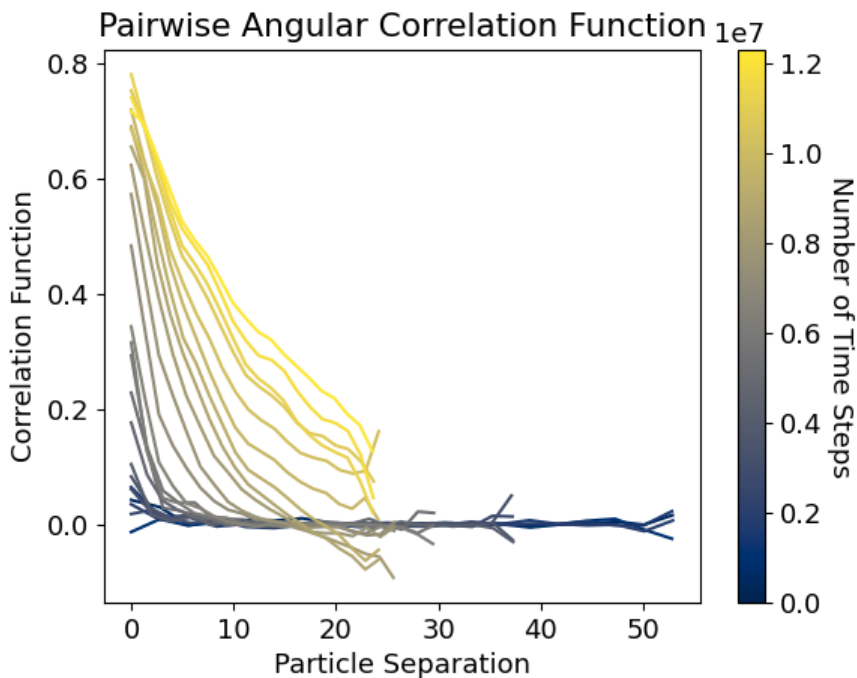
The problem with the previous approach is that it assumes an axially symmetric molecule, and considers the correlation of the molecule wise director (i.e. the vector between the two end atoms in the molecule) across space, or in a pair-wise context. These don't fully describe the system, and in particular likely won't be able to identify a 'zig-zag' system (where the orientation of the kink varies but the overall molecule director is uniform).

Single-Arm Correlation Functions

To avoid some of the issues above, we define the director along one of the 'arms' - (rigid halves) of the molecule. This should be able to resolve any chevron patterning, however we run into confusion of what arm to choose! Initially we choose this arbitrarily (each molecule has numbered atoms, and the director is placed along the half of the molecule with lower atom numbers). However this is unsatisfactory as molecules are placed in the simulation region randomly, so this choice has no physical meaning, and means directors may be anti-aligned. It may be better to ensure they all lie on rods facing an arbitrary direction (ie increasing x) through conditional logic, however this has not yet been implemented (and indeed it may be simpler to use the approaches below instead).

In the initial implementation , we observe no significant change in the pair-wise correlation function:
(Above: Original Version, with director given by displacement between end atoms of molecule.
Below: Altered Version, with director given by a (randomly chosen) arm of the molecule.)





Other Choices of Director

Finally, Daan suggested two new ways to characterise the herringbone structure. Firstly, consider correlation between the normal vector to the plane of each molecule. This should be expressed best in the second order correlation function g_2 . Additionally, take the vector along the bisector of each molecule, and calculate g_1 . I suspect this last method may be successful in giving an oscillating pattern for the zigzag phase, so would be very interested to see what it turns out.

I have therefore evaluated the orientational correlation function for four different methods of calculating the director:

- 'molecule' calculates director between ends of the molecule
- 'arm' calculates director along first arm of molecule
- 'bisector' gives the director along the bisector of the join angle
- 'normal' gives the bisector out of the plane of the molecule

These were initially applied to the `fixed_angle` directory, which did not provide conclusive results (having a decay in all cases with no subsidiary maxima or oscillating components). The chevron phase doesn't seem to be being detected, so I will consider alternative methods here, and review the previous literature.

I then went on to apply it to the simulation results for the elongated simulation region, which provide a longer lengthscale (and potentially a 'swirled' phase pattern.) However the same trends were observed, with a much faster decay (and smaller long-lengthscale order) than the 'traditional' methods I have been using.

First Order Correlation Function

Daan specifically suggested the first order correlation function (i.e. the expected value of the first order Legendre Polynomial rather than the second order polynomial that has been traditionally used up to this point. No correlation is observed over long length scale.

Biaxial Phase Search

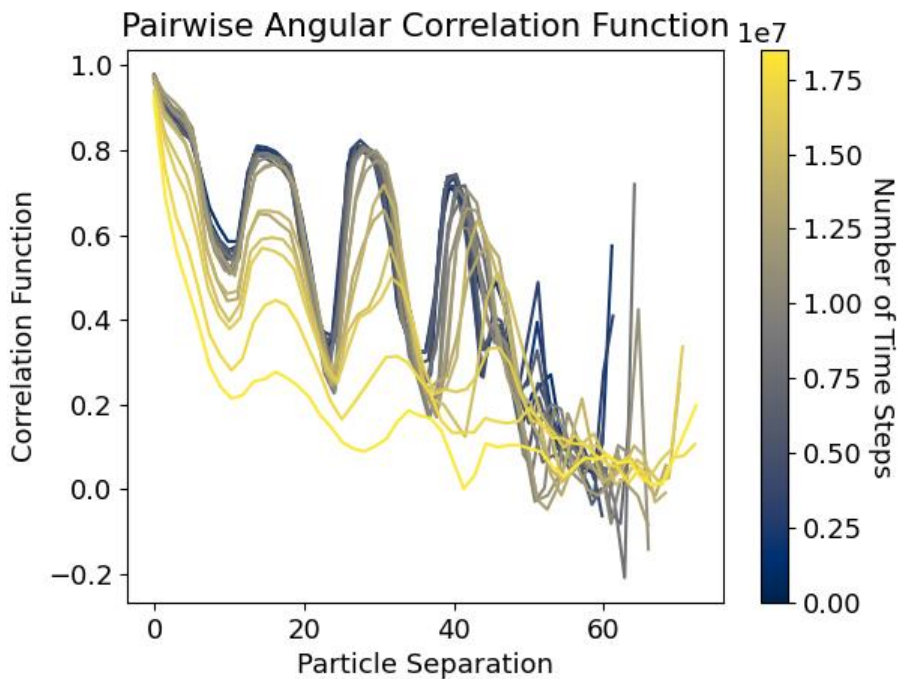
15 March 2021

00:16

This is based on the idea that it might be possible for our nunchuck systems to form a biaxial nematic phase (a phase for highly isotropic particles with three different lengthscales for length, width and height, where the vectors along both long lengthscales are well aligned).

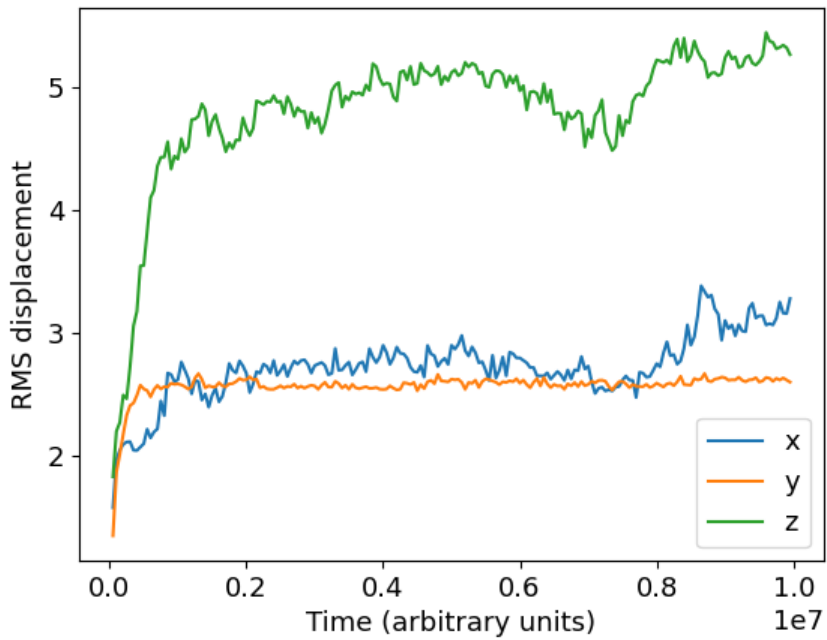
For a particle with dimensions a,b,c ($a>b>c$), we find that the biaxial phase is favoured when $b \sim \sqrt{ac}$, which occurs for the nunchuck particles 15 atoms long at an opening angle of 120°.

We ran a simulation of these (with slow expansion to focus on the smectic phase) from a crystalline state, and observed the following pair wise correlation function:

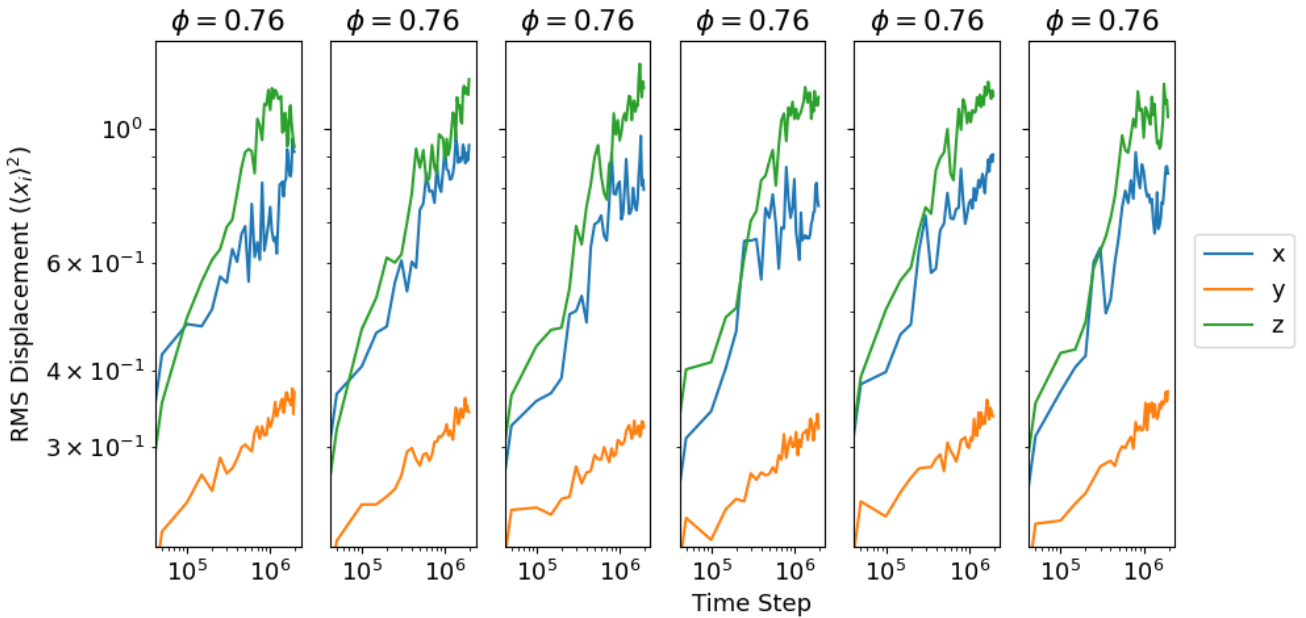


Initially I believed this could correspond to periodic order within the sample, however this was not obvious from the images. I now believe this is actually a interesting and little studied flaw in this method; peaks correspond to smectic layers, while the troughs correspond to a very small (order of 1) number of particles that have become misaligned with the layers. Hence this is an artifact of this sampling method, which doesn't account for/display the number of particle pairs in each radius bin/at each separation, meaning that it may be disproportionately affected by very small numbers of particles, as the majority of particles are approximately an integer number of particle lengths away (centre-to-centre distance) in the smectic phase.

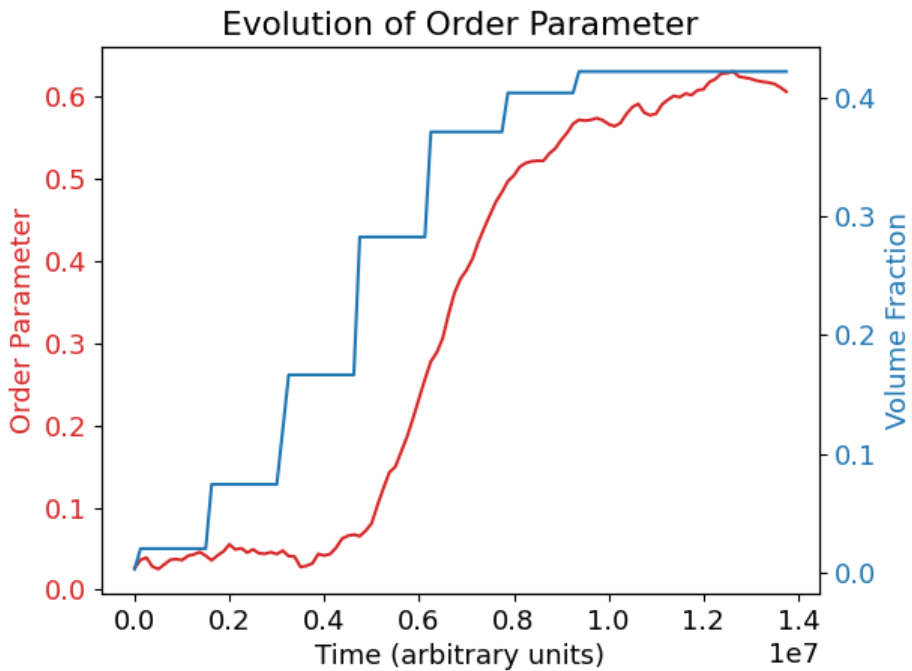
I was also aware that the smectic phase would be stabilised if the simulation region was approximately an integer number of particle lengths long, and so ran subsequent simulations with a fixed aspect ratio mimicking this. This displayed a remarkably stable smectic phase, as expected. We also observed some anisotropy in the rms displacement (ie directional diffusion) coefficients over the timespan of the simulation:



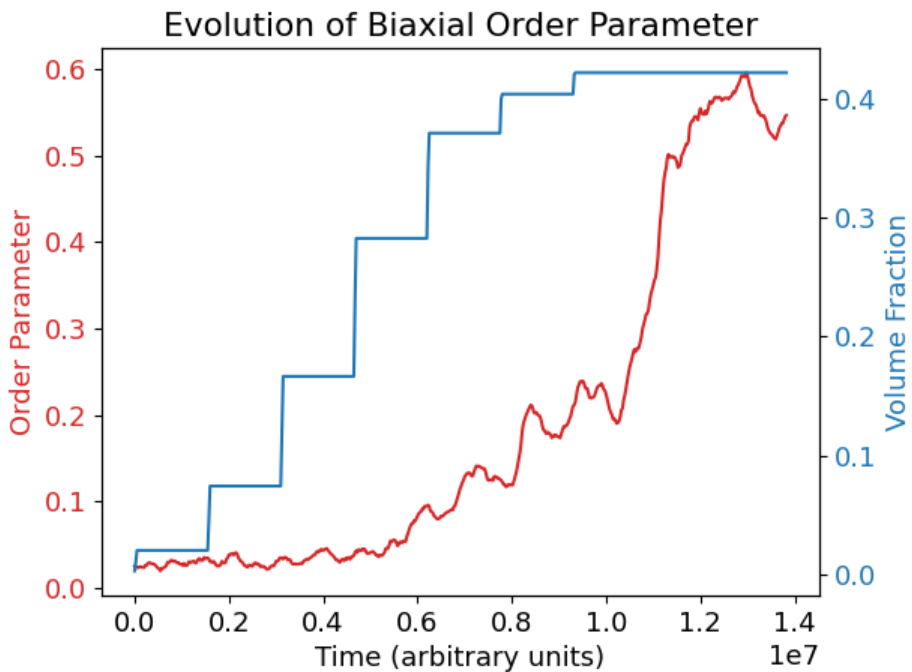
The smectic layers are oriented in the x-z planes, and so anisotropy in the y axis is expected for the smectic phase. However, anisotropy within the x,z plane suggests a degree of biaxiality to the simulation, otherwise these components would be expected to be equal (as observed in the rigid rods case). Six simulations at this volume fraction compound evidence for a slight anisotropy between these axes, with consistently high mobility in the z direction in this case:



Further simulation revealed this biaxiality may even be detected in contracting simulations from an initially dilute system. Here we observe the nematic order parameter for the particle director along the molecular axis (a vector connecting the ends of the particle):



In addition to this, we notice a subsequent formation of order for particle directors oriented along the bisector of the molecule (ie perpendicular to the molecular axis) below. This suggests biaxial order, which is not observed in nunchucks with wider opening angles (and certainly not in the rigid rod simulations).



Dynamics - Diffusion Coefficient

20 March 2021

13:00

While some research of the static phase behaviour of this system has already been conducted, very little is known about the dynamics of the system. There are many interesting questions here, particularly with regards to the viscosity parameters and shear wave behaviour in the system, or even elastic coefficients of the crystalline phase. However, to start with, the diffusion constants in the three cartesian directions (particularly in the crystalline phase) would be particularly interesting to investigate!

Theory

The diffusion coefficient t is given by:

$$\langle (x(t) - x_0)^2 \rangle = 2NDt, \text{ for N dimensions and at time t.}$$

This is measured in two ways. Firstly we iterate over all time steps, considering the rms displacement over the time period from the start of the simulation to that point. However this covers multiple different conditions and potentially phases.

Therefore we also take a single measurement of the rms displacement (averaged over all particles) between the configurations at the start and the end of each equilibration run, and divide by six times the equilibration time to estimate the diffusion coefficient. This measures D for that particular volume fraction, or phase.

These values in themselves are fairly meaningless however, it would be more interesting to find the directional diffusion coefficients.

These are affected by the size of the box; really need to account for the periodic boundary conditions here!

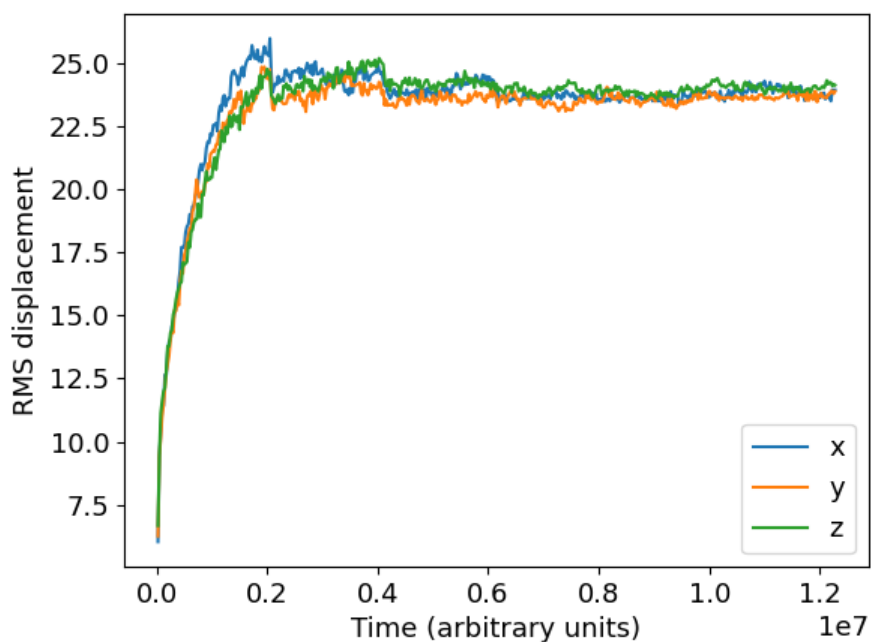
Periodic Boundary Conditions

These complicate matters, by making it harder to track the distance travelled. We will log each time a particle crosses a boundary (separately for x, y and z), and add/subtract the appropriate dimension for the box length to that component of the final position, before determining the absolute value of the displacement from the initial position.

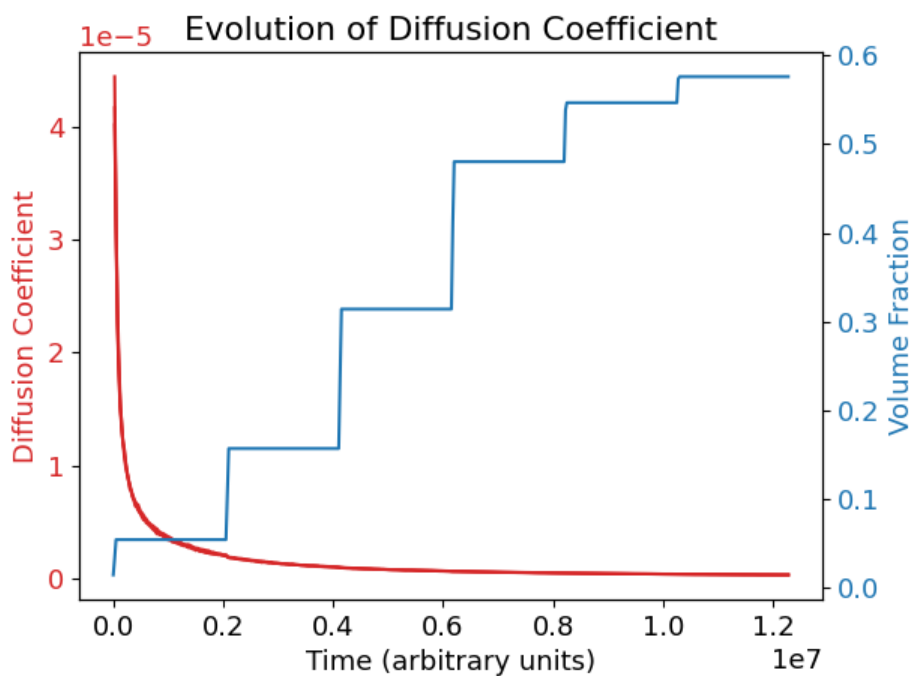
This has not yet been implemented however, due to the complexity of implementing it over multiple timescales. This may account for the decay of the diffusion coefficient over large timescales, as the displacement of particles that have crossed the periodic boundaries are underestimated.

Results

Initially I tracked the rms displacement over time. I was able to separate this into three components, and , as shown in plots of the form below. These plots were taken for an isotropic system, but similar plots have been recorded for all systems of interest; they are not reproduced below for brevity!

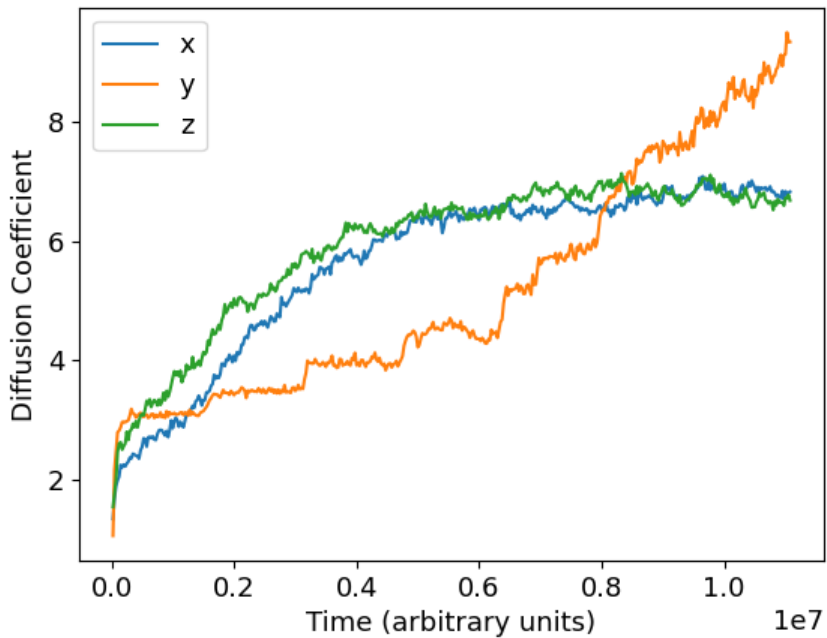


If we divide the rms displacement by the time measured, we may obtain the diffusion coefficient on that particular timescale. I have obtained that on across all timescales here, and plotted it in comparison with the order parameter. As expected the diffusion coefficient decays over time.



Crystalline Expansion

NB this graph is incorrectly labelled; should have rms displacement on y axis. This clearly shows anisotropic effects, however we would not necessarily expect the rms displacement to plateau at long times, but rather be linear (so diffusion constant is constant). This plateau is likely an effect of the periodic BC, which will be corrected for in the next implementation.



Evaluation

The discrete changes observed in the rms displacement (particularly in the isotropic case) correspond to expansion phases, where the volume of the system changes discretely. This means we are sampling over different phases (when considering the displacement between initial position before the volume change and final position after the volume change) and so this approach may not be particularly useful. I therefore describe a new approach on the next page.

Dynamics - Sampling Time

25 March 2021

11:57

Sampling Time

While we may sample diffusion over a range of different time scales, I am focusing on longer timescale changes (to ensure diffusive motion rather than ballistic motion is being sampled).

More importantly, I have implemented methods to sample the diffusion coefficient in a particular phase (ie when the volume is held constant, so that we do not include displacement over the mixing phases, as was used previously). It is worth noting that the current approach considers the entirety of the equilibration phase, and so assumes that this is long in duration in comparison to the timescale required to form any new phases. This seems primarily validated by observations of the timescale required for the pressure to settle, but I must be aware of this.

Periodic Boundary Conditions

This approach has also made it easier to track periodic boundary crossing, as we only need to track one set of crossings (over one timescale) rather than tracking them over multiple timescales.

At each timestep, we test whether the displacement of each particle (in each cartesian axis) is greater than half of the corresponding box dimension. If so, it is most likely that the particle has

crossed over the boundary. (In reality the displacement between each step is much smaller than this value, typically over a few % of the corresponding box dimension; this is verified by ensuring the results don't vary under small changes in this cut-off).

We keep track of these crossings using an 'extra_displacement' vector; this is the difference between the particles apparent position under the periodic boundary conditions and the particles true position. For example, if the particle crosses from the positive to negative x boundary (which are set at +/- 50 for this example), its apparent position is $x=-49$ whereas its true position (for calculation of the rms displacement) is $x=51$. Therefore the corresponding value in the extra_displacement array is +100 (the box dimension). It is worth noting explicitly that this value would be negative had the crossing occurred in the opposite direction. This may be added to the final apparent displacement to give the final true displacement.

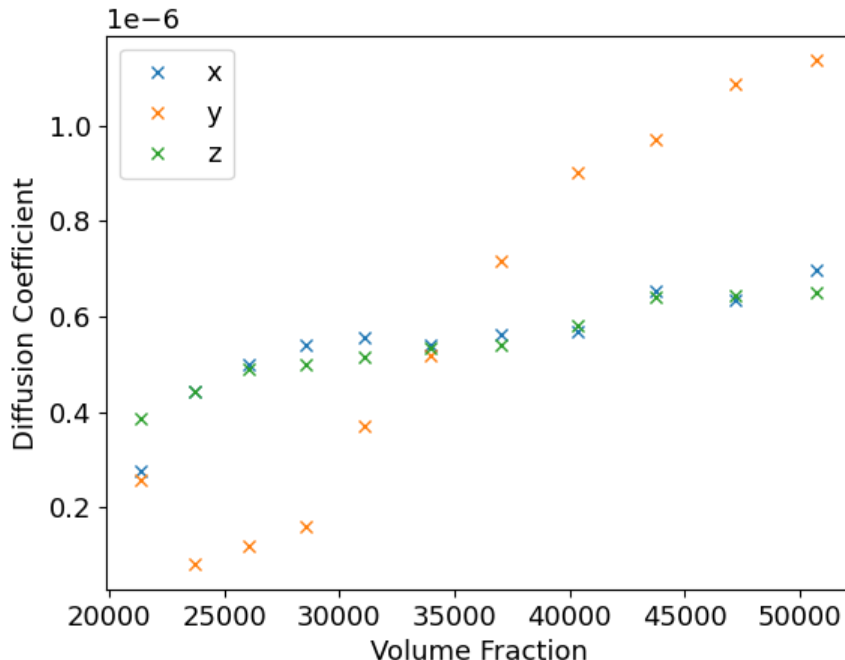
By only considering one timescale, we only need to keep track of one such extra_displacement array, and can also avoid recording the time of each boundary crossing, reducing the memory requirements significantly, and also reducing computational complexity significantly, as multiple crossing in opposite directions automatically cancel out without explicit consideration.

This has been tested thoroughly through manual particle tracking to ensure the correct values are obtained (on small particle number systems), and also on constant drift systems (that undergo multiple crossings in the same direction, which is also accounted for correctly here).

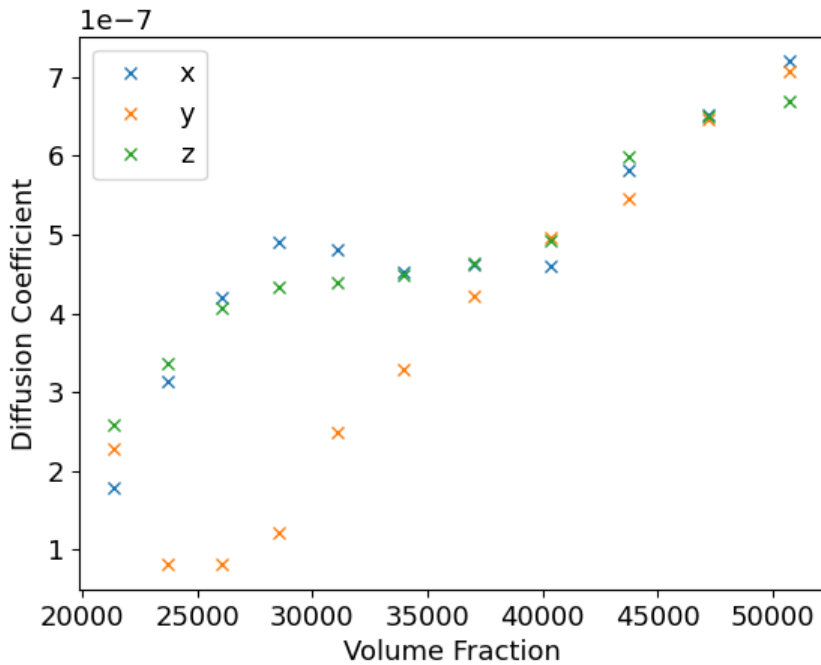
Results

NB These graphs are mislabelled with 'volume fraction' instead of 'volume' on the x axis - volume is what is plotted here.

Before implementation of BC (with the time sampling approach):



After implementation of BC (with the time sampling approach):



As expected here, the three lines join together in the high volume limit; as the phase is isotropic and so there is no difference between each direction. Below this, the diffusivity in the y direction is much lower, as might be expected for a smectic phase. Meanwhile, the data for the x and z axis are in good agreement, as would be expected for such a system with no difference between these axis. The plateau in x,z directions (possibly during the smectic->nematic phase transition) has not been explained.

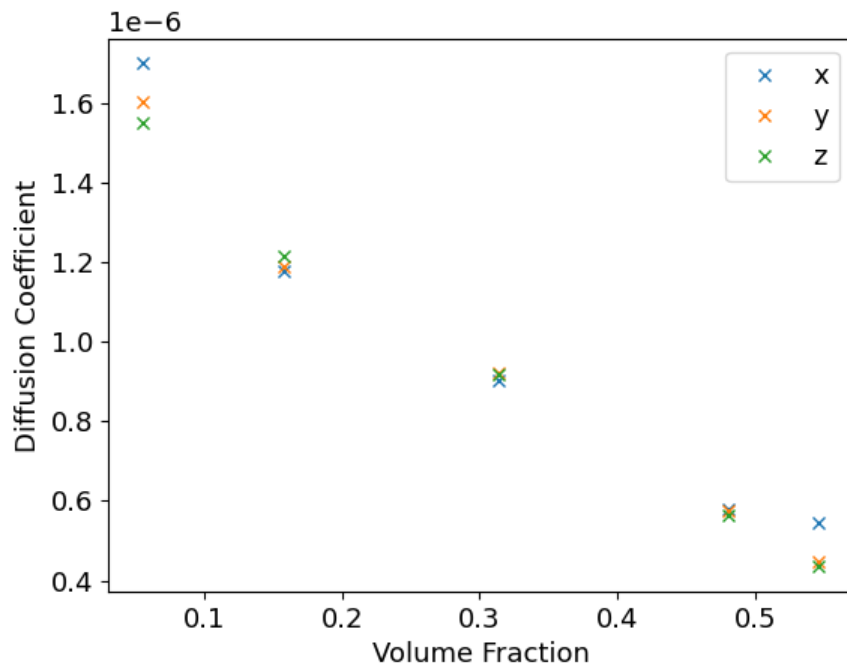
Dynamics - Further Analysis

29 March 2021

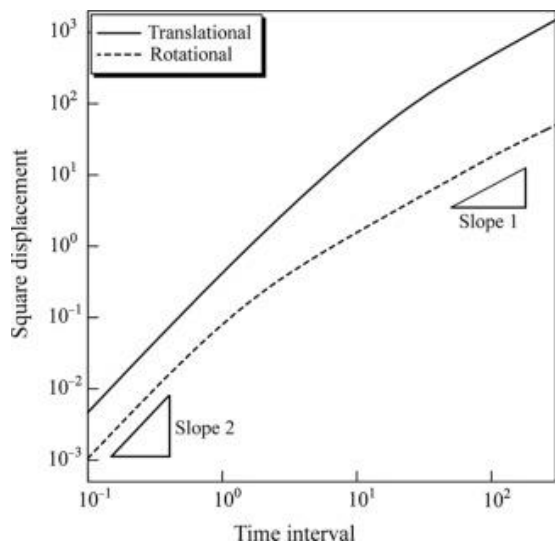
11:58

Particle Diffusion

Here we plot the diffusion coefficient against volume fraction for the isotropic case; there seems to be a strong linear trend here! - *add data for other cases*

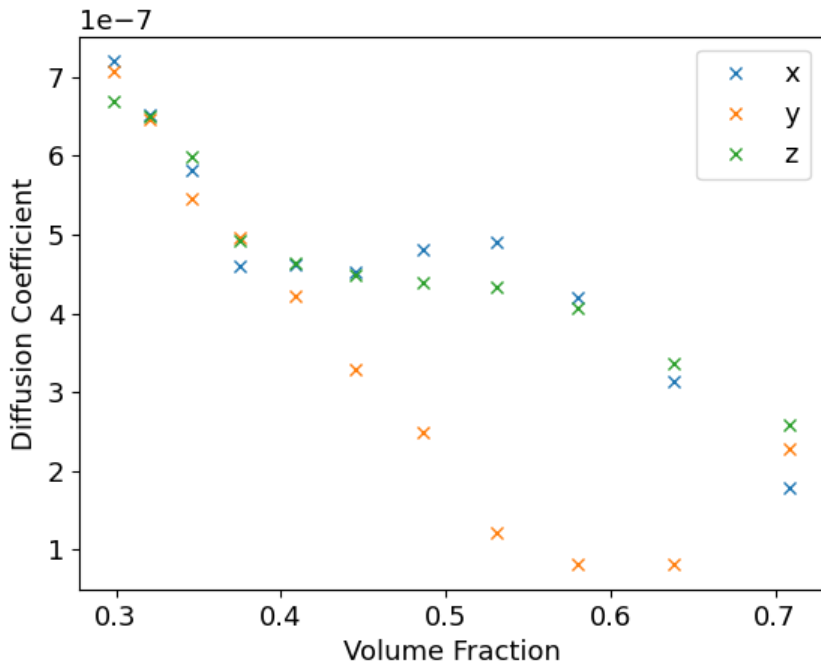


It would be extremely useful to plot the mean squared displacement over time, on a log-log plot; this describes the nature of the motion extremely well (as below): -*give results for isotropic, crystalline and rigid rod cases here*

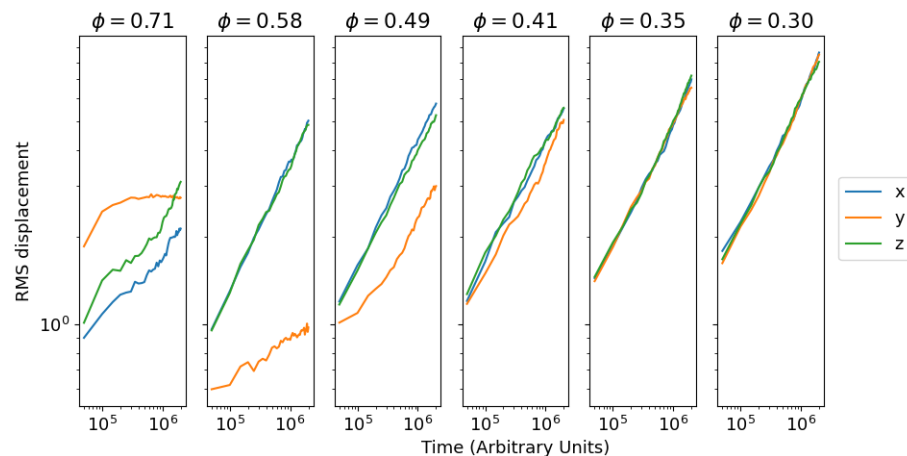


Crystalline (Full) Transition:

The diffusion coefficient varies over volume fraction as below:



We may also consider the rms displacement over time, for equilibration runs at different volume fractions:



Fitting a linear best fit line in log space (to the x coordinate here):

For vol frac = 0.71, slope = 0.23

For vol frac = 0.58, slope = 0.44

For vol frac = 0.49, slope = 0.43

For vol frac = 0.41, slope = 0.41

For vol frac = 0.35, slope = 0.43

For vol frac = 0.30, slope = 0.43

A similar trend is observed for the isotropic case, suggesting a tendency towards a value of 0.5. This is expected, as the squared displacement should be linear with time (so rms displacement goes as $\text{sqrt}(t)$, and has a slope of 0.5 in logspace). The behaviour is subdiffusive in the concentrated limit.

For rigid rods, we obtain values much closer to the ideal 0.5 value (in range 0.47-0.50 for crystalline phase).

For vol frac = 0.6378, slope = 0.4732

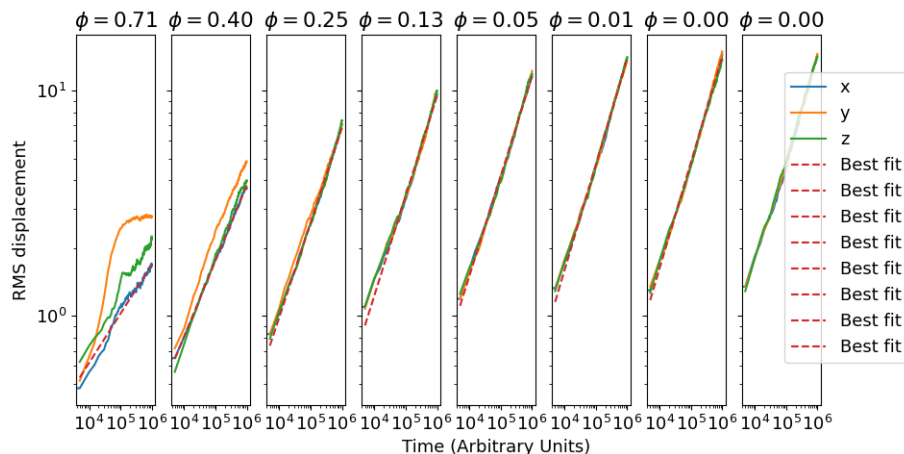
For vol frac = 0.5429, slope = 0.4977

For vol frac = 0.4676, slope = 0.4831

For vol frac = 0.4080, slope = 0.5099

For vol frac = 0.3220, slope = 0.4856

Dilute Limit



Smectic phase in first image (better observed in other plots).

Nematic phase decays in second plot (nematic phase has y line above others, as there is free particle movement along the axis of the particle, which is well aligned with the y axis from the initial smectic phase).

Isotropic phase after this, with no differences between the three directions.

Erika has suggested investigating the dilute and semidilute diffusion fractions.

These are separated by whether the overlap of effective sphere around each particle overlaps or not. This is estimated to happen when the volume fraction is greater than the volume fraction of a particle in its sphere:

$$\text{Semi-dilute lower limit: } \frac{\text{mol length} \times \pi \times r^2}{\frac{4}{3} \pi \times (\text{mol length}/2)^3} = \frac{6 \times 0.56^2}{10^2} = 0.0189$$

Theoretical work from her current student David predict's the following results:

Dilute: Should be $1+2.5*\text{vol_frac}$

Semidilute: Strong reduction in diffusion coefficient

For nunchucks (*dilute case, sampled over 50 rods, 1.5 mill time steps*)

Taking only the x average:

For vol frac = 0.290692, slope = 0.4510

For vol frac = 0.069905, slope = 0.3932

For vol frac = 0.019638, slope = 0.5196

For vol frac = 0.003800, slope = 0.3863

For vol frac = 0.000894, slope = 0.4625

For vol frac = 0.000038, slope = 0.5068

Taking the average across three coordinates

For vol frac = 0.290692, slope = 0.3903 -*Ignore this; still anisotropic*

For vol frac = 0.069905, slope = 0.4185

For vol frac = 0.019638, slope = 0.4971

For vol frac = 0.003800, slope = 0.4907

For vol frac = 0.000894, slope = 0.4549

For vol frac = 0.000038, slope = 0.4895

For rigid rods (*otherwise same as above*)

For vol frac = 0.281068, slope = 0.4269, error = 0.002134

For vol frac = 0.088465, slope = 0.5135, error = 0.003381

For vol frac = 0.022089, slope = 0.5165, error = 0.002598

For vol frac = 0.004652, slope = 0.4663, error = 0.002446

For vol frac = 0.001103, slope = 0.5113, error = 0.003351

For vol frac = 0.000079, slope = 0.5014, error = 0.002162

The variation in these values is much greater than in the larger samples above; I think it worth replicating this analysis for larger systems.

Dynamics - David's Prediction

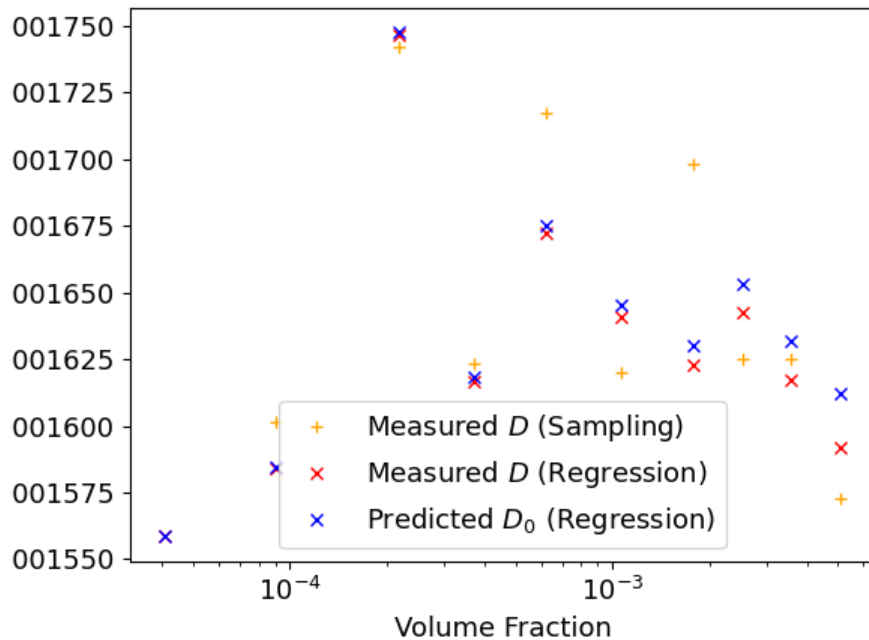
07 May 2021

10:20

David has predicted that $D = D_0(1 + 2.5\phi + \mathcal{O}(\phi^2))$

We therefore calculated D_0 from each run, in hope it would be constant. This is plotted below in blue, while D is given in red. This data is based on regression over the whole period, whereas the yellow sampling points are from an alternative method where only the particle displacement from the start to the end of the simulation is used.

This is a repeat of previous analysis, but over longer sampling periods with 500 particles (running for about 12 hours), to identify whether we were able to obtain the statistics required to test this hypothesis (put forward by David).



The difference between the red and blue points shows the effect of David's predictions on finding D_0 by including the volume fraction correction factor. However this difference is much less than the overall spread observed, and so we have insufficient statistics to be able to give concrete identification of any trends there.

Daily Logs

Chapter Introduction

30 October 2020

18:47

At the start of the project, I made the choice to document the major milestones and setbacks in this project in thematic order, as I believed this would be more useful for further reference, and so this is given in the Project Records.

This chapter instead provides a chronological account of the research process. It gives an outline of the day-to-day progress of this project, in a way that matches the git log of the associated repository. It should be noted that this section is not the sole record of any content essential to the understanding the overall development of the ideas in this project, and indeed there will be a large degree of overlap with other sections of the lab-book.

Rather, this is to outline the daily time and effort put into the project, the more mundane challenges I faced and how these were also resolved. This includes issues accessing data, plotting data or simply writing functioning code. After new year, I decided to only document progress in the coding; while a significant proportion of my time is being spent in literature reviews and reading around the previous research in this area, it seems silly to document this all twice!

N.B Some important points/milestones are highlighted **in bold**.

October

16 October 2020

21:14

5th Oct - Endeavoured to conduct introductory research/reading into the project aims in preparation for a expression of interest meeting (following the listing of the project on TiS).

Compiled notes on liquid crystal phase behaviour, particularly the definitions of nematic and smectic phases (mentioned in the project abstract); these had previously been covered in 1A Materials Science, but was useful revision.

6th Oct –Further preparatory work for the initial interest meeting, looking at OxDNA. Having discussed potential PhDs with academics in Oxford working on this technique, it was not new to me, but still useful to recap the fundamentals of it (and introduce myself to LAMMPS).

7th Oct - Initial meeting with Jiaming to discuss the scope of the project. This (as with all future meetings) will be recorded in more detail in the Meetings Summary chapter, but this gave a summary of the expectations of the project.

There is less OxDNA work than I had anticipated, with the bulk of the initial work in LAMMPS, however apparently there is the possibility to return to OxDNA later on (I am initially implementing a potential derived from OxDNA by Jiaming into LAMMPS).

10th Oct - Further reading into liquid crystals, supplementing previous knowledge. Specific coverage of the distinction between thermotropic and lyotropic liquid crystals (based on the driving force behind the phase transitions they undergo)

13th Oct - Met with Erika to indicate willingness to accept the project, and outline aims for the project - detailed in the initial steps page within the project records.

The ultimate aim of the project is to detect the so-called 'swirl' phase observed by Jiaming last summer, and test whether this is observed in semi-flexible nunchucks as well as fully flexible molecules.

However, will initially start on 2D hard spheres and rods to build up knowledge of the techniques involved, and ideas on how to quantify phase transitions.

Also documented the features and capabilities of LAMMPS, to understand how this fits into the aims we want to achieve in this project, and whether it is the suitable tool to use. It seems well designed and has capabilities beyond that which will be required here.

14th Oct - Start of literature review - slow progress initially here as a lot of the concepts are unfamiliar and require tangential reading/research. Focused on the Xing 2009 Y-shaped nanoparticles paper, as this is from the Eiser group and uses some of the same techniques I expect to use.

Particularly relevant is the use of complementary simulation techniques to consider different levels of coarse-graining, and a comparison of the different software packages available.

15th Oct - Reviewed Gleeson 2016 Nunchucks paper - considers a very similar system to the one we are considering. However the molecules are likely too large and results inconclusive. The addition of sticky patches on the molecules may mean they are finding what they want to find, and there is little evidence this mechanical model represents reality accurately.

16th Oct - Start setting up virtual lab-book, and filling out sections/ considering how I wish to plan the project. Will record work chronologically, as requested by the dept, but also thematically, as I believe this may be easier to keep track of my ideas.

18th Oct - Document the basic methods and functionality of LAMMPS, including how to load and run scripts.

Install LAMMPS software (twice!), and document this process. I installed the lmp_serial executable as recommended for windows, and the parallel processing is not stable on windows operating systems.

20th Oct - Following recommendation from Jiaming, I also installed Ovito, as a useful visualisation package that works natively with the output files of LAMMPS. This visualisation would be tricky to do manually through python and so I am glad this step is not necessary.

Also met with Erika to discuss aims for the project, and specifically how to test the stability of the system by verifying energy conservation. This can be done directly in LAMMPS by summing the potential and kinetic components at each step.

We also discussed how to determine phase transitions; a likely here would be a discontinuity in pressure of density. However it is more formally described by considering a change in the average director - a concept I needed to revise from IA materials again.

23rd Oct - Initial testing of LAMMPS, using built in example of 'colloids' system. The results can be visualised in Ovito, and the testing is documented within the LAMMPS chapter.

25th Oct - Modified the colloids example to test a hard spheres system. This was difficult, and took most of the day, as the text based language of LAMMPS has many unique commands, all of which I had to look up to determine the meaning of. This is a steep learning curve, as it is very specialised, and unlike other programming languages I have come across before, however it gave me a much better understanding of how LAMMPS functions.

This also seemed like a good point (now I was writing up my own code) to **set up a git repo for this project**, to allow version control (and simply have an online backup of my work).

27th Oct - Meet again with Erika to discuss the motivations behind this project (and field of research in general). This includes display technology, but also DNA origami and other biophysical self-assembly problems. She also gave a number of suggestions of different works of literature to review, which are detailed in the Meetings Summary chapter.

Went on to review the Fernandez 2020 Banana colloids papers - from one of Daan's former postdocs. This gives evidence of a 'splay-bend nematic' phase which seems visually similar to that observed by Jiaming, however the size of the particles used is much larger, and so may not be determined by thermodynamic principles.

Also outlines potential future applications in display technologies, due to having the advantageous property of faster switching speeds.

November

01 November 2020

15:30

2nd Nov - My main aim for today was to make use of the thermo data output from the Lammps simulation. This involved scraping the data from the Lammps output file into a numpy dataframe, while removing the (variable length) header. It took a while to find a method that worked consistently with different header sizes and output file formats, but I wanted to ensure this was forwards compatible, and continued to work even if I later needed to change the form of the output file.

3rd Nov - Previous simulation code from Jiaming implemented a shrinking simulation region, so I wanted to set up a 2D hard spheres system in a fixed simulation region ab initio; this required extensive use of the LAMMPS documentation to understand how to 'build' a simulation (something I am not familiar with from previous courses), but I have now built up.

This also required getting my head around fixes in LAMMPS, something which took much of the day and required detailed documentation in the LAMMPS chapter of the lab book. I have not covered Langevin thermostats etc before, but have been trying to draw analogies to the ensembles covered in Part II thermodynamics.

Met with Erika and Jiaming, mainly to discuss my research today in fixes, and also the choice of parameter values in LAMMPS. Jiaming has assured me that much of this is very arbitrary, indeed temperature is relative, and expressed by a relative value, with only relative changes being relevant.

Conversion to physical values may only be through experiment - i.e. matching values at a known phase transition. Variation in temperature parameters tends to have minimal effect on the simulation output.

4th Nov - Implemented the rigid rods demo today. Overall the code had become slightly confused, so cleaned up any extraneous variables, and went through documenting the example line by line, so I was clear on what each line did in this new language.

Also added automated running of the analysis code from the lammps executable, via linking it directly to the shell; handy for later analysis!

9th Nov - Focus on cleaning up git repo; ensuring cloud back ups of non code work (or large data files) separately (i.e. of the literature review) without that cluttering up the repo.

Read up on the theory behind the LJ potential, and particularly on the logic behind the cut-off version. Code suggested by Jiaming is inconsistent with LAMMPS safe practice here, so was updated to ensure cut-off implementation is stable.

13th Nov - Met with Jiaming and Erika to discuss the overall project direction, and greater specifics on the nunchucks system I will consider. It is likely I will consider two separate cases; one where the opening angle between the two arms of the nunchuck is fixed, and one where it is capped at a certain value (but free to vary below this).

This also clarified a number of important matters about the simulation size required etc; this has been a matter of trial and error for many years and so Daan's expertise here is invaluable! The details of these outcomes are detailed in the Meetings Summary chapter.

18th Nov - I am aware of python integration to LAMMPS (from having browsed the software website) but needed to look into this further. This will be particularly useful for me, as I have already written analysis code to plot thermodynamic outputs from simulations, and will likely use python to automatically generate specific input files in the future as well.

21th Nov - Researched the units system used in LAMMPS. I believe natural units (the default lj units option within LAMMPS) will be simplest to work with, but may give difficulties later on when converting to physical systems, and so this is worth investigating further. I documented this within the LAMMPS chapter of the lab book.

23rd Nov - Began to consider the phase behaviour of the rigid rods system. This was simple to implement manually, but ideally I need to be able to loop over various thermodynamic variables (most likely shrinking time) here to measure multiple points in the phase plot efficiently. While I would intuitively use a 'for loop' (or equivalent) for this, there is no direct equivalent in LAMMPS and so I have to consider an alternative approach more native to this software. I have not yet observed the formation of any order in this system.

24th Nov - Continuing and documenting work from yesterday. This involved recording phase plots at different temperatures, and fixing incompatibility errors in the nunchucks generation file. This seems to have incomplete documentation (and require modules that don't exist!) so I after much research today I will have to go back to Jiaming with my issues here.

Met with Erika and Jiaming to discuss the project plan submission, as well as expectations for work over the holiday (I am concerned that the combination of PhD applications, interview preparation

and major exam preparation may leave me unable to make significant progress here; however they have confirmed that this is not an issue! I also raised a concern that DNA is a chiral molecule (suggesting it may favour the formation of cholesteric phases which we do not account for in our analysis), however on the length scale of DNA fragments we are considering this effect is negligible and so unlikely to disrupt the nematic phase behaviour observed.

28th Nov - Started writing project plan. I have mainly left the literature review section blank for now, but focused on describing the system we are considering, and the phase behaviour we are looking for, as well as suggesting ways we may quantify this. I have also provided an outline for the whole report here.

29th Nov - Started collating papers for the initial literature review in the project plan, I have written very little of this section today, as it turned out that identifying the key papers was more time consuming than expected and I went down many dead ends! Having found a few key review articles on this (or related areas) greatly assisted this search, pointing me in the right direction to the papers I needed.

30th Nov - Considerable **work to describe phase changes through discontinuities in pressure**. This was based on a graph by Jiaming which shows a sigmoid change in the pressure of the system as the phase transition (isotropic -> nematic) occurred, however I have not yet been able to replicate this, or have any visual evidence a nematic phase is forming.

Also have completed and stored multiple data collection runs today, having generalised the phase plotting code to an arbitrary loop variable (instead of simply looping over different system temperatures). This will be particularly important for the rigid rods system, where we do not expect (or want to focus on) thermotropic phase transitions driven by a change in system temperature.

December

01 December 2020

10:00

1st Dec - Compiled literature and papers collected into a literature review for my initial report; a time consuming process but very satisfying in giving me a greater understanding of the origin of this field. An interesting diversity in the papers considered 'seminal' in this field - many recognise the theoretical contribution of Onsager for example but experimental credit seems to be spread between different groups, with differing opinions on the authors of the most significant contributions. I am concerned any view I take here will be personal, and influenced by the papers I have read, and so hope not to omit any well-deserving authors here.

2nd Dec - **Produced first draft of the project plan**, tying together all the work of the previous few days. It was my expectation that this would require redrafting, however Erika is very happy to sign off on it, and so I will submit this directly to the department.

Further discussion with Erika about requirements to restructure my simulation approach, I have not observed any nematic phase and this is likely due to insufficient running time. It would be more efficient to alternate compression and equilibrium phases, to measure different volume fractions while avoiding recompression. However this will require significant reworking of my code, and I have decided to start this in a new directory to preserve the previous method should it be required in the future.

Daan has also provided illuminating suggestions on the possibility of running such simulations 'in reverse' - i.e. starting from an ordered crystalline system and expanding the system. The primary goal of this is to ensure we observe the same phase transitions at the same volume fractions as in the shrinking method - any hysteresis here may suggest our system is not actually in equilibrium.

6th Dec - Literature review of papers suggested by Daan in the previous meeting; particularly his papers on the simulation of liquid crystals and hard core models. While much of this used Monte Carlo approaches instead of Molecular dynamics simulations, much of the work on phase categorisation in particular is highly relevant. There are also many approaches regarding the mechanical properties of the molecules, and their associated free energy that may be worth considering.

10th Dec - Research on possible implementations of higher order loops in LAMMPS. In particular, it is important to be able to preserve the current state of the system (LAMMPS automatically defaults to a novel system, closing and reopening the current file when looping over it), meaning it is not automatically possible to extend simulations on the same configuration as would be required here.

It may be possible to do so manually (write out a complete sequence of compression and equilibration steps in the input file, however this is very sub-optimal and will limit the ease of future work when trying to plot detailed phase diagrams, so a better alternative is sorely needed.

11th Dec - Produce a workable version of the manual loop previously mentioned, as a proof of concept. This has been subsequently adapted for further plotting of my results, however an alternative continues to be needed; I have contacted Jiaming about this (as of last week) but heard nothing back yet.

12th Dec - Develop the loop introduced yesterday, to loop over different values of the variable 'mix steps'; a time consuming process as no proper documentation exists for this process. Managed to develop my code to allow multiple equilibrium runs however, essential for automated phase analysis and a big step forward!

14th Dec - As a result of a PhD interview invitation, have consolidated all the work completed so far in this project, ready for discussion if necessary, A review of some of the seminal textbooks on molecular dynamics simulation was particularly helpful.

15th Dec - A further invitation necessitated the (rather last minute!) production of a presentation of my results thus far; so I produced formal versions of the plots already obtained, alongside a presentation script - the focus here was on the future direction of the project and the previous generation of the project plan was extremely helpful here.

At this point, PhD interviews took over, with a very busy week for this. Aware these would continue in the fortnight after the New Year, and Major Topic exams followed suit after this, I put this project to bed until after these exams occurred. My hand was slightly forced here my personal circumstances/illness, and I would have hoped to have progressed further by the end of this term.

Reviewing my goals, I have indeed successfully installed LAMMPS, and ran test cases successfully here. I have also been able to write my own simple test case (2D hard spheres) completely from scratch, and then extend this work into rigid rods simulations. While the hard spheres themselves will likely not contribute to the final report, they were extremely useful in developing my skills and knowledge of the simulation systems considered here.

I have also implemented multiple methods to measure the phase of my system, both through the equilibrium pressure values and also the evolutions of thermodynamic variables such as pressure and internal energy. However, I have not been able to achieve my ultimate aim of verifying the isotropic->nematic phase transition in a rigid rods system, as predicted by Onsager theory. This is partly due to issues in restructuring my code, which I hope to resolve in the new year to probe this system further.

January

24 January 2021

23:01

As described in the December entry, I was unable to make further progress on my project in the first half of this month, due to conflicting demands on my time though PhD interviews (from 4th - 15th Jan) and Major Topic Exams (18th - 22nd Jan). After these, I was excited to make progress on the work completed previously, and make up for lost time!

From this point on, I will only document progress in the coding; while a significant proportion of my time is being spent in literature reviews and reading around the previous research in this area, it seems silly to document this all twice!

24th Jan - Took all day but finally worked out a way to **automatically loop over different mix steps values**; requires two separate files (one for initiation, and a second one that can then be repeated while acting on a restart file generated by the previous loop).

25th Jan - Tidied up the code written yesterday, to make the loop more readable, and applicable to different looping variables, extended run times (with regular data saving built in, if the simulation fails at any point). Applied these techniques to 1000 particle simulations in an effort to generate a full phase plot for the rigid rod system.

26th Jan - Analysis of yesterday's simulation gives evidence for a nematic phase transition, which is easily tracked in Ovito. This was also easily visualised in the thermodynamic variables of this plot, and I was excited to present these results to Jiaming today. I have concerns that the simulation region may need to be an integer number of molecules lengths long to observe a stable nematic phase, however Jiaming denies this.

I may also look into accessing further computational resources, as the simulation above took 3 hours. While this was not unreasonable (and is in fact very much on par for this type of simulation on a personal laptop), it is also becoming limiting in terms of what is computationally possible. I will not be able to increase the particle number or equilibration time significantly, while continuing to run such simulations. Therefore it may be necessary to use other computational resources; Jiaming has suggested the Cambridge High Performance Computing centre, as well as Erika's GPU. However this can be tricky to set up, not helped by the remote nature of all work at the moment, and so I will continue to use my personal laptop when possible.

30th Jan - Tidied up data from previous data collection, and developed code to automate the data scraping process. This enabled me to generate code to plot the system director evolution over time, a precursor to the order parameter.

31st Jan - Implemented an oblong simulation region, to aid nematic phase formation (according to Jiaming). This was a time consuming process, and involved adapting the initialisation python code (to

generate the starting configuration) as well as the LAMMPS running code - this took longer than anticipated!

The results from initial simulations in this configuration was unexpected, Jiaming's predictions do not seem to be holding up with particles not aligning along the long axis of the region spontaneously; I believe this may be the stochastic nature of the simulation dominating any driving force for this specific alignment. This method also throws up separate issues; ordered phases may be 'nucleated' at two separate points in the region, and this extended aspect ratio means they may stabilise in the region around these points before interacting with each other. As a result, the ordered phase can actually consist of regions with different directors. While this grained structure is typical of physical systems, it complicates the analysis significantly as there is no longer a single system director. Subsequent simulations will tell whether this was an unlucky occurrence or a more frequent one!

February - 1

01 February 2021

14:30

1st Feb - Now that I have data (and am able to run simulations), this project becomes a task of data extraction. Surprisingly, this is actually something I have very little experience in, and so a good portion of today was spent teaching myself how to read and parse text files (or rather how to code these processes in python), so that the positions of each particle could be extracted from the LAMMPS output files.

Once this was completed, I was able to generate an array of all molecule start and end positions at a given timestep, and so therefore could determine the average director of the system.

2nd Feb - Armed with the mean director of the system, I was finally **able to calculate the order parameter** (based on the assumption that the system director was equal to the mean of the individual directors in the system). From this I was able to plot the evolution of the order parameter and volume fraction over time in the system. This could be applied to an extended time duration simulation that I ran last night, to capture the full nematic transition. Some of the results obtained were unexpected, with negative order parameters and a much lower maximal value than expected; using the mean director as the system director may not be the optimal approach.

I met with Jiaming this afternoon to discuss the issues I have been having in achieving highly ordered states, with a uniform nematic vector, even after long equilibrium runs. Jiaming has no ideas why this may be occurring, but suggests that there is a significant random element to the nature of the phase formed, and whether the nematic phase director lies along the long axis of the simulation region (which has not been occurring up to this point).

Jiaming added that the most ordered phases are typically obtained from expanding from the lattice configuration of a perfectly ordered system. In fact in the phase diagram he produced, these points were not obtained from a simulation run, but rather added by eye.

5th Feb - Now that I am getting results, I started writing a 'Project Progress' report; this will not be submitted (although some of it may be transferred into the final report), but rather serve as a more formal record of my progress (and graphs that I may wish to include in my final report). I also wished to take this opportunity to record the methods of analysis that I have used, such as the calculation of the order parameter etc.

6th Feb - After an extensive literature review this morning, I came across a paper by Eppenga et al. (1984) that introduces a novel eigenvalue method to calculate the nematic order parameter, in a system where the global director is not known (i.e. in the absence of any external director from an electric field or similar). The mathematical details of this were slightly complex initially, however I have managed to **implement this updated, tensor based method to calculate the order parameter** today (with much greater success than the original method for order parameter calculation).

7th Feb - I reproduced all plots of my order parameter, and updated my progress report both with these plots, and a description (and complete derivation!) of how this method worked. With this greater understanding of the tensor method, I was also able to clean up my code on this area, and remove unnecessary elements of the program for optimised running. I initialised long simulation runs to identify the location of the nematic phase transition (ie the critical volume fraction).

8th Feb - After analysing the data from last night's simulation, I was able to reconfigure a long simulation run with more optimised mixing steps to provide a greater resolution on this nematic transition.

9th Feb - Was rather busy today with minor course work, but (as I fear may become a regular part of my term), I started and ended the day by analysing the results from the previous night's simulations, and adapting the simulation parameters to better identify the critical volume fraction where the phase transition occurs. This is an arduous process on LAMMPS, as the start and end volume fraction of each mixing step cannot be specified directly, only the duration of the step (and the damping of the thermostat, however this cannot be converted to a rate of volume change). Therefore, trial and error is required to identify best sequence of mixing steps to maximise the resolution around the phase transition in a given runtime (i.e. by undergoing fast contraction before the phase transition, and slow contraction around it).

10th Feb - This is the first time I have met with Erika since the end of last term, however I was able to share significant progress since then, including nematic phase formation. She was able to suggest that the 'mixed nematic' phase I observed in longrun2, with a non-uniform director orientation across the simulation box, was a common unphysical artifact of simulations not accounting for boundary effects, which provide a uniform orientation for phase formation. Erika also highlighted the importance of comparison with simulation results from an expanding system (starting from a crystalline phase). As well as verifying the nematic \rightarrow isotropic phase transition (and ensuring there is no hysteresis here with the phase transition occurring at the same volume fraction, it would also allow observation of the smectic \rightarrow nematic phase transition in theory).

11th Feb - While this is an ongoing effort, I am fairly confident my simulations of rods with an aspect ratio of 10 match the predictions given by Onsager well. This could easily be extended (and more conclusively verified) through consideration of rods with alternate aspect ratios. Sadly the nunchucks.py initialisation file is not generalisable in this respect, being written exclusively for 10 atom long particles. For now, it is simplest to break the central bond of the molecule, to consider a system of molecules formed of 5 atoms instead, with half the aspect ratio of the rods previously considered.

12th Feb - Analysis of the half-length rod system configured yesterday revealed that no nematic/ordered phase formation was observed, as was expected from Onsager's analysis given the limited volume fractions that can be achieved (both through LAMMPS and in a system of hard sphere force centres, which are limited by their packing efficiency).

Additionally I have researched parallel execution on LAMMPS, to speed up my simulation times, as they are becoming prohibitively costly. However true parallel execution on LAMMPS is only stable on Linux operating systems, and so cannot be used on my windows laptop - sadly COVID-19 has limited my access to linux resources which might otherwise be available in person at the department. I was able to **implement multi-threading** however, which was sped up simulation times by approximately 40%.

February - 2

14 March 2021

11:30

14th Feb - This weekend seemed the perfect time to tackle the looming challenge of **running simulations from an initial crystalline state**. This was a complex task, and required a complete rewriting of the nunchucks.py file, an arduous task as this has no documentation and some unusual syntax/non standard programming approaches. I developed a minimum working example, for small systems, where the number of particles along each axis is specified initially (instead of the total number of particles and the box size). This is why simulations starting from a crystalline phase have 1024 particles rather than 1000, as this fills the box with 4 layers, each with 16x16 molecules in them. This approach could then be easily extended to larger systems.

Additionally, I continued the project of identifying the critical volume fraction in the nematic phase, also for rods of an extended aspect ratio as well as those of a reduced aspect ratio. This was done through adapting the dilute nunchucks code further, although admittedly adjustments to the aspect ratio are made manually not automatically; I hope this is the last of the aspect ratio sample sizes and so the time investment to change this parameter is not worth the time investment.

15th Feb - Following the significant progress in crystalline initial states achieved yesterday, I was able to initialise a new directory for nunchuck simulations sampling decreasing volume fractions (i.e. with expanding mixing stages). However this proved more complex than anticipated, and I was not sure of the interpretation of the thermostat, and hence the implementation of an expanding ensemble in this representation.

I also decided it was really time to crack on with the nunchuck molecules, as they are the main focus of this project; therefore I initialised new directories to focus on analysis of these systems. For low flexibilities (or large angles between rods), we can easily observe similar nematic phases to those previously seen in the completely rigid rod systems. However, with greater flexibility I could not observe any long range order (positional or orientational).

16th Feb - In today's meeting, we looked in more detail at Jiaming's swirl phase, however it turns out this was composed of multiple images stitched together despite initial claims to the contrary, and there doesn't appear to be any pattern in a single image. Daan also suggests this is unlikely to form anyway, as this restriction of translational entropy would be unlikely to be entropically favourable. The image itself may show short range order due to local restriction of molecular orientation (two particles next to each other will probably have some alignment), but no long range order (which would indicate a new phase).

This was frustrating, as the project was initially based on this evidence, however I hope I will be able to find more conclusive evidence for alternative phases. I have continued to run initial simulations on a range of rigidities to identify suitable candidates for ordered phase formation, however have not observed any ordered phase formation in the semi-flexible cases considered today.

17th Feb - As an alternative method to detect order within the fixed rigidity case, I have introduced a histogram plot of the opening angles of the molecules, to determine whether there is any deviation from the initial isotropic distribution. This might represent a restriction on the configurational entropy of the molecules as a preferred angle is formed, and hence an entropically driven phase transition.

19th Feb - Today I tried to clear up loose ends on the rigid rods front, as I really want to be able to focus on the nunchucks simulations from now on. I wrote up my findings from the extended aspect ratio rods in the project progress report, as well as planning further work that was necessary on these systems, particularly in the crystalline case.

I also introduced a Kernel density plot to measure the angle distribution in the fixed rigidity nunchuck system, as I believe this continuous representation may be more illuminating than the discrete density histogram. This required the instillation of seaborn, a module I am unfamiliar with, however it was not difficult to get working.

20th Feb - Further data collection and analysis on both the nematic rigid rod transition from the crystalline state, and also the fixed rigidity nunchucks. Beginning to find the optimised mixing step lengths for this transition, and a significantly longer simulation was able to give a **peak in the angle KDE, and some non-zero order parameters for the fixed rigidity case!**

21st Feb - Recent success with the crystalline rigid rod simulations has not only verified the nematic order, but also suggested a smectic phase, so I have developed a new order parameter based on the Fourier component of the density to detect this (following a long search in the literature for a suitable approach that didn't involve simulated/experimental light scattering. It is worth noting this transition does not appear to occur at a single volume fraction, but rather continuously over a range of phi.

22nd Feb - I realised that longer nunchuck molecules may be more conducive to ordered phase formation, and so adapted my analysis files for angle distribution to take the molecule length as an input constant. This mainly affected the data selection from the raw output files, so that the middle and end atoms in a molecule could still be accurately identified, and should work for even and odd numbered molecules.

I also initialised further simulations for the fixed rigidity case, to illuminate the ordered transition, and in the fixed angle case to redo simulations that crashed overnight earlier in the week.

23rd Feb - Analysis of yesterday's simulations provided more conclusive evidence for a preferred angle in the fixed rigidity case, with development of a larger peak at wider opening angles (although I am as of yet unable to isolate this peak from the origin, and so not sure if the preferred configuration is simply straight molecules).

27th Feb - I have been looking through some of the experimental literature, and this raised questions on the validity of this (highly coarse-grained) representation of DNA. For example, I am aware of the chiral nature of DNA, and many of the experimental studies seem to observe the formation of cholesteric rather than nematic phases as a result of this. I will raise this in the next meeting, along with the dependence of intramolecular opening angle potential on base pair configuration (this may be negligible if it is dominated by the phosphate backbone).

I have also realised I need to correct my current work here, as it does not account for particles crossing over the boundary of the simulation region (their director is no longer properly represented by a vector between the two end particles). This error is minimised by choosing adjacent particles (which are much less likely to be separated by the simulation boundary) however ideally this would be fixed fully. This would require transforming end particle positions across the simulation region if the particle crosses the box boundary (or simply rejecting data from particles with an end-to-end 'distance' greater than expected (i.e. on the order of the size of the simulation region)

March - 1

01 March 2021

23:02

Mar 1st - Following an extensive literature search for ways to characterise the apart order I have observed in the fixed rigidity (and to a certain extent in the preliminary fixed angle) studies, I have come across the pair-wise orientational correlation function, which provides a distance dependant measure of the order parameter (varying over the separation distance between the pair of particles concerned). I have started to implement this, but am not clear how to do so effectively, and so am binning particles by separation distance and then finding their average correlation coefficient initially.

I did however learn how to write a module in python, so that I might import functions from a previous analysis file (phase_plot) without actually running the file itself

Mar 2nd - Much of today was spent on testing and improving the correlation function introduced yesterday, a more mammoth task than previously anticipated! Initial work was spent improving the binning process through use of the nditer iterators native to python. I also implemented a mask on the array of particle separations to avoid recalculation of these values; this comes at the cost of storing a million pairwise distances! I was also to halve this cost by storing the matrix in upper triangular form however.

Mar 4th - In today's group meeting, I expressed concern that the box size may be insufficient to observe periodicity in the phase structure; ie if there is a twisted-nematic or swirled phase that has a repeating pattern, then the length-scale of this may be greater than the box itself. This would mean that $g(r)$ would not extend to great enough radii to observe secondary peaks. Erika has suggested that Sofia Kanterovich (Univ. Vienna) has a cluster (ESPResSo) and may be able to simulate this system with much large particle numbers to observe this. This system is compatible with LAMMPS and so could be a promising avenue for further work, potentially over the summer due to current timescale conflicts and lead time in preparing collaborative work.

Mar 5th - I improved the correlation function plotting functions, in particular adding a colour map to better visualise the evolution of time between each curve; this was a graphic process I had not encountered before (and indeed I have never been formally introduced to the object oriented style of programming required for such plotting) so a slight learning curve on this matter, but good skills investment for the future!

Late this evening my improved plots displayed a consistent secondary peak, a very exciting development as this suggests periodic order in the system. These are the first non-decaying plots I have been able to observe, and as such I am very pleased with the progress I have made here!

Mar 6th - Sadly I realised the exciting discovery last night may instead be a product of incorrect application of periodic boundary conditions (and so particles at either ends of the box that have a large 'measured' separation actually have a much lower 'true' separation through the boundaries of the box, explaining their raised correlation. Accounting for this computationally does not seem trivial, and I spent a great deal of the day working through this problem on paper before I was sufficiently confident in my approach to implement it. Sadly it seems to have been successful in removing these spurious secondary maxima completely; not such a new result after all!

Mar 7th - Further data collection for the correlation plots was initialised, in hope of resolving any other features through greater sampling statistics.

Mar 8th - Returning to the traditional nematic phase, I have worked further to attempt to isolate this transition, identifying the critical volume fraction at which occurs. Sadly this is a non-trivial task, especially as the ordered phase formation appears to occur much slower in anisotropic particles (an effect that might have been expected even if such non-equilibrium phenomena have not been fully documented in the literature - likely as the practical applications of this are minimal, and the relevance to physical systems very limited; indeed it is more a measure of the effectiveness of the numerical integrator rather than anything else).

Mar 9th - Today I met with Erika and Jiaming again, to discuss categorisation of the more exotic phases I am now observed; Erika has suggested to correlate between the orientation of individual arms, which should help elucidate zig-zag/herringbone structure (which my current method of a director between ends of the molecule will not do). Finally, Daan suggested two new ways to characterise the herringbone structure. Firstly, consider correlation between the normal vector to the plane of each molecule. This should be expressed best in the second order correlation function g_2 . Additionally, take the vector along the bisector of each molecule, and calculate g_1 .

Daan also kindly gave a presentation on how to calculate the pair-wise orientational order correlation function using spherical harmonics; the details are in the notes which have been saved separately. He explains that we want to measure a correlation function that is invariant under a global rotation of the system; the simplest of these is $\cos(\theta)$. However it is worth noting we tend to use the second order Legendre polynomial, instead of simply the first order $\cos(\theta)$, as that averages to zero for molecules with no dipole. This is best expressed using spherical harmonics, and should decrease the running time require significantly.

Mar 10th - Investigating a completely different approach completely, I decided to extend my search for novel phases to nunchucks with much smaller opening angles, in the fixed angle regime. This is inspired by Erika's belief that such systems may yield columnar phases; while separate order parameters may be needed to test for this, a simple nematic test on the molecule normal vectors should suffice initially.

Mar 11th - Sadly no ordered phases whatsoever where observed in the small angle cases, and it does appear that entanglement in this phase may be much more difficult to resolve, which (combined with poor tessellation/volume packing in the hypothetical ordered phase) does not bode well for the potential of this system. Further tests will however be conducted to validate this further, with systems of regular opening angles 60 and 90 deg initialised for future analysis. The motivation

for these choices is that an ordered value, with regular symmetry, may be more likely to form highly ordered columnar phases due to optimal mesogen packing.

Much of today was spent **rederiving Daan's spherical harmonic approach before implementing it in python**, a complex and fiddly process but hopefully worth it in the future analysis time, as this is by far the most costly element of my analysis suite.

Mar 13th - Benchmarking of Daan's approach against my conventional (brute-force) one revealed significant savings (in run time but more significantly in RAM usage), while giving replicable plots. I was then able to document and implement the alternative correlation methods he and Erika had suggested earlier in the week, calculating the bisector and normal vectors for each molecule as well as the traditional director.

Mar 14th - Analysis of the small angle data collected earlier in the week (both with the traditional order parameters and this new correlation function) revealed no order in these systems (as was expected from a visual assessment of the systems). The correlation function was generalised to include first order correlations as well as second order, dictated by the order of the associated Legendre polynomial.

March - 2

15 March 2021

18:30

Mar 15th - Initialise a fixed angle crystalline simulation. This is a complex process of trial and error, and the molecules must be placed in their linear configuration in the cubic lattice, before slowly relaxing into their bent state. These bent molecules do not pack as efficiently, and so the simulation region must expand slightly to account for this change, otherwise the internal energy of the system explodes as particles are forced to overlap. However, we wish to maintain as higher initial volume fraction as possible (specifically maintaining the length of the long axis to maintain the smectic phase) so that we can sample as wide a range of volume fractions as possible. Therefore this is a trial and error process, experimenting with how little initial stabilising expansion we can get away with.

Subsequent long time simulations of this state were initiated, for future data analysis. Care was taken to ensure the stability of such simulations in the early stages (i.e. at high volume fractions).

Mar 16th - The full crystalline simulations were analysed, giving a complete picture of the phase transitions available to this system between the crystalline and isotropic regions. There is certainly a smectic phase, although it is unclear whether this decays to the isotropic directly or through a separate nematic phase. Nevertheless, a video of this complete transition is extracted, potentially for use in the supplementary material.

Mar 17th - I finally bit the bullet and **rewrote the nunchucks.py initialisation code to allow for an arbitrary arm length**, specified in the arguments. I have taken a different approach to Jiaming and only allowed for odd-numbered molecule lengths, so that there is only one point of rotation at the centre of the molecule rather than two; this matches the OxDNA model better, and seems more physical (I also see no need for this additional degree of freedom as its introduction was purely arbitrary).

Mar 19th - Further data collection and analysis for the 120 degree bond in the crystalline phase, as it is still believed that regular bond angles will produce the most favourable ordered phases (if they should exist). No conclusive order is found here, beyond the quasi-nematic and smectic phases.

Met with Daan to discuss the scaling of the spherical harmonic approach; establishing that the calculation inevitably scales an $O(N^2)$ even if spherical harmonics are used to evaluate the angular components, as the pair-wise separation calculations must scale with the square of the number of particles. Further simulations may be conducted on Erika's GPU. I have tried to get remote access to this, but we will likely need to use a root account to set up a separate account for me on here.

Regarding further simulations, the phase transition with bend rigid rods can be hard to pin down, and so it is worth completing further simulations here, both varying the rods length (5 molecules per arm etc) and the separation angle (135 deg, 105 deg). While some research of the static phase behaviour of this system has already been conducted, very little is known about the dynamics of the system. There are many interesting questions here, particularly with regards to the viscosity parameters and shear wave behaviour in the system, or even elastic coefficients of the crystalline phase. I have suggested that the diffusion properties in particular may provide an alternative route to look at (for?) new phases, as they reflect the symmetries of the system.

Mar 20th - Initial consideration of directional diffusion coefficient, as a method of phase tracking. First, tracking of the scalar diffusion coefficient was implemented, followed by reduction into directional components. This is most easily done along the cartesian axes, and so most applicable to crystalline phases (which are initiated in this basis, whereas dilute systems spontaneously form order in an arbitrary basis).

Mar 21st - Continuing yesterday's initial work to consider the dynamics of the system, I had to consider more inventive ways to account for the periodic boundary conditions again; I decided it was best to track any time a particle crossed the boundary (through a maximum allowed displacement per step), along with the direction of the crossing, and then subtract the offset from the crossing from the final position to give a final position in true (rather than periodic) space, from which the overall displacement can be measured. This accounts for multiple crossings well, and has little memory requirements. I also initiated a simulation for the full crystalline \rightarrow isotropic phase transition, for subsequent dynamic analysis.

Mar 22nd - Diffusion data was collected for this crystalline system, and clear anisotropy observed in the smectic phase. Further analysis is required (and further iteration) to ensure all phase transitions are simulated at high resolution, so that changes in the dynamic properties over the phase transition may be observed.

I also decided it was time to start work on my project report, to avoid leaving myself too much to do at the last minute, and that the writing was not rushed! Primary focus today was outlining the structure of the report, and setting up a Latex file.

Mar 23rd - Met with Erika and Jiaming today, primarily to discuss the requirements for the report (such as how much code to include etc). Also discussed the dynamic results I have been obtaining, and established it would be useful to plot the mean squared displacement over time, on a log-log plot; this describes the nature of the motion extremely well (although accounting for periodic boundary conditions will be non-trivial here!)

Mar 24th - Further simulation data of the diffuse system was collected to produce plots that reflected the phase transitions observed in this system, with a fine enough sampling resolution. I

also began writing the methods section of the report, documenting the processes used and parameter values in LAMMPS for reproducibility.

Mar 25th - Most work today was theoretical, formalising the derivation of all order parameters used, and justifying my choice in order parameter through a literature review. The derivation of Eppenga's Q-tensor method was written out in full.

Mar 28th - Initial studies on the dynamic behaviour in the dilute regime; Erika's previous student David has generated a number of predictions about the dependence of diffusion coefficient on volume fraction in this region and I hope to verify these computationally. However the simulation methods of LAMMPS are optimised for concentrated systems, and seem to struggle with large simulation regions in the dilute, hence I am working out the best way to run these.

Mar 29th - Generated an analysis file to plot the continued RMS displacement of the sample over time, including a method that accounted for boundary crossings in this (at the time of the crossing, rather than at the end of the sample period, as had previously been done). Also finalised the methods section for the report, including methods used for the diffuse regions.

Mar 30th - Reconfigured the dilute data analysis, and considered additional results on this front, with a much longer sampling time for increased statistics. Despite this, the particle number has had to be reduced to account for the large decrease in simulation evaluation rate, and the noise is still greater in magnitude than the correction term predicted by David.

Also began to outline the results I wanted to publish in my report. I had to be selective here, as I have hundreds of graphs, and so choosing those that best outline the arc of this research was the first challenge here (then the 'story' could be built around these key elements).

April

02 April 2021

21:42

Apr 1st - I combined plots of nematic and smectic ordering for better visualisation of the temporal sequencing of these transitions, and related critical volume fractions. I also research and produced a complete appendix on the application and use of Onsager theory within my project for use in my project report.

Apr 2nd - Further **analysis of diffusion in the dilute limit**. Only the net diffusion coefficient is considered here, as the system is completely isotropic. Despite longer time sampling, it is still not possible to separate the first order volume fraction from the noise, despite sampling over a range of volume fractions (into the semi-dilute limit).

The diffusion coefficient is observed to decrease as volume fraction is increased, and the use of a $(1+2.5/\phi)$ factor does not offset this to give a constant estimate for D_0 . The variability in diffusion coefficient is also much greater than the magnitude of this adjustment in the dilute regime.

Apr 4th - Final analysis of the nematic transition from the crystalline state in the rigid rods system, to fully identify this phase transition (and produce publication quality graphs for use in the report). This also allowed identification of the smectic point in this transition, although this remains ambiguous as the phase transition is likely to be continuous.

Apr 8th - Production of a final draft of my report, incorporating the literature review from the previous project plan as well as the latest diffusion results. A full conclusion and abstract have not been included.

Apr 13th - Meeting with Erika to discuss standard of figures presented in the report (including accessibility for colour-blind/visually impaired readers). Summarise that further work will be required to identify first order corrections to the diffusion coefficients in the dilute limit, as well as more general characterisation of a potential biaxial phase.

At this point I had two weeks until minor topic exams, and so my focus shifted to preparing for this full-time.

May

02 May 2021

00:05

Final minor exam on 4th May and so I was able to return to focusing on the project after this point.

May 4th - Initialised simulation of dilute system, which much greater particle numbers (overnight), as a last attempt to reduce the stochastic noise sufficiently to test David's hypothesis.

May 5th - Analysis of diffusion data in dilute limit; noise has reduced but still significant. Adapted plotting methods to highlight any deviation from the expected ('zeroth order') prediction that might test David's hypothesis. However this provided a final confirmation that I do not have the computational resources available to test this hypothesis, due to the significant amount of residual noise in the system that can only be reduced by increasing the sampling statistics of the simulation (increasing the computational cost).

May 6th - Start work on a presentation to Erika's wider group on my project work; again this is focused around the graphs I want to present and the script written from there/ I want to make this look professional and so have used the appropriate logos from the university as well as researching good practice in academic presentations.

I wrote a description for the methodology section of the presentation, as well as refreshing my notes on the parameters used within LAMMPS.

May 7th - Prepare presentation material and graphs on the rigid rods section of the presentation.

Met with Erika and Jiaming to discuss the applications and motivations of this study. Primarily we care about anisotropic liquid crystals as they may lead to the formation of new phases. This are of direct interest in liquid crystal technology; for example there is already some evidence that anisotropic liquid crystals gives rise to phases that offer wider viewing angles for display screens. Such phases are much easier to test and identify in silico, and so such simulation approaches demonstrate what might be possible (along with the associated molecule parameters most likely to be successful), without using costly experimental resources (especially with expensive custom-made DNA molecules!)

I was also able to share my (slightly disappointing) conclusion in the investigation into David's theoretical predictions.

May 8th - Added introduction, nunchuck results and a conclusion to my presentation script, as well as tidying up the slides and ensuring I am ready to present this.

Investigate potential phase hysteresis through comparative plotting of the expanding and contracting simulations; while exact comparison here is not accurate (or truly valid), this certainly confirms that minimal hysteresis is present in the nematic transition, as anticipated.

Finally, I initiated further simulations to explore the potential existence of twisted or biaxial nematic phases in the fixed angle nunchuck system, which have potentially been observed already, but not fully validated.

May 9th - Correlation analysis of the potential twisted nematic phase shows no evidence for a secondary maxima in the pair wise correlation function. Visual inspection of this system shows apparent periodicity of this phase is twice that of the simulation region; if it does exist then we don't have the resources to capture it here!

The biaxial phase analysis is less conclusive, and so I revisited the literature for further approaches to phase identification here (detailed in the literature review section). Then a final, long equilibration simulation was initialised, with an expected runtime of 20 hours.

May 10th - Tentative **identification of a biaxial nematic phase** through the nematic order parameter applied to the bisector vector (as well as the traditional molecular director). Further analysis of a stabilised crystalline system verified this identification, with anisotropy observed in the x and z diffusion coefficients. Also **delivered presentation of project to Erika's group** (and Daan) and fielded questions on the project in general.

May 11th - Developed code to identify the biaxial nematic phase through formal nematic order analysis on the molecular bisector. This was applied both to the target system (with an opening angle of 150 degrees) and a control system (with an opening angle of 179 degrees) to ensure that it is zero when uniaxial nematic order is present.

May 12th - Updated results section of the final report to reflect the new findings, and increase clarity (as it was rather verbose initially)

May 13th - Met with Erika and Daan to discuss a few recent findings on the biaxial phase, which seems to be becoming more conclusive! I do not think I have enough evidence to present a full picture in my report (nor enough space to do it, more pertinently!) but Erika has suggested providing a reference to future work on this (particularly as we hope to publish these results over the summer).

Literature Review

Chapter Introduction

13 October 2020
19:09

This chapter provides a record for some of the primary papers consulted as part of the initial literature review. It is not intended to be a record of every paper I have read, or every paper I deem

relevant to my project/ may cite in my final report. It has been used, however, as a continual source of reference throughout the project on both theoretical and computational matters, as well as giving a broader (particularly experimental) context to the work presented here.

I introduce the most relevant papers individually, followed by other groups of papers organised by topic.

Papers have not been cited fully here; typically a title (along with lead author surname and publication year) suffices; the aim is that sufficient detail is provided for the paper to be relocated and cited more fully if/when desired. I must also declare that many sections (particularly the abstracts of papers) are reproduced here 'word-for-word' and are not my own words, rather I have collated them as a reference for personal use. I make no claim that all the words here are my own.

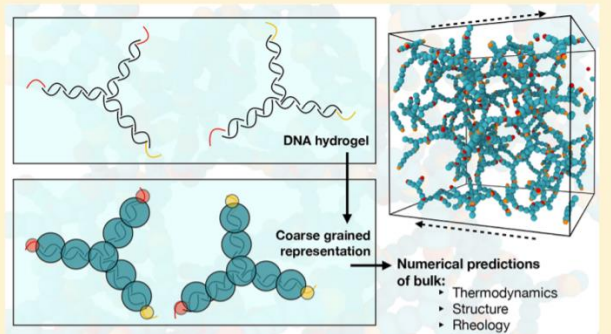
Xing 2009 - Y-shaped Nanoparticles)

13 October 2020

20:09

Structural and Linear Elastic Properties of DNA Hydrogels by Coarse Grained Simulation

ABSTRACT: We introduce a coarse-grained numerical model that represents a generic DNA hydrogel consisting of Y-shaped building blocks. Each building block comprises three double-stranded DNA arms with single-stranded DNA sticky ends, mimicked by chains of beads and patchy particles, respectively, to allow for an accurate representation of both the basic geometry of the building blocks and the interactions between complementary units. We demonstrate that our coarse-grained model reproduces the correct melting behavior between the complementary ends of the Y-shapes, and their self-assembly into a percolating network. Structural analysis of this network reveals three-dimensional features consistent with a uniform distribution of inter-building-block dihedral angles. When applying an oscillatory shear strain to the percolating system, we show that the system exhibits a linear elastic response when fully connected. We finally discuss to what extent the system's elastic modulus may be controlled by simple changes to the building block complementarity. Our model offers a computationally tractable approach to predicting the structural and mechanical properties of DNA hydrogels made of different types of building blocks.



The Y-shapes comprise three arms made of soft beads, with the terminal beads having attractive patches that represent the ssDNA sticky ends.

Model Types

Atomistic Models

- Considers detailed dynamics of nucleotides
- Investigates DNA folding and molecular interactions
- Extremely computationally expensive

Bead Spring

- Models up to 3000 base pairs as a single bead
- Obtain bulk material properties easily

OxDNA

- Offers intermediate level of coarse-graining
- Used to simulate DNA nanotechnology and molecular machines

We can use OxDNA to obtain mechanical properties of a nanoparticle, which then may be used to model the particle in bulk, using a more coarse-grained (less computationally expensive) approach.

Simulation Details

All coarse-grained molecular dynamics simulations are performed using Langevin dynamics, in which the trajectories of each bead are computed according to:

$$m \frac{d^2\mathbf{x}}{dt^2} = -\nabla U(\mathbf{x}) - \lambda \frac{d\mathbf{x}}{dt} + \eta(t)$$

where \mathbf{x} and m are the position and mass of a single bead, respectively. $U(\mathbf{x})$ is the bead interaction potential (that is, the sum of the relevant V terms), the damping parameter λ is large to approximate overdamped conditions, and $\eta(t)$ is a noise term from interactions with a stochastic heat bath via random forces and dissipative forces.

We use the number of connected patchy pairs to characterize the connectivity of the network. This quantity increases during equilibration, reaching a plateau whose value depends on T and the number density ρ . We use the degree of association θ to evaluate the connectivity of the network, which we define here as:

$$\theta = \frac{M}{(Q_{\text{valence}} N)/2}$$

Here M is the number of connected patchy pairs, N is the total number of Y-shaped units, and Q_{valence} is the building-block valency, which is 3 in our model by construction. As the denominator represents the maximum number of connected patchy pairs for a system of N units, θ varies between 0 at high temperatures, where we have a gas of Y-shapes, and 1 at very low temperatures, when all possible bonds in the system are formed.

Simulation Summary

- Bead spring model implemented in LAMMPS
- Attractive patches to mimic sticky ends of ss-DNA (to promote polymer formation)
- Cut-off LJ potential employed here (interaction forces are not nucleotide dependant and so much less expensive to model)
- Initial config generated by placing molecules randomly in cubic box (periodic BC) with no overlap

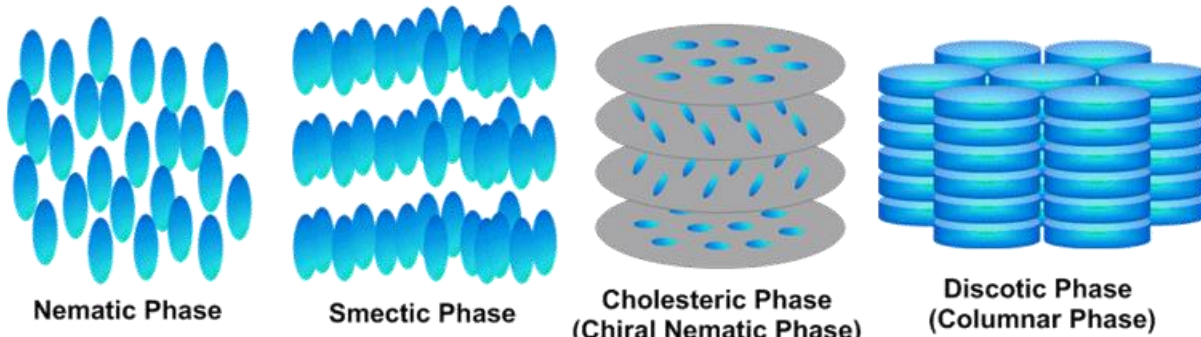
Gleeson 2016 - Nunchucks

13 October 2020

20:13

Smectic phase in suspensions of gapped DNA duplexes

Abstract



Smectic ordering in aqueous solutions of monodisperse (*uniform size*) stiff double-stranded DNA fragments is known not to occur, despite the fact that these systems exhibit both chiral nematic and columnar mesophases. Here, we show, unambiguously, that a smectic-A type of phase is formed by increasing the DNA's flexibility through the introduction of an unpaired single-stranded DNA spacer in the middle of each duplex. This is unusual for a lyotropic system, where flexibility typically destabilizes the smectic phase.

We also report on simulations suggesting that the gapped duplexes (resembling chain-sticks) attain a folded conformation in the smectic layers, and argue that this layer structure, which we designate as smectic-fA phase (*a novel smectic-A type of phase, where 'f' stands for 'folded'*), is thermodynamically stabilized by both entropic and energetic contributions to the system's free energy. Our results demonstrate that DNA as a building block offers an exquisitely tunable means to engineer a potentially rich assortment of lyotropic liquid crystals

Summary

Phase transitions of double-stranded B-form DNA (dsDNA) in aqueous saline solutions have been extensively studied in the past, revealing a series of multiple lyotropic liquid crystal (LC) ordered phases at sufficiently high concentrations, depending mainly on the length of the dsDNA molecules and the sample preparation method

Here, we report conclusive small-angle X-ray scattering (SAXS) evidence, as well as computer simulations, that reveal it is possible to form a smectic phase in suspensions of short dsDNA fragments by introducing a flexible single-stranded DNA (ssDNA) region in the middle of the duplex. The stabilization of the lyotropic smectic phase by introducing a flexible spacer is not obvious and somewhat counter intuitive, since one would expect that a significant decrease in the system's stiffness will destabilize the smectic phase²⁹. On the basis of a combination of physical arguments and our simulation results, we propose a specific model for the smectic layer structure in which the gapped duplexes predominantly adopt a folded configuration, with the rigid parts of our DNA-based chain-sticks lie side by side. We designate this novel smectic-A type of phase as a 'smectic-fA' phase, where 'f' stands for 'folded'.

Experimental Details

Nunchucks are constructed to exploit the large difference in the persistence length between (double stranded) dsDNA (50 nm) and (single stranded) ssDNA (2 nm) to fabricate DNA duplexes possessing a central flexible region which is tunable in length. These DNA duplexes thus consist of two stiff dsDNA fragments which are connected by a flexible ssDNA strand, resembling chain-stick like molecules.

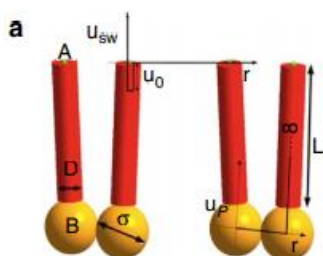
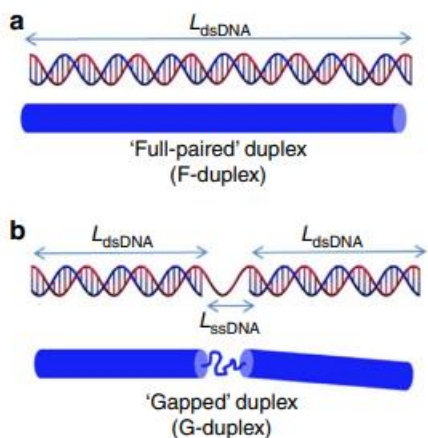
In particular, the length and the position of the paired (L_{dsDNA}) and unpaired (L_{ssDNA}) bases region (see Fig. 1a,b right) can be controlled with sub-nanometre precision, at the level of a single base. The systems involved in this study are two gapped duplexes (G-duplex) with a fixed length of the stiff dsDNA parts, $L_{dsDNA} = 48$ bp/16 nm (using 0.33 nm per bp), and two lengths L_{dsDNA} of the ssDNA flexible spacer, corresponding to 1 and 20 thymine (T) bases.

Simulation Details

They have carried out Monte Carlo (MC) simulations. The G20T-duplexes are modelled in a coarse-grained manner as two hard cylinders with length $L = 16$ nm and thickness $D = 3$ nm (aspect ratio = 5.3). Each cylinder is decorated with two interacting sites, designated A and B. Referring to Fig. 5a, site B is the centre of the orange sphere (diameter s), while site A is the centre of the small green sphere (diameter d) at the opposite end of the red cylinder. Site B is located along the symmetry axes at a distance $L/2 + s/2$ from the centre of mass of the cylinder. The interaction potential u_P between sites B is taken as 0 if $r < s$ and N otherwise, where r is the distance between the sites. The interaction range s (that is, the diameter of the sphere associated to attractive sites B) in our simulations is taken equal to half of the contour length (12.6 nm) of the flexible 20T-spacer; this length has been estimated, assuming the length of each base, to be 0.63 nm. If the two cylinders belong to two distinct gapped duplexes, the interaction potential between their sites B is 0 for each r . Site A is located on the symmetry axis of the cylinder at a distance equal to $L/2 \pm 0.15D/2$ from the cylinder's centre of mass, and sites A belonging to two distinct cylinders interact via a square well potential.

Evaluation

This article simulates the phase behaviour of nunchucks under a simplified model. However we believe this article is restricted, with the model of nunchucks not fully representative of their actual mechanical behaviour, and the conclusions limited by concentration and L_{ssDNA} range considered.



Bilteer 1998 - LC Simulations

20 February 2021

12:59

Simulations of Liquid Crystals - Billeter & Pelcovits

We first give some background on the various liquid-crystal phases and how the degree of order in these phases can be quantified. Next, we discuss how to set up a molecular-dynamics simulation using a well-established phenomenological model for liquid crystals, the Gay-Berne model. We also discuss some of the methods that can be used to assist in determining the structure of the phases. We focus on thermotropic liquid crystals, where phase is determined by temperature (as opposed to lyotropic liquid crystals, where phase is determined by mesogen concentration).

Overall this paper gives a basic overview of liquid crystal mesogens and phases, however with a focus on thermotropic liquid crystals. Very useful discussion on simulation practicalities, and smectic phases.

Nematics - basic motivation for order parameter

If we begin with a completely disordered liquid (the isotropic phase), and cool the system, the simplest mesophase that can form IS the nematic phase. In the nematic phase, the long axes of the molecules align with each other on average. However, the positional order is short-ranged like that of a conventional liquid.

The average direction of alignment is called the director \mathbf{n} . Note that \mathbf{n} is equivalent to $-\mathbf{n}$, if the system can be rotated by 180° perpendicular to the director with no changes in physical properties. The degree of alignment along \mathbf{n} is described by an order parameter:

$$S \equiv \langle P_2(\cos\theta) \rangle = \langle \frac{3}{2}\cos^2\theta - \frac{1}{2} \rangle,$$

Where the brackets $\langle \dots \rangle$ denote an ensemble average, P_2 is the second-order Legendre polynomial, and θ is the angle of the long molecular axis with respect to \mathbf{n} . In the isotropic phase, $\cos(2\theta) = 1/3$ and hence $S=0$. Note that first order quantities such as $\cos(\theta)$ will disappear here as the \mathbf{n} and $-\mathbf{n}$ director vectors are equivalent in these mesogens.

Smectics - useful description of different smectic phases (A,B,C,F,I)

Upon further cooling, nematic phases can form smectic phases, in which the oriented molecules form a stack of two-dimensional layers (see Fig. 1). Within the layers, the molecular center-of-mass positions may be random (smectic A) or may form a hexatic phase (smectic B), in which each molecule is surrounded by six neighbors in a roughly hexagonal configuration. The hexagons all have the same orientation with respect to some fixed direction in the plane of the layers, but do not occupy sites consistent with any rigid, long-range lattice structure (see Fig. 2). The degree of this hexatic order (also known as bond-orientational order) is measured by the order parameter:

$$\Psi = \langle e^{6i\theta_6} \rangle,$$

where θ_6 is the angle between the vector connecting nearest neighbour molecules and some fixed axis in the plane of the layers. In more exotic smectic phases the molecules in the layers are tilted with respect to the normal to the layers (smectic C, F, and I).

Other - neighbour lists (leapfrog algorithm) and nematic theory

This then gives further theory on modelling such particles, such as the orientation-dependant Gay-Berne potentials used for the ellipsoidal mesogen particles. This is extended through the use of quaternions in the Hamiltonian equations to track the molecule orientations.

There is a discussion of the use of the potential cutoffs, so that we may use a neighbour list to avoid considering pair-wise interactions with particles outside of this cut-off. This is then updated every T steps (ie 10 or so), assuming molecules change separation slowly. A leapfrog algorithm is used for this, and detailed in this paper. There is also discussion of energy conservation and boundary effects.

This paper references the work of D.Frenkel in Phase Transitions in Liquid Crystals, edited by S.Martellucci and A.N.Chester (Plenum, New York, 1992). This notable work utilises hard spherocylinders (cylindrical rods with half-sphere caps) to demonstrate that nematic phases can be formed from an anisotropic repulsive potential with no attractive parts.

Paolini (1993) - Soft Core Model

28 February 2021
12:19

Simulation of site-site soft-core liquid crystal Models - Paolini et al 1993

Very useful discussion of model parameters (cut-off radii etc), despite focusing on thermotropic phase transitions.

Abstract

Suggested mechanisms responsible for liquid-crystalline ordering include non-spherical excluded volume effects, anisotropic attraction forces and flexibility. It has been shown using hard-core models that non-spherical excluded

volume effects are the essential factor and can qualitatively explain the phenomenology of the problem. However, the simulation of hard-core models is technically demanding. A simpler and more direct alternative is to use a model

with a soft-core site-site potential. We employ here a system of molecules composed of a few (11) atoms, constrained to form a multilinear molecule, and in mutual interaction via a continuous repulsive site-site potential of the form r^{-12} . Our results show that such a model is capable of exhibiting nematic and smectic liquid-crystal phases.

Soft-Core Model

model systems consisting of hard-core anisotropic molecules such as ellipsoids of revolution or spherocylinders have been extensively studied, showing that steric repulsion is sufficient to describe the occurrence of a number of liquid-crystalline phases. However, the simulation of hard-core models is technically rather complicated.

In the present work we choose a simpler approach: our model consists of a set of linear molecules interacting via a soft-core continuous potential. This approach is more straightforward and less specialized than hard-core or molecular models, and appears as a good candidate for exhibiting liquid-crystalline behaviour, because the potential naturally gives rise to anisotropic excluded

volume effects. Indeed, a purely mechanical analysis of the system, based on long molecular dynamics runs over a wide range of temperatures, shows evidence of a rich phase diagram including solid, smectic, nematic and isotropic phases.

Model Details -*very similar to mine*

$$V(r) = 4\epsilon(\sigma/r)^{12},$$

The model employed is a system of N rigid linear molecules ($N = 600$ in all calculations reported here, previous studies with smaller N were hampered by small-size effects) with periodic boundary conditions in the three directions. Each molecule is composed of 11 centres of force and interacts with other molecules via a site-site atomic potential of the form:

$$V(r) = 4\epsilon(\sigma/r)^{12},$$

, where $r = \text{abs}(r_i - r_j)$ is the distance between two atoms belonging to different molecules. Of the 11 sites of each molecule, only the two at the extremes are true atoms, each of mass $m = 1.993 \times 10^{-23}$ g, while the others are massless centres of force, i.e. they contribute to the site-site interactions but bear no mass. The centres of force are constrained on a line, at an interatomic distance $a^*/2$, where $a^* = 1.2\sigma$ is chosen as the effective atomic diameter. A cut-off $r_c = 1.7\sigma$ is used for pair interactions. Such a model is geometrically comparable to a spherocylinder of length-to-width ratio $L/D \sim 5$. We chose this ratio on the basis of [20] (in which a system of hard spherocylinders for various length-to-width ratios is studied) in order to be able to simulate a system with a phase diagram spanning various mesophases.

Also has a very useful discussion on initiating simulations from a crystalline phase, and the justification behind decisions taken here; an approach that should be replicated in my report!

We note that, to avoid unphysical diffusion driven by the periodic boundary conditions [21] it is necessary that the system be large enough in all directions. Exploratory simulations performed on a smaller system, having only two layers along the x-axis, showed evidence of a columnar phase (crystalline order within a layer, but strong diffusion parallel to the nematic director) which disappeared as the system size was increased. ***-Importance of sufficient system size, and justification that mine should be sufficiently large.***

Order Parameter

Extensive discussion of different order parameters, particularly worth considering when detecting the smectic phase. ***Also contains a very useful derivation of the Legendre polynomials as an order parameter. Also details the position dependant order parameter!***

Dussi 2018 - Columnar Phase

27 February 2021

23:30

On the stability and finite-size effects of a columnar phase in single-component systems of hard-rod-like particles - Dussi et al. (2018)

Gives useful literature review outline, and explains the nematic order parameter in the same way I calculated it.

Abstract

Colloidal rod-like particles self-assemble into a variety of liquid crystal phases. In contrast to the formation of the nematic and smectic phases for which it is well understood that it can be driven by entropy, the stabilisation mechanism of a prolate columnar phase (Col+), observed for example in fd-virus suspensions, is still unclear. Here, we investigate whether or not a Col+ phase can exist in a purely entropy-driven single-component system. We perform computer simulations of hard particles with different shapes: spherocylinders, top-shaped rods, cuboidal particles, and crooked rods. We show that the Col+ phases observed in previous simulation studies are mere artefacts due to either finite-size effects or simulation boxes that are incommensurate with the stable thermodynamic phase. In particular, we observe that the characteristic layering of the stable smectic or crystal phase disappears when the dimension of the simulation box along the direction of the layers is too small. Such a system-size effect depends both on particle shape and the competing phases, and appears to be more pronounced for less anisotropic particles.

Phase Classification

The different phases can be distinguished on the basis of the microscopic arrangement of the particles. Nematic phases (N) display only long-range orientational order, i.e. the particles are on average aligned along a common direction; smectic (Sm) phases have an additional 1D positional order, i.e. the particles are arranged in smectic layers; and finally, columnar (Col) phases feature a 2D positional order, i.e. particles form columns that are arranged on a 2D lattice.

In the case of biaxial particles, LC phases can be further divided into (i) prolate uniaxial (often denoted with a subscript +), (ii) oblate uniaxial (subscript -) and (iii) biaxial phases (subscript b), depending on whether the long-range orientational order of the system is associated to (i) the long, (ii) short or (iii) both particle axes. Further classification is possible based on the symmetry of the positional order.

History

In 1949, Onsager showed in his seminal work that a system of infinitely thin hard rods exhibits a purely entropy-driven phase transition from an isotropic to a nematic phase at sufficiently high densities [13]. Upon increasing the density of the system, the alignment of the rods along a common director becomes favourable at the expense of orientational entropy, but this loss is more than compensated by a gain in translational entropy.

In the 1980s, Frenkel et al. employed computer simulations on various hard-particle systems, such as ellipsoids, spherocylinders and disks, to provide evidence for the entropy-driven formation of not only the nematic phase [14] but also the smectic [15] and the columnar phases [16]. Quoting Daan Frenkel from his 1999 review paper: ‘the idea of entropy-driven phase transitions is an old one. However, it has only become clear during the past few years that such phase transformations may not be interesting exceptions, but the rule!’ [17].

Indeed, the number of theoretical and simulation studies on entropy-dominated systems has steadily increased since then [18–27], not only because of their fundamental interest but also due to the concurrent developments in synthesis routes to produce colloidal particles and nanoparticles [28–30].

Results

- Extended discussion on the potential stability of columnar phases for freely rotating hard spherocylinders.

- Further consideration of systems comprised of top-shaped rods, cuboids and crooked rods.
- Includes discussion of nematic and smectic order parameters.

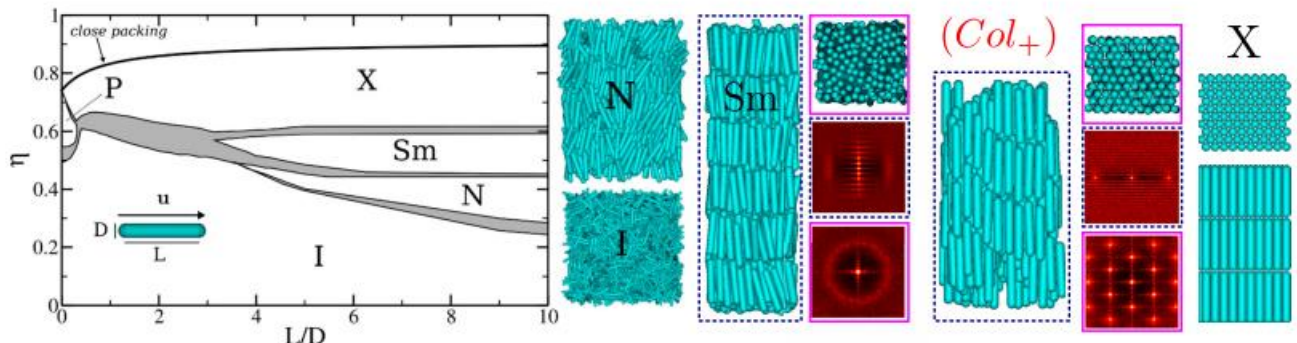


Figure 1. Phase diagram of hard spherocylinders in the packing fraction η -aspect ratio L/D representation, data adapted from Bolhuis and Frenkel [39]. The different stable phases indicated in the phase diagram are: isotropic (I), plastic crystal (P), nematic (N), smectic (Sm) and crystal (X) phase. Representative snapshots of isotropic, nematic, smectic (metastable), prolate columnar (Col_+) phase and crystal phase (X) with the AAA stacking are also shown. For the last three phases, both top and side views are shown. For Sm and Col_+ phases, the diffraction patterns obtained by projecting the particle positions onto the respective plane (top and side view) are also shown.

This paper considers hard spherocylinders as a case study, and so has many useful results on pressure etc which are useful for comparison.

Banana Colloids

27 October 2020

16:48

Shaping colloidal bananas to reveal biaxial, splay-bend nematic, and smectic phases - Fernandez 2020

Summary

A team of researchers from Oxford and Utrecht has developed a new system of micrometre-sized banana-shaped particles. With these bananas they experimentally confirm the existence of the so-called ‘splay-bend nematic’ liquid crystal phase, which was predicted forty years ago, but had remained elusive until now. (Other nematic systems are common, while nematic have been harder to form, but relevant for their chiral and biaxial phases).

Such banana shaped molecules are not only ideal systems to study phenomena such as the spontaneous chiral symmetry breaking in systems of achiral molecules, but are also excellent candidates for achieving faster switching speeds in display technologies.

Abstract

Understanding the impact of curvature on the self-assembly of elongated microscopic building blocks, such as molecules and proteins, is key to engineering functional materials with predesigned

structure. We develop model “banana-shaped” colloidal particles with tunable dimensions and curvature, whose structure and dynamics are accessible at the particle level. By heating initially straight rods made of SU-8 photoresist, we induce a controllable shape deformation that causes the rods to buckle into banana-shaped particles. We elucidate the phase behaviour of differently curved colloidal bananas using confocal microscopy. Although highly curved bananas only form isotropic phases, less curved bananas exhibit very rich phase behaviour, including biaxial nematic phases, polar and antipolar smectic-like phases, and even the long-predicted, elusive splay-bend nematic phase.

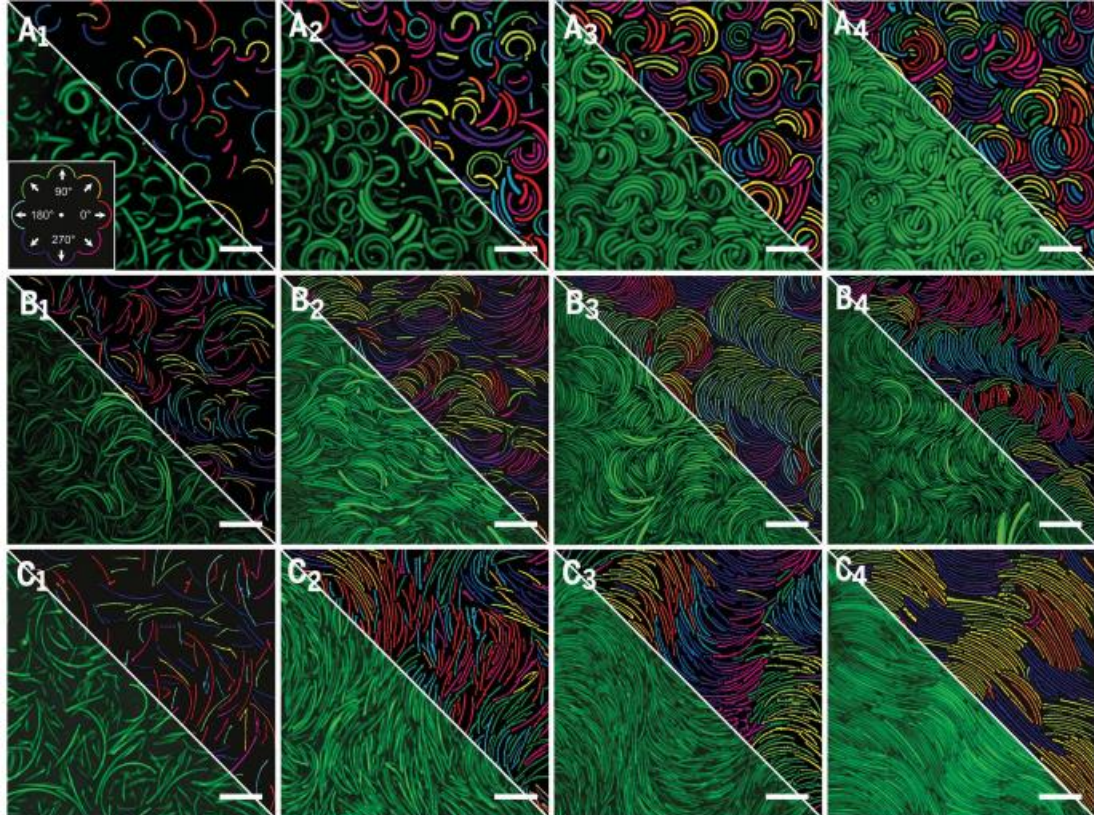


Fig. 4. Phase behavior of banana-shaped colloidal particles with different curvatures. (A to C) Confocal microscopy images of colloidal bananas with an average curvature of [(A1) to (A4)] $k = 0.25 \text{ mm}^{-1}$ and packing fractions $f = 0.12$, 0.26 , 0.61 , and 0.84 , respectively; [(B1) to (B4)] $k = 0.10 \text{ mm}^{-1}$ and $f = 0.27$, 0.63 , 0.79 , and 0.82 , respectively; and [(C1) to (C4)] $k = 0.07 \text{ mm}^{-1}$ and $f = 0.29$, 0.60 , 0.67 , and 0.79 , respectively. The top-right overlays on the images show the bananas colored according to their polar orientation q as defined in the inset in (A5) and the color legend in (A1). (A5), (B5), and (C5) show the polar angle distributions of the corresponding confocal microscopy images. The insets show schematics of the bananas with their mean curvatures. Scale bars are 10 mm.

A detailed characterization of the measured $\hat{n}(y)$ is shown in Fig. 5C, where the spatial modulations of its components parallel (n_y) and perpendicular (n_x) to the nematic director are shown for all five packing fractions. To unambiguously identify the splay-bend nature of these phases, we fit the measured nematic director field with the theoretical expression for the director field of a splay-bend nematic phase (12), given by $\hat{n}(y) = \left\{ \sin[\theta_0 \sin(\frac{2\pi}{p}y)], \cos[\theta_0 \sin(\frac{2\pi}{p}y)] \right\}$, where θ_0 and p are the amplitude and pitch-length of the modulation, respectively (12) (fig. S18).

Worth considering how phase identity was confirmed; in this case a theoretical prediction of the director field was available for comparison.

Evaluation

This paper has useful context of the scale and importance of current research, as well as detailing their method for phase identification and quantification.

However, the findings themselves may be limited. The primary issue here is that the scale of the mesogens is too large, so the system may be granular rather than truly thermodynamic. This means they may be forming equilibrium phases as a result of mechanical shear rather than thermodynamic forces.

On the spontaneous symmetry breaking in the mesophases of achiral banana-shaped molecules - Dozov (2001)

Abstract

We propose that the natural tendency of banana-shaped mesogen molecules to induce a local bend of the nematic director can result in pathological elasticity, with negative bend elastic constant. Under this hypothesis, a simple Landau-like phenomenological model predicts a symmetry-breaking transition inside the nematic phase, from uniform textures toward spontaneous periodic distortion, either oscillating splay-bend or conical twist-bend helix. The predicted lower symmetry nematic phases are expected to show interesting polar properties, similar to those already reported for banana-shaped smectogens.

Introduction

The nematic liquid crystals are liquids with long-range orientational order. The nematic molecules are oriented preferentially along the nematic director n , a unit vector parallel to the local macroscopic optical axis. However, there is no vector order parameter describing the nematic phase —due to flip-flop and free rotation of the molecules around their long axis, the directions n and $-n$ are equivalent and molecular dipoles average to zero on macroscopic scale. The phase is then described by a tensor order parameter $Q = (3/2)S(nn^T - I/3)$, where I is the unit tensor and S is the scalar order parameter [1].

The nematic order arises because the long and highly polarisable molecules like to align parallel to one another. The main energy contribution, stabilising the nematic phase, is due to the van der Waals dispersion forces, either directly to their anisotropy [2], or to their isotropic part modulated by the steric anisotropy of the molecules [3].

[Rev. Mod. Phys. 90, 045004 \(2018\) - Physics of liquid crystals of bent-shaped molecules \(aps.org\)](#)
may also be relevant

Cholesteric Phases in DNA (T/E)

20 February 2021
17:21

Incorporating particle flexibility in a density functional description of nematics and cholesterics - Tortora and Doye (2019) - *Theory*

Abstract

We describe a general implementation of the Fynewever-Yethiraj density functional theory (DFT)* for the investigation of nematic and cholesteric self-assembly in arbitrary solutions of semi-flexible polymers. The basic assumptions of the theory are discussed in the context of other generalised Onsager descriptions for flexible polyatomic systems. The location of the isotropic-to-nematic phase transition is found to be in good agreement with molecular simulations for elongated chains up to relatively high polymer flexibilities, although the predictions of the theory in the nematic regime lead to gradual underestimations of order parameters with decreasing particle stiffness. This shortcoming is attributed to increasing overestimations of the molecular conformational entropy in higher-density phases, which may not be easily addressed in the formalism of DFT for realistic particle models. Practical consequences of these limitations are illustrated through the application of DFT to systems of near-persistence-length DNA duplexes, whose cholesteric behaviour is found to be strongly contingent on their detailed accessible conformational space in concentrated solutions.

*Density-functional theory (DFT) is a computational quantum mechanical modelling method used in physics, chemistry and materials science to investigate the electronic structure (or nuclear structure) (principally the ground state) of many-body systems, in particular atoms, molecules, and the condensed phases. Using this theory, the properties of a many-electron system can be determined by using functionals, i.e. functions of another function. In the case of DFT, these are functionals of the spatially dependent electron density. DFT is among the most popular and versatile methods available in condensed-matter physics, computational physics, and computational chemistry.

Motivation - *Biological applications*

The self-organisation of polymer solutions into partially-ordered mesophases is a phenomenon of considerable biological relevance, whose occurrences span the formation of phospholipid bilayers for the assembly of cell plasma membranes 1, the arrangements of F-actin filaments in the cytoplasm 2, and of haemoglobin chains in sickle-cell anaemic blood 3. This natural ubiquity, combined with a sustained industrial interest in the practical applications of polymeric liquid crystals 4–6, has spawned a wealth of fundamental and applied investigations of their phase behaviour in a variety of contexts 7,8.

History - *Development from Onsager theory*

First account of the emergence of order in polymer solutions comes from Onsager, who demonstrated the existence of a concentration-driven transition from a liquid-like isotropic state to an orientationally-ordered nematic state in dispersions of anisotropic colloid. The onset of nematic organisation simply results from the competition between orientational entropy and excluded-volume interactions, for which exact explicit expressions may be obtained in the limit of rigid rod-like particles with infinite particle aspect ratios.

Classical density functional theory then extended this to non-uniform fluids. Further work was required to apply these findings to rods of finite stiffness (as opposed to the ideal rigid rods considered by Onsager). Strately extended Onsager's work to account for mirror symmetry breaking in the weakly-chiral case. However the representation of conformational free energy is non-trivial in the case of semi-flexible particles here.

- Khokhlov and Semenov suggested combining various extensions of the original Onsager excess free energy in the limit of hard rigid cylinders with a mean-field description of several flexible chain models.
- Fynewever and Yethiraj conversely suggested accounting for the effects of flexibility directly through the excess free energy contribution, while retaining the Onsager expression for the ideal free energy.

Cholesteric Behaviour of DNA Duplexes

DNA constitutes a well-studied semi-flexible biopolymer with relatively-high stiffness, whose persistence length has been measured to be 130 base pairs (44 nm) at salt concentration 0.5M, although the precise value is somewhat dependent on solution, conditions and sequence. DNA is also chiral, both in terms of its excluded volume — it is a grooved double helix with the major groove larger than the minor groove — and its electrostatics — it has a double helical pattern of negative charges associated with the phosphate groups along the backbone.

This paper focuses on (and compares to two previous studies on) DNA duplexes with length on the scale of the persistence length (i.e. about 146 base pairs, with an aspect ratio of about 20), with a focus on the dependence of the cholesteric pitch on DNA concentration and solution conditions. These previous studies* considered the isotropic to cholesteric transition at differing solute concentrations. This paper uses computational techniques (through OxDNA) to emphasise the importance of flexibility in DNA duplexes of this length (which has not typically been considered in previous studies).

**E.g. Phase Transitions in Concentrated DNA Solutions: Ionic Strength Dependence by Teresa E. Strzelecka and Randolph L. Rill*

Re-entrant cholesteric phase in DNA liquid-crystalline dispersion particles - Yevdokimov et al. (2016) - *Experiment*

Abstract Sections

In this research, we observe and rationalize theoretically the transition from hexagonal to cholesteric packing of double-stranded (ds) DNA in dispersion particles. The samples were obtained by phase exclusion of linear ds-DNA molecules from water-salt solutions over a range of concentrations. At low concentrations and room temp, we find ds-DNA cholesteric molecule packing, typical of classical cholesterics, with hexagonal packing at higher concentrations.

However, slightly counter-intuitively, the cholesteric-like packing reappears upon the heating of dispersions with hexagonal packing of ds-DNA molecules, for sufficiently great salt concentrations. The obtained new cholesteric structure differs from the classical cholesterics observed in the low salt concentration range, hence the term 're-entrant'. Our conclusions are based on the measurements of circular dichroism spectra, X-ray scattering curves and textures of liquid-crystalline phases.

Experimental Phases (*History*)

Various DNA phases obtained by dissolution of lyophilized double-stranded (ds) DNA samples (of high and low molecular masses) in water-salt solution (with an adjustment of concentration through a buffer solution) have been known since 1961 [1–7]. An alternative method to prepare ds-DNA phases is to increase the ds-DNA concentration by ultrafiltration through a membrane whose pore size allows passage to water and ions but not to ds-DNA molecules [8–10].

Many works in this field have been dedicated to the problem of packing ds-DNA molecules in structures (phases) formed by such methods [11–14]. The performed studies proved the formation of ds-DNA liquid-crystalline (LC) phases. Bulk ds-DNA phases resemble viscous solutions in which neighbouring DNA molecules are orientationally ordered, while keeping their ability to slide relative to each other. Upon the increase of the linear ds-DNA concentration in water-salt solution, the isotropic solution transforms (via either blue phases or precholesteric stages) into the cholesteric LC phase. Under poly(ethylene glycol)—osmotic pressure compression the hexagonal densely packed structure becomes favourable and more concentrated phases can be considered even as true crystals [15–19].

LC Chevron Phases

14 March 2021

15:40

Landau-de Gennes theory of the chevron structure in a smectic-A liquid crystal - Kralj & Sluckin (1994)

Abstract

We make a ***theoretical study of the chevron and tilted structures*** in the smectic-A phase of a liquid crystal. ***These structures have been observed to occur in cells in which the director is oriented in the plane of the wall.*** We examine the hypothesis of Limat and Prost [Liq. Cryst. 13, 101 (1993)] that the layer buckling and the tilting is a consequence of a mismatch between layer thickness in the bulk and at the surface. We use the covariant form of the Landau-de Gennes free energy expressed in terms of the nematic director field $n(r)$ and the smectic complex order parameter $\psi(r)$. The threshold condition for and evolution of the chevron and tilted structure are obtained as a function of liquid crystal elastic properties, cell thickness, and surface orientational anchoring strength. The threshold and amplitude evolution exhibit almost universal behaviour as a function of a dimensionless chevron number σ .

We give a possible explanation of the hysteresis effect observed in the liquid crystal 4O.8 [4-octyl-n-(4'-butoxybenzylidene)aniline]. We estimate the energy barrier for the chevron-tilted-structure transition and discuss the case where the stress imposed by surface positional anchoring is partially relieved by incorporating a lattice of wedge dislocations.

Introduction

Recently there have been many studies of smectic liquid crystals (LC's) confined between parallel bounding plates in the so-called bookshelf structure. In this structure the layers are perpendicular to the cell walls. An understanding of the stability of the bookshelf structure is of considerable importance in the development of display devices based on smectic LC technology. The perfect bookshelf geometry in practice, however, only rarely occurs. More often the so-called chevron structure, shown in Fig. 1, is seen. In this case the smectic layers are symmetrically tilted, with a kink in the middle of the cell. The chevron structure is believed to be the consequence of the mismatch between the natural smectic layer separation d_0 and the separation d , imposed by the surface interaction.

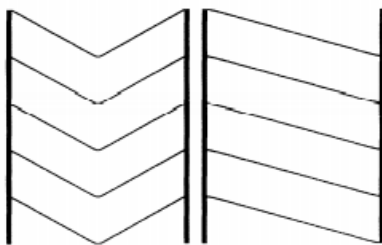


FIG. 1. Schematic representation of the chevron (left) and tilted (right) structures, showing the structure of the smectic layers within a cell. In the Sm-3 phase the nematic molecules tend to be oriented along the layer normal.

Gives detailed free energy calculations for the chevron defect, and control of its formation through Landau theory.

Smectic-C “chevron,” a planar liquid-crystal defect: Implications for the surface-stabilized ferroelectric liquid-crystal geometry - Clark et al. (1988)

Abstract

The recent discovery of “chevron” structured smectic-C (SC) layers in surface-stabilized ferroelectric liquid-crystal (SSFLC) cells enables the understanding of many commonly observed features of SSFLC director and layer structure. We present the full three-dimensional layer structure of zigzag walls, the predominant SSFLC defect, which we find to mediate change in chevron direction. We show that stabilization of the director field in SC chevron cells occurs at the chevron interface, so that SC chevron cells behave as two nearly independent cells optically and electrically in series.

Description

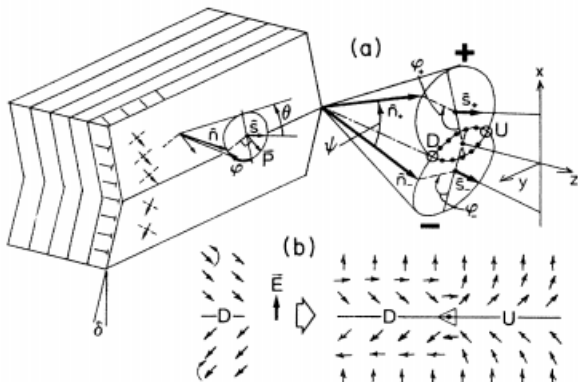


FIG. 1. Geometry of the director field at a smectic-C chevron interface. (a) The SC is a locally biaxial structure of liquid-like layers in which $\hat{n}(\mathbf{r})$ is tilted at an equilibrium angle θ relative to the local layer normal $\hat{s}(\mathbf{r})$ and is free to reorient azimuthally through the angle ϕ on a cone of axis \hat{s} . Subscripts + and - refer to quantities on opposite sides of the chevron.

Considers specifically a chevron orientation structure around a defect, rather than corresponding to long range orientational order. Corresponds to a discontinuity in the order parameter at a planar sheet, parallel to which there is full translational invariance. There is further consideration of the orientational elastic energy of such a defect.

Experimental results obtained via polarised light microscopy, with visual characterisation of the chevron structure.

Chevron Layer Structure in the Smectic A Phase of 8CB - Takanishi et al. (1989)

Abstract

The smectic A layer structure of a homogeneously aligned 8CB liquid crystal (25 μm in thickness) has been studied by X-ray diffraction analysis. Contrary to the common recognition, it is found, for the first time, that the local layer structure of this type of cell changes to a chevron layer structure from a book-shelf structure, as the temperature decreases away from the N-SA phase transition point. The formation of the chevron layer structure is also recognized by the characteristic defects: zig-zag defects appear as a boundary of two opposite chevron structures with focal conics.

Results

This paper differentiates between a 'bookshelf' structure - the regular Smectic A phase where molecule axes are perpendicular to the molecule layers, and a less conventional 'chevron' phase.

Experimentally, this is achieved by confining the sample between glass plates, and is measured by x-ray diffraction.

They believe the chevron structure in the smectic phase is induced to decrease the layer thickness while keeping the overall volume constant. There is no analysis of the order parameter here however, with the phase structure characterised only by the tilt angle. The smectic phase is enforced by the boundary plates, and does not apply in cases.

Biaxial LC Phases

11 May 2021

14:49

Theory and simulation of biaxial nematic and orthogonal smectic phases formed by mixtures of board-like molecules - Vanakaras (2003)

Abstract

Variational cluster calculations and Monte Carlo simulations are applied to hard-body board-like models of biaxial molecules forming liquid crystalline phases. The molecular long axes are assumed for simplicity to be fully oriented. Depending on the extent of transverse anisometry in the molecular shape, these systems can exhibit biaxial nematic phases as well as uniaxial and biaxial orthogonal smectic phases. It is shown that the region of thermodynamic stability for the biaxial nematic phase is considerably broadened in binary mixtures of molecules with the same cross section but differing in their long dimension

Introduction

The existence of thermotropic biaxial nematics is one of the long standing problems in liquid crystal science. They have been constantly attracting experimental, theoretical and computer simulation research interest for over three decades and yet no stable low molar mass thermotropic biaxial nematic phase has to date been conclusively identified by experiment. In fact, reports on the observation of any type of real biaxial nematic phase, be it in a lyotropic or polymeric system, are scarce in the literature. Indeed, there are several instances of systems that were initially reported as biaxial nematics but these were later found not to be so. However, preliminary reports provide strong indications that thermotropic biaxial phases may have been stabilised in at least two different cases, namely bent-core mesogens and rod-plate systems. Indeed, an orthogonal biaxial smectic phase has already been reported for banana shaped molecules.

Biaxial Order Parameter

The aim of the theoretical calculations is to determine the liquid crystal phase behaviour of a binary mixture composed of lath-like particles with their **molecular z-axes perfectly oriented parallel to the macroscopic Z-axis**. The translations of the molecules as well as rotations about their z-axis are unrestricted. Under these conditions, the least ordered phase of the system is a homogeneous phase with uniformly distributed molecular rotations about the z-axis.

This implies for the principal order parameters $\langle \cos(2\phi) \rangle = \langle \cos(4\phi) \rangle = 0$, where the **angle ϕ describes rotations about the molecular z-axis**, and the angular brackets denote equilibrium ensemble averages. This phase is described as uniaxial nematic, NU, and the macroscopic Z-axis is a C1 axis. The system can exhibit two more uniform phases but of higher orientational order, consistent with the molecular symmetries: The first phase is described as tetratic nematic, NT, wherein the macroscopic Z-axis is a C4-axis. Here $\langle \cos(2\phi) \rangle = 0$ and $\langle \cos(4\phi) \rangle \neq 0$. The **second is described as biaxial nematic phase, NBX**, and the macroscopic Z-axis is a C2-axis. **Here $\langle \cos(2\phi) \rangle \neq 0$ and $\langle \cos(4\phi) \rangle \neq 0$.**

The elusive thermotropic biaxial nematic phase in rigid bent-core molecules - Achayra et al (2003)

Abstract

The biaxial nematic liquid crystalline phase was predicted several decades ago. Several vigorous attempts to find it in various systems resulted in mis-identifications. The results of X-ray diffraction and optical texture studies of the phases exhibited by rigid bent-core molecules derived from 2,5-bis-(p-hydroxyphenyl)-1,3,4-oxadiazole reveal that the biaxial nematic phase is formed by three compounds of this type. X-ray diffraction studies reveal that the nematic phase of these compounds has the achiral symmetry D2h, in which the overall long axes of the molecules are oriented parallel to each other to define the major axis of the biaxial phase. The apex of the bent-cores defines the minor axis of this phase along which the planes containing the bent-cores of neighbouring molecules are oriented parallel to each other.

Keywords. Biaxial nematic phase; banana liquid crystals; X-ray diffraction; bent-core liquid crystals.

Introduction

Nematic liquid crystals (NLCs) possess long-range orientational order, along a spatial direction known as the director, and represented by the unit vector n , but with no positional ordering. An aligned NLC behaves as a uniaxial optical medium through which a beam of polarized light propagates along n without a change in its polarization. Based on the symmetry considerations, the existence of a biaxial NLC phase, which possesses two orthogonal optic axes along which the polarization of propagating light remains unaffected, had been predicted some time ago. One of the optic axes of the biaxial nematic phase is along the primary director n along which the long axis of the molecules is oriented, and the second optic axis lies along the secondary director m in the plane perpendicular to n . To this day, only the existence of lyotropic biaxial nematic phases has been confirmed.

This gives a useful introduction into the optical properties of biaxial nematics, but again detection focuses on crystallographic approaches, comparing simulated scattering patterns with experimental ones.

Hard competition: stabilizing the elusive biaxial nematic phase in suspensions of colloidal particles with extreme lengths - Dussi et al. (2018)

Abstract

We use computer simulations to study the existence and stability of a biaxial nematic Nb phase in systems of hard polyhedral cuboids, triangular prisms, and rhombic platelets, characterized by a long (L), medium (M), and short (S) particle axis. For all three shape families, we find **stable Nb states provided the shape is not only close to the so-called dual shape with $M = \sqrt{LS}$ but also sufficiently anisotropic** with $L/S > 9, 11, 14, 23$ for rhombi, prisms, and cuboids, respectively, corresponding to

anisotropies not considered before. Surprisingly, a direct isotropic-Nb transition does not occur in these systems due to a destabilization of Nb by a smectic (for cuboids and prisms) or a columnar (for platelets) phase at small L/S, or by an intervening uniaxial nematic phase at large L/S. Our results are confirmed by a density functional theory provided the third virial coefficient is included and a continuous rather than a discrete (Zwanzig) set of particle orientations is taken into account.

"Biaxial nematic phases have long held promise for applications in novel opto-electronic devices, but their limited window of thermodynamic stability (and for a long time even their very existence) has been of great concern"

Order Parameters

"We distinguish the different liquid-crystalline phases with a variety of scalar and tensorial order parameters [16]."

nematic phases. In fact, to precisely quantify the degree of (macroscopic) biaxial alignment of a nematic phase an additional (scalar) order parameter \mathcal{B} is employed. Notice that different notations and slightly different approaches are employed to calculate the biaxial order parameter in computer simulations [25, 28, 29, 42, 50]. We follow the procedure in Refs. [28, 29] that consists in first identifying an appropriate orthonormal basis for the laboratory reference frame that is aligned with the two main directions of the biaxial phase. For each configuration, we identify the largest $S^{\hat{a}}$ and we define the z-axis of the laboratory reference frame as $\hat{\mathbf{Z}} \equiv \hat{\mathbf{n}}_{\hat{a}}$, with \hat{a} the principle main axis of the particle. Then, we identify the second largest nematic order parameter $S^{\hat{b}}$ and we define the second axis of the laboratory reference frame as $\hat{\mathbf{Y}} \equiv \hat{\mathbf{n}}_{\hat{b}} - (\hat{\mathbf{n}}_{\hat{b}} \cdot \hat{\mathbf{Z}})\hat{\mathbf{Z}} \simeq \hat{\mathbf{n}}_{\hat{b}}$. Analogously, we define the third axis of the laboratory frame by orthogonalizing the third nematic director: $\hat{\mathbf{X}} \equiv \hat{\mathbf{n}}_{\hat{c}} - (\hat{\mathbf{n}}_{\hat{c}} \cdot \hat{\mathbf{Z}})\hat{\mathbf{Z}} - (\hat{\mathbf{n}}_{\hat{c}} \cdot \hat{\mathbf{Y}})\hat{\mathbf{Y}}$, with \hat{c} the third symmetry axis of the particle. Finally, we compute

$$\mathcal{B} = \frac{1}{3} \left(\hat{\mathbf{Y}} \cdot \mathcal{Q}^{\hat{b}} \cdot \hat{\mathbf{Y}} + \hat{\mathbf{X}} \cdot \mathcal{Q}^{\hat{c}} \cdot \hat{\mathbf{X}} - \hat{\mathbf{Y}} \cdot \mathcal{Q}^{\hat{c}} \cdot \hat{\mathbf{Y}} - \hat{\mathbf{X}} \cdot \mathcal{Q}^{\hat{b}} \cdot \hat{\mathbf{X}} \right), \quad (S2)$$

where \mathcal{B} is normalized such that it ranges from 0 to 1. Low values of \mathcal{B} correspond to an isotropic phase or to a uniaxial phase and high values to a biaxial phase. In

Gives a complete and theoretical treatment of the system.

Biaxial Liquid Crystals - Taylor et al (1969)

Abstract

Convergent light observations have been made on three liquid crystalline substances with nematic and smectic phases. The nematic phase was observed to be uniaxial as expected, but smectic C was found to be biaxial. The optic axial angle $2V$ for smectic C was found to be on the order of $20'$ for all three compounds. Also, the tilt angle for smectic C is nearly $45'$ for all three liquid-crystal systems. Anisotropy of the degrees of order is suggested as a partial explanation for the biaxial character of smectic C.

Introduction

We have studied three compounds which exhibit a nematic phase and a single smectic phase of the type classified by Sackmann and Demus' as type C. The smectic phases classified by Sackmann and Demus correspond to different molecular arrangements and are separated from each other by first-order phase transitions. The nematic phase has a long-range order such that the long axes of the molecules are nearly parallel and the parallelism of the long axis generally varies continuously throughout the bulk of the liquid. Assuming a random arrangement of the centre of mass and free rotation about the long molecular axis, nematic liquids would be uniaxial. **All observations do show the nematic phase to be uniaxial.** Smectic A is a system in which the molecules are arranged in layers with the long molecular axis perpendicular to the layer.¹ If the centres of mass within the layers are random and free rotation is assumed, then smectic A would be uniaxial. Experimentally, **all smectic-A phases have been shown, in general, to be uniaxial.** Smectic C is generally considered to have a structure such that the molecules are arranged in layers but with the long molecular axis tilted with respect to the layer normal. In general, it has been assumed that all smectic phases including smectic C would show uniaxial character and, in fact, Friedel¹ argued that all smectic phases would be uniaxial. Recently, Saupe pointed out that due to symmetry considerations, smectic C should be biaxial. **The observations we report in this Letter show that smectic C phases are biaxial.**

Focus on Smectic C phase, with tilt in molecular director from layer normal. Not observed in these systems, and indeed is possibly outdated as I believe other biaxial nematics have been subsequently shown to exist.

Observation of a Biaxial Nematic Phase in Potassium Laurate-1-Decanol-Water Mixtures -Yu & Saupe (1980)

Abstract

The phase diagram of the ternary system potassium laurate-1-decanol-D₂O was studied over concentration ranges where nematic phases are likely to occur. Two uniaxial nematic phases which are separated by a biaxial nematic phase are found. In limited concentration range the following phase sequence may be observed reversibly on heating and on cooling: isotropic-uniaxial nematic (positive optical anisotropy)-biaxial nematic-uniaxial nematic (negative optical anisotropy)-biaxial nematic-uniaxial nematic (positive optical anisotropy)-isotropic.

Widely cited as the first evidence of lyotropic biaxial liquid crystal phases. Method of characterisation is based purely on optical properties, as is common experimentally, and so less relevant to this work.

N.B The double angle relation $\cos(2\phi) = 2\cos^2 \phi - 1$, which should scale with the traditional order parameter $S_n = \frac{1}{2}(3\cos^2 \phi - 1)$.

The angle ϕ is a rotation about the major optical axis (the y axis in my case), and so should be able to be measured from an arbitrary point? It seems to vary with starting angle though, and I think setting $\phi = 0$ along the minor optical axis (ie the average bisector direction) is reasonable.

Gay-Berne Simulations

27 February 2021

19:23

N.B The Gay-Berne potential accounts for the orientation of anisotropic particles, and reduces to the LJ potential in the case of spherical particles.

Molecular dynamics simulations of flexible liquid crystal molecules using a Gay-Berne/Lennard-Jones model - Wilson (1997)

Abstract

Molecular dynamics simulations are described for liquid crystal molecules composed of two Gay-Berne particles connected by an eight-site Lennard-Jones alkyl chain. Calculations have been carried out for 512 molecules in the NVE and NPT ensembles for simulation times of up to 6.4 ns. The system exhibits the sequence of phases: isotropic liquid, smectic-A, smectic-B, and the simulations demonstrate the spontaneous growth of a smectic-A liquid crystal over a period of approximately 6 ns on cooling from the isotropic liquid. Model molecules are seen to remain flexible and able to change conformation in the smectic-A phase. As temperature is reduced molecules become elongated as the number of gauche conformations drops, leading to a small increase in the spacing of smectic layers. The latter is seen through the temperature dependence of the Gay-Berne radial distribution function resolved parallel to the direction of orientational order. Results are presented which show an odd–even variation of orientational order parameters for bonds in the alkyl chain, and a change in effective torsional potentials as the system is cooled from isotropic liquid to a smectic-A phase.

N.B Note that phase transitions here were thermotropic

Simulation Details

Here a hybrid Gay-Berne/Lennard-Jones model is employed to study the phase behaviour of a model liquid crystal dimer system composed of two mesogenic units linked via a flexible alkyl chain. In the model system, bond lengths were fixed between the centres of adjacent sites.

They employed the NPT ensemble using the Anderson thermostat, and implementing a Monte Carlo procedure to alter the volume of the system V . Following Eppenga and Frenkel, changes were made in $\ln(V)$. A random number d was chosen uniformly from the range $(-d_{\max}, d_{\max})$, giving a new volume $V_{\text{new}} = V_{\text{old}} \exp(d)$, with d_{\max} chosen to allow acceptance ratios in the range 35–50%.

For isotropic scaling of the system the length scaling factor is given by $\exp(d/3)$. For anisotropic scaling, a box dimension L_x, L_y, L_z was chosen at random with the box length scaling factor given by $\exp(d)$. Both isotropic and anisotropic scaling methods were tried for different state points. At the highest densities, anisotropic scaling was used exclusively, allowing the box shape to vary. This avoids the possibility of translationally ordered phases forming with layers which are incommensurate with the box dimensions.

To form the initial nematic phase, a low density array was configured, with molecules in an all-trans conformation aligned parallel to the z axis of the simulation box. Molecules were arranged with a

random centre of mass vector and atomic velocities taken from a Maxwell-Boltzmann distribution. This low density configuration was rapidly compressed to provide a pseudo-nematic starting configuration.

Order Parameter

During the simulations, orientational and translational ordering of the Gay-Berne sites was monitored; the former through the calculation of the orientational order parameter $S = \langle P^2 \rangle - \langle \cos(\theta) \rangle / \langle \cos(\theta) \rangle$ (*i.e. the second Legendre polynomial*), and the latter through the radial distribution function g , where \mathbf{r}_{ij} is the vector between the centres of mass of particles i and j .

$$g(r) = \frac{V}{[N_{\text{GB}}]^2} \left\langle \sum_i^{N_{\text{GB}}} \sum_{j \neq i}^{N_{\text{GB}}} \delta(\mathbf{r} - \mathbf{r}_{ij}) \right\rangle,$$

Finally, it also provides some detail on the angle distribution:

Following Wilson and Allen,²¹ the dihedral angle distribution can be written in the following form

$$S(\phi) = C \exp \left[-\frac{V(\phi)}{k_B T} \right], \quad (10)$$

where C is a normalization factor and $V(\phi)$ is an effective torsional potential or conformational free energy. $V(\phi)$ is composed of contributions from both intramolecular interactions V_{int} (mainly the Ryckaert-Bellemans potential and 1–5 nonbonded interactions), and an intermolecular part V_{ext} which depends strongly on molecular environment. Extract-

GPU-Accelerated Molecular Dynamics Simulation to Study Liquid Crystal Phase Transition Using Coarse-Grained Gay-Berne Anisotropic Potential - Chen et al. (2016)

Useful detail on simulation settings

Abstract

Gay-Berne (GB) potential is regarded as an accurate model in the simulation of anisotropic particles, especially for liquid crystal (LC) mesogens. However, its computational complexity leads to an extremely time-consuming process for large systems. Here, we developed a GPU-accelerated molecular dynamics (MD) simulation with coarse-grained GB potential implemented in GALAMOST package to investigate the LC phase transitions for mesogens in small molecules, main-chain or side-chain polymers.

For identical mesogens in three different molecules, on cooling from fully isotropic melts, the small molecules form a single domain smectic-B phase, while the main-chain LC polymers prefer a single-domain nematic phase as a result of connective restraints in neighbouring mesogens. The phase transition of side-chain LC polymers undergoes a two-step process: nucleation of nematic islands and formation of multi-domain nematic texture.

Gives details of this alternative MD simulator for the GB potential

Motivation

Adequate descriptions of the LC systems require an accurate model for both inter- and intra-molecular interactions, and also require system sizes that are large enough to observe the effects of molecular ordering. A combination of coarse-grained Gay-Berne (GB) model and graphics processing units (GPU)-accelerated algorithms should be a highly promising way to provide simulation accuracy and efficiency in the study of larger systems considering more details of anisotropic particles, especially for LC phase transitions. Coarse graining as one of the conceptual and technical ways that smooths over or averages out some of fine details, has been widely used to simulate the longer time- and larger length-scale dynamics and phase behaviours. The coarse graining of LC through representing groups of atoms by single interaction sites leads to a remarkable acceleration in molecular simulation.

Simulation Settings - very useful for comparison!!

To study the LC phase transition of mesogens in different molecules, simulations are in NVT ensemble with periodic boundary condition is used. For mesogens in small molecular LC systems, the simulations are performed with 1000 mesogens. These three system have the same volume ($V = 15\sigma_0 \times 15\sigma_0 \times 15\sigma_0$) and volume fraction of particles ($\rho = 0.47$). Further, to confirm finite size effect in the simulation systems, we also carried out simulation in the simulation box with double size.

A standard leap-frog algorithm for anisotropic systems is used to solve the equations of motion, and the dimensionless MD time step $dt^* = (m\sigma_0^2 / \epsilon_0)^{(1/2)} dt = 0.001$. The reduced temperature $T^* = k_B T / \epsilon_0$ is controlled using Nose-Hoover thermostat with a relaxation time $\tau_T = 0.1$, where k_B is the Boltzmann constant. To observe the phase behaviour of the model systems, the simulated annealing process is applied to gradually cool down the systems from equilibrated isotropic melts. Systems are equilibrated for at least 1×10^{10} time steps for mesogens in small molecules and polymers, respectively. The mean properties are represented by statistical averages over ten samples evenly taken from the last 3×10^6 time steps.

Also outlines the derivation of the order parameter from the Q tensor!

Other Theory Papers

27 October 2020

14:13

Details of the simulation of the pair correlations of orientation (as well as a history of the field) is given in a separate page within the 'Project Records' section.

Tracing the phase boundaries of hard spherocylinders - Bolhuis and Frenkel (1997)

Abstract

We have **mapped out the complete phase diagram of hard spherocylinders as a function of the shape anisotropy L/D**. Special computational techniques were required to locate phase transitions in the limit $L/D \rightarrow \infty$ and in the close-packing limit for $L/D \rightarrow 0$. The phase boundaries of five different phases were established: the isotropic fluid, the liquid crystalline smectic A and nematic phases, the orientationally ordered solids—in AAA and ABC stacking—and the plastic or rotator solid. The

rotator phase is unstable for $L/D > 0.35$ and the AAA crystal becomes unstable for lengths smaller than $L/D = 7$. The triple points isotropic-smectic-A-solid and isotropic-nematic-smectic-A are estimated to occur at $L/D = 3.1$ and $L/D = 3.7$, respectively. For the low L/D region, a modified version of the Gibbs–Duhem integration method was used to calculate the isotropic-solid coexistence curves. This method was also applied to the I-N transition for $L/D > 10$. **For large L/D the simulation results approach the predictions of the Onsager theory.** In the limit $L/D \rightarrow \infty$ simulations were performed by application of a scaling technique. The nematic-smectic-A transition for $L/D \rightarrow \infty$ appears to be continuous. As the nematic-smectic-A transition is certainly of first order nature for $L/D < 5$, the tri-critical point is presumably located between $L/D = 5$ and $L/D = \infty$. In the small L/D region, the plastic solid to aligned solid transition is first order. Using a mapping of the dense spherocylinder system on a lattice model, the initial slope of the coexistence curve could even be computed in the close-packing limit.

Introduction

Intuitively, one associates increased order with a decrease in entropy. ***It is therefore surprising that a large number of phase transitions exist in which both the structural order and the entropy of the system increase.*** In particular, all ordering transitions in systems of particles that have exclusively hard-core interactions are of this type. Already in the forties, Onsager showed that thin hard rods must form a nematic liquid crystal at sufficiently high densities. Computer simulations of a variety of models of non-spherical hard-core models have since shown that excluded volume effects could not only account for the stability of nematics, but also for the existence of smectic and columnar liquid-crystalline phases (for a review, see Ref. 12!).

Methods

In our simulation studies of the equation of state of hard spherocylinders, we generated initial conditions both by expansion and by compression. Specifically, we prepared the configurations of a dense spherocylinder system in the following ways

- Expansion of a solid phase. A close-packed fcc lattice of spheres with its $\sim 111!$ plane in the xy plane was stretched in the z direction by a factor of (L/D) in order to accommodate a close-packed crystal of spherocylinders. This ABC-stacked lattice was subsequently expanded to the desired density and allowed to equilibrate. In the crystalline and smectic phases, the box shape should have the freedom to fluctuate in order to obtain an isotropic pressure.
- Compression of an isotropic liquid phase. At low density an ABC-stacked lattice of spherocylinders was allowed to melt into an isotropic liquid using NVT Monte Carlo. This configuration was subsequently compressed to the desired density using constant-NPT Monte Carlo and allowed to equilibrate again with constant-NVT Monte Carlo.
- Starting from a smectic configuration. The configuration obtained was subsequently compressed by NPT MC or expanded and allowed to equilibrate again.
- Starting from a nematic configuration. In studying the nematic-smectic transition by compression, it is preferable to start with a defect-free nematic phase. However, the nematic phase that forms upon compression of the isotropic liquid usually contains long-lived defects. To prepare a defect-free nematic phase, we first generated a hexagonal crystal lattice, then we allowed the spherocylinders to rotate but not yet translate in order to suppress an initial fast relaxation to the smectic phase.
 - After a few thousand cycles translation was allowed as well and the system was allowed to equilibrate. The equilibrated nematic configuration was compressed by NPT MC to the desired density and equilibrated again. In principle, we kept the box shape fixed in the nematic phase. However, close to the smectic phase boundary, where

appreciable smectic fluctuations are already present in the system, we found it advantageous to use VSMC even in the nematic phase, to speed up equilibration

Simulation Practicalities

To study the equation of state in the isotropic and solid phases for low L/D values, relatively small systems could be used O(10^2) particles. For the meso-phases it was often necessary to go to larger systems (O(10^3) particles.

Bulk of the simulation work here is done using a Monte Carlo approach; which is more accurate at sampling the entire subspace to find a global energy minimum phase. However this is difficult for phases which require large-scale changes to form order, so MD simulations are also used for nematic and smectic phase transitions. As a result of the reliance on MC however, a large section of the paper is devoted to calculating the free energy of various configurations. This paper also discussed the calculation of system pressure, as this is a primary factor in determining when a phase transition occurs.

The numerical study of the spherocylinder phase diagram for systems of longer rods is not different in principle from the study for shorter rods. However, in practice, there are many differences. Almost all of these differences imply that simulations of longer rods are more time consuming. For one thing, the simulation of long rods requires large system sizes. *The simulation box should be large enough to accommodate at least two rod lengths in order to avoid the situation that one particle can, at the same time, overlap with more than one periodic image of another particle.*

It is usually assumed that the nematic-to-smectic transition in the Onsager limit is continuous. However, there is no hard theoretical evidence to support this conjecture - this is discussed further in the paper

Evidence for algebraic orientational order in a two-dimensional hard-core nematic - Frenkel & Eppenga (1984)

Simulations of purely repulsive thin rigid rods in a 2D system

Abstract

We present Monte Carlo simulations on a two-dimensional (2D) fluid of N infinitely thin hard rods of length L ($N < 3200$). This system has an isotropic phase at low densities and a "nematic" phase at high densities. Although true long-range orientational order is not excluded a priori, the simulations indicate that the nematic phase has algebraic order. We find no evidence for a first order isotropic-nematic transition; rather, all the available evidence points towards the occurrence of a disclination-unbinding transition of the Kosterlitz-Thouless type. The heat capacity C_p peaks at a density some 20% below the estimated disclination-unbinding transition point. We discuss earlier simulations on 2D nematics in the light of the current results. We have computed the virial coefficients of the hard-needle fluid up to B5 and find that B4 is very small, while B5 is negative.

Results

Focuses on a proof by Straley that no true long-range order can exist in 2D nematics if the intermolecular potential is separable (i.e. can write as a product of functions for radial and orientational separation).

In order to distinguish between true long-range order, algebraic order and shortrange order it is essential to study system-size dependence of the nematic order parameter. We did this both by performing simulations on a variety of system sizes ranging from $N = 30$ to $N = 3200$ and by computing the order parameter for smaller subsystems formed by dividing a large system into 4, 16, or 64 blocks of equal area.

Our simulations suggest that a 2D nematic of hard needles has only quasi-LRO, i.e., the nematic order parameter vanishes in the thermodynamic limit and all order parameter correlation functions decay algebraically (i.e. polynomially).

Simulation study of a two-dimensional system of semi flexible polymers - Dijkstra & Frenkel (1994)

Abstract

We report (*Monte Carlo*) computer simulations of a two-dimensional system of semi flexible polymers consisting of infinitesimally thin hard segments connected by joints of variable flexibility. As the density is increased, we observe a transition from the isotropic phase to a "nematic" phase with quasi-long range orientational order. This transition appears to be of the Kosterlitz-Thouless type. We observe that, whereas at low densities the most rigid polymers have the lowest compressibility, the opposite is true at high densities. We argue that such behaviour is to be expected. Finally, we study the scaling behaviour of the elastic constants for splay and bend in the nematic phase and find good agreement with the relevant theoretical predictions.

Introduction

The study of semi flexible polymers was initiated by Flory in 1956, who modelled the polymers by self-avoiding random walks on a three-dimensional lattice. In his mean-field calculation, he obtained a first order phase transition from an isotropic phase to an orientationally ordered state, when the fraction of bent bonds exceeds a critical value. Other mean-field theories also predict this phase transition for three-dimensional lattice polymers. However, these results have been disputed on the basis of several exactly solvable models for three-dimensional polymers which show a continuous phase transition.

In this paper, we present a simulation study of a two dimensional off-lattice model of semi flexible polymers. In particular, we investigate whether this system exhibits an isotropic to nematic phase transition. We performed a series of grand canonical Monte Carlo (GCMC) simulations of semi flexible polymers with varying flexibility.

Results

For a dilute system the pressure decreases when the polymers become more flexible, but increases in dense systems. If we increase the density, we observe an isotropic-nematic phase transition with algebraic decay of orientational order. This transition appears to be of the Kosterlitz-Thouless type. The scaling behaviour of the elastic constants is found to be in good agreement with the theoretical predictions.

Methodology is rather focused on Monte-Carlo logistics, or mechanical properties (splay etc) and so less relevant to my project. May be able to compare semi-flexible nunchuck simulations to the phase diagrams here (they only have one bending point but this would give an OoM estimate.

Isotropic, nematic, and columnar ordering in systems of persistent flexible hard rods - Hentschke & Herzfeld (1991)

Considers flexible and semi-flexible polymer chains, and the effect of flexibility on phase transitions

Abstract

We extend previous work on the Khokhlov-Semenov approach to long-range order in solutions of persistent flexible main-chain polymers by including hexagonal columnar ordering. The description of long-range positional order uses a recent model developed for rigid rodlike particles, which is based on the trade-off of translational entropy between liquidlike and crystal-like dimensions. For moderately flexible polymers, we find an isotropic-nematic-columnar phase sequence with increasing polymer concentration. ***As the polymers become more flexible, the isotropic-nematic transition recedes to higher concentrations, until finally, near the wormlike chain limit, a direct isotropic-to-columnar transition occurs.*** We show that the corresponding triple point occurs at longer persistence lengths for polymers of increasing contour length. In addition, we show that the longitudinal packing in the columnar phase becomes much tighter with increasing molecular flexibility to accommodate greater lateral freedom. Finally, we compare our theoretical equation of state with experimental measurements for poly-benzyl-L-glutamate (PBLG).

Introduction

Khokhlov and Semenov (KS) were able to calculate the mean-field orientational (or confinement) entropy of a persistent flexible cylindrical fibre for arbitrary L/P. Their result does not depend explicitly on the external potential combining the polymer but is given in terms of the distribution function $f(n(\tau))$, where $n(\tau)$ is a tangential unit vector at position τ along the polymer contour. By expanding their expression for the orientational entropy at the two limits $L/P \ll 1$ and $L/P \gg 1$, and by employing a second order virial approximation of the hard-core interparticle interactions, ***KS obtained the isotropic-to-nematic coexistence densities, as well as the order parameter at the transition.*** However, the KS approach does not describe the effects of persistent flexibility on translationally ordered lyotropic liquid-crystalline phases, such as smectic phases.

Results

In this work, we calculate a phase diagram for hard flexible rodlike polymers in terms of polymer volume fraction v , polymer contour length L , and polymer persistence length P . If, for a given L the rods are sufficiently stiff (i.e. P is sufficiently large), then we obtain an isotropic-to-nematic-to-columnar phase sequence with increasing volume fraction. As the rods become more flexible, however, the isotropic-to-nematic phase transition recedes progressively to higher concentrations. Finally, for a small enough P , the nematic phase disappears, and there is a direct transition from the isotropic to the columnar phase. With increasing L , the corresponding triple points shift to larger values of P . However, as L approaches infinity, the triple-point value of P asymptotically approaches a finite value, so that for persistence lengths beyond this value there is always a stable nematic phase, even for an arbitrarily large contour length.

Gives an interpolated expression for sigma (orientational free energy) combining expressions for flexible and rigid polymer rods. This enables prediction of the critical volume fraction at the phase transition for different L/D ratios. The results are only given for larger values of L/D however, which may be harder to interpret.

$$\sigma = [\sigma_{\text{rigid}}^{(0)} + (s\sigma_{\text{rigid}}^{(0)} + \sigma_{\text{rigid}}^{(1)}) (L/P) \\ + s\sigma_{\text{wormlike}}^{(0)} (L/P)^2] / [1 + s(L/P)],$$

Structure and Interfacial Tension of a Hard-Rod Fluid in Planar Confinement - Brumby et al. (2017)

Abstract

The structural properties and interfacial tension of a fluid of rodlike hard-spherocylinder particles in contact with hard structureless flat walls are studied by means of Monte Carlo simulation. The calculated surface tension between the rod fluid and the substrate is characterized by a nonmonotonic trend as a function of the bulk concentration (density) over the range of isotropic bulk concentrations. As suggested by earlier theoretical studies, a surface-ordering scenario is confirmed by our simulations: the local orientational order close to the wall changes from uniaxial to biaxial nematic when the bulk concentration reaches about 85% of the value at the onset of the isotropic–nematic phase transition. The surface ordering coincides with a wetting transition whereby the hard wall is wetted by a nematic film. Accurate values of the fluid–solid surface tension, the adsorption, and the average particle–wall contact distance are reported (over a broad range of densities into the dense nematic region for the first time), which can serve as a useful benchmark for future theoretical and experimental studies on confined rod fluids. The simulation data are supplemented with predictions from second-virial density functional theory, which are in good qualitative agreement with the simulation results.

Describes the effects of walls on our hard rod system, describes density functional theory for a confined rod

The Study of the Structure and Properties of Nematic, Smectic and Cholesteric Liquid Crystals by the Molecular Dynamics - Tsykalo (1985)

Introduction

This paper discussed the main results of studying anisotropic systems by methods of computer experiments (the molecular dynamics method and that of Monte Carlo). It gives the description of the molecular dynamic model and the technique of molecular dynamic modelling liquid crystals of different types (nematic, smectic, cholesteric, as well as films of liquid crystals). Special attention is paid to the choice of the pair potential of interaction which takes into account anisotropic of the dispersion attraction and form peculiarities of molecules as well as specific contributions to the interaction energy (which result in the formation of twisted cholesteric structures, smectic layers, etc.) The model of “a molecule in a molecule” is suggested to describe the smectic state.

According to the results of computer experiments some values were calculated such as structure characteristics of different liquid crystals and films of liquid crystals (order parameters, orientational and translational distribution functions, coordination numbers), characteristics of dynamic behaviour of particles (mean square displacements, time correlation function, time of correlation and that of relaxation), as well as physical and chemical properties (pressure, energy, heat capacity, sound velocity, coefficients of compressibility, coefficients of self-diffusion).

Method

In this paper liquid crystals of three types-nematic (NLC), smectic (SLC), cholesteric (CLC) were studied by the molecular dynamics method. Special attention was paid to the pair potential of interaction, where a Gay-Berne potential was used.

In the SLC case the **model of a “molecule in a molecule” is used**. A smaller ellipsoid is located in every large elongated ellipsoid. Large ellipsoids interact with one another according to the law of power repulsion (the first addendum of the potential takes into account relatively “soft” repulsion of end chains of smectics molecules and more “rigid” repulsion of central parts of these molecules). Smaller ellipsoids attract each other (the second addendum of the potential takes into account dispersive attraction of benzene ring of molecules central parts).

The statistical problem was solved by numerical integrating the system of motion equations for 108, 168 or 256 ellipsoidal particles (each of which had five powers of freedom) placed into the basic sample which had the form of a cube or a rectangular parallelepiped. Periodical boundary conditions were imposed on the planes of the basic sample, which presented the possibility to simulate an infinitely large system with translational periodicity.

Results

Peculiarities of molecules locations in smectic layers can be described by the binary distribution functions $g(r/\sigma_0)$. Their forms give the possibility to distinguish SLC A (the comparatively smaller first maxima and attenuation of oscillations at large distances) from SLC B (the higher first maximum and availability of long-range ordering which shows itself in the existence of oscillation even at large distances). The molecular dynamics method for SLC was used to determine not only orientational order parameters, but also translational and mixed order parameters. **In case of CLC, one can observe spontaneous twisting of conditionally chosen molecular layers so that the directors for such layers composed a typical cholesteric spiral.**

Structure of CCH5 in the isotropic and nematic phases:
a computer simulation study Wilson & Allen (2006)

Abstract

We have studied the single particle structural properties of the nematogen trans4-(trans-4-n-pentylcyclohexyl)cyclohexylcarbonitrile (CCHS) by molecular dynamics simulation using realistic atom-atom potentials. On going from the isotropic phase at 390K to the nematic phase at 350K, the molecules become significantly longer and thinner, as indicated by the equivalent molecular moment of inertia spheroid and the distribution of trans and gauche bonds. This change is only partly accounted for by the lowering of the temperature, there being a significant quenching effect due to the change in the molecular environment. This quenching effect is also apparent in the distribution of molecular shapes seen in molecular width-breadth contour maps. In the nematic phase, at 350K, the distributions of alkyl tail bond orientations with respect to the director show a pronounced odd-even effect, with peaks in the distributions occurring alternately parallel to, and at an angle to, the director.

Methods

We have carried out molecular dynamics calculations on samples of 128 CCHS molecules at three temperatures: 350 K and 370 K in the nematic phase (corresponding respectively to average order parameters of 0.62 and 0.38), and 390 K in the pretransitional region of the isotropic phase. The simulations were carried out for, respectively, 662, 720 and 648 ps, using the AMBER potential energy function:

$$V_{\text{total}} = \sum_{\text{bonds}} K_r (r - r_{\text{eq}})^2 + \sum_{\text{bending angles}} K_\theta (\theta - \theta_{\text{eq}})^2 + \sum_{\text{dihedral angles}} \frac{V_n}{2} (1 + \cos(n\phi - \gamma)) + \sum_{i < j} \left(\frac{q_i q_j}{R_{i,j}} + \frac{A_{i,j}}{R_{i,j}^{12}} - \frac{C_{i,j}}{R_{i,j}^6} \right), \quad (1)$$

The parameter values used here, more details of the dihedral angle calculations and conformational changes are given in the paper, ***which provides a useful example of generating such a potential energy.***

Also gives an extensive description of use of the Q-tensor approach for calculating the order parameter.

Liquid Crystal Phase in DNA - Assawasunthonnet Thesis

Abstract

Liquid crystal phase is an emergent phase in many of the condensed matter and biological systems it has properties between those of normal crystalline solid and liquid. In this paper a brief introduction to different types of liquid crystal ordering is given. Features and properties observed in liquid crystals are presented. The rest will discuss a specific system namely the liquid crystal phases due to the helix-helix interaction in DNA. Qualitatively I will argue that DNA in electrolyte solution should exhibit liquid crystal phase transition. Experimental results confirming the existence are presented. A theory based on mean field approach will also be discussed

Contents

- Provides an introduction on the history and (very) basic theory of liquid crystals phases in DNA
- Details of application to (and detection via) NMR
- Basic introduction to Landau theory in the context of the nematic phase
- Application of Poisson-Boltzmann theory to consider interactions between DNA strands

Other Experimental Papers

20 February 2021

13:00

A useful summary the historical developments in this field (ie the liquid crystal phases of DNA) is provided in 'clark.pdf'; a presentation by Nakata et al.

Nakata/Zanchetta et al. - DNA duplex Liquid Crystals

This group wrote two separate papers on these systems, detailed below:

End-to-End Stacking and Liquid Crystal Condensation of 6–20 Base Pair DNA Duplexes - 2007

Abstract Section:

Short complementary B-form DNA oligomers, 6 to 20 base pairs in length, are found to exhibit nematic and columnar liquid crystal phases, even though such duplexes lack the shape anisotropy required for liquid crystal ordering. Structural study shows that these phases are produced by the end-to-end adhesion and consequent stacking of the duplex oligomers into polydisperse anisotropic rod-shaped aggregates, which can order into liquid crystals.

Introduction:

The ability of duplex DNA to form liquid crystal (LC) phases when hydrated has been known since the late 1940s and played a crucial role in deciphering its structure, through the measurement of the x-ray structure factor of a single chain uncomplicated by interchain correlations (1–3).

Since that time, the LC phases of solutions of duplex B-form* DNA (B-DNA) have been extensively characterized by optical, x-ray, and magnetic resonance methods for chain lengths N, ranging from mega-base pair semiflexible polymers down to approximately 100 bp rigid rodlike segments**, comparable in size to the B-DNA bend persistence length 50 nm (13).

These studies of long DNA (lDNA) have revealed an isotropic phase (I); chiral nematic (N), uniaxial columnar (CU), and higher-ordered columnar (C2) liquid crystal phases; and crystal (X) phases, with increasing DNA concentration. The appearance of such LC phases has been accounted for theoretically by modelling B-DNA as a repulsive rigid or semiflexible rod-shaped solute. The basic model is Onsager's treatment of monodisperse repulsive hard rods (length L, diameter D) (14), which, if they are sufficiently anisotropic in shape, nematic order for volume fraction $\phi > 4D/L$.

*Common form of DNA (when hydrated).

There is a useful review article on this matter (with a superb bibliography) [Colloidal DNA - ScienceDirect \(cam.ac.uk\)](#) by Podgornik et al.

** [Liquid crystal formation in DNA fragment solutions - Kassapidou - 1998 - Biopolymers - Wiley Online Library \(cam.ac.uk\)](#) (Liquid crystal formation in DNA fragment solutions, K. Kassapidou et al.)

Phase separation and liquid crystallization of complementary sequences in mixtures of nanoDNA oligomer - 2008

Abstract Section:

We have studied the phase behaviour of mixtures of 12- to 22-bp-long nanoDNA oligomers using optical microscopy. The mixtures are chosen such that only a fraction of the sample is composed of mutually complementary sequences, and hence the solutions are effectively mixtures of single-stranded and double-stranded (duplex) oligomers. When the concentrations are large enough, such mixtures phase-separate via the nucleation of duplex-rich liquid crystalline domains from an isotropic background rich in single strands.

Motivation

We know that biological molecules are crowded in the cellular interior, and this close packing may lead to spontaneous organisation/ordering of biological macromolecules. In particular, highly concentrated DNA in the cell nucleus may form ordered mesophases in vivo, although it is unknown if this represents an evolutionary advantage.

This liquid-crystalline phase behaviour has previously been observed by self-complementary 6- to 20-bp nDNA sequences and for mutually complementary sequences in the same length range. Here we explore the phase behaviour of mixtures of nDNA where some of the sequences are complementary (and able to pair in double strands), and some are not (therefore remaining in solution as single strands).

We have found that in concentrated mixtures of DS and SS nDNA, the system phase-separates into duplex (DS)-rich liquid crystal (LC) domains coexisting with a duplex-poor isotropic phase. This leads to the physical segregation of 4- to 6-nm-long complementary chains from non-complementary ones (that remain as SS-DNA). This segregation is required to form LC phases, as the complementary sequence concentration would not be sufficient to form LC phases alone.

It is also worth noting that this phase formation is reliant on end-to-end adhesion of duplexes (and no LC phases form if this is suppressed via steric hindrance at the duplex ends for example). This work informs research more generally on the entropic forces driving phase formation on the nanoscale.

Experimental Details

- Use of optical microscopy and fluorescence to identify phase structure, although fluorescent moiety disturbs LC ordering.
- Focus on temperature variation to determine thermotropic phase behaviour, and measurement of the energy driving of phase separation

Liquid Crystal Ordering and Isotropic Gelation in Solutions of Four-Base-Long DNA Oligomers - Fraccia (2016)

While from the same group, this considers a different self-assembly process to form liquid crystals from short oligomers

Abstract

Liquid crystal ordering is reported in aqueous solutions of the oligomer 5'-ATTAp-3' and of the oligomer 5'-GCCGp-3'. In both systems, we quantitatively interpret ordering as stemming from the chaining of molecules via a "running-bond" type of pairing, a self-assembly process distinct from the duplex aggregation previously reported for longer oligonucleotides. While concentrated solutions of 5'-ATTAp-3' show only a columnar liquid crystal phase, solutions of 5'-GCCGp-3' display a rich phase

diagram, featuring a chiral nematic phase analogous to those observed in solutions of longer oligonucleotides and two unconventional phases, a columnar crystal and, at high concentration, an isotropic amorphous gel. The appearance of these phases, which can be interpreted on the basis of features of 5'-GCCGp-3'molecular structure, suggests distinctive assembly motifs specific to ultrashort oligonucleotides.

Background

Here, we report that solutions of ultrashort DNA oligomers have a (surprisingly) rich phase diagram at and above room temperature (T) and at concentrations about 1 M nucleobases, featuring chiral nematic and columnar LC phases, columnar crystals, and high-density isotropic gel.

Previous investigations described a mechanism for LC ordering of DNA oligomers through a three-step self-assembly process. First, oligomers hybridize into duplexes, which are stable at T below their melting. Second, duplexes form linear aggregates. Such aggregation is mediated by either base stacking of terminal bases in the case of blunt-ended duplexes or by pairing of terminal sections when duplexes terminate with interacting overhangs. Third, linear aggregates align and form a LC phase.

Although these steps mutually strengthen, with LC ordering enhancing chaining and duplex stability, no LC ordering was previously observed for oligomers too short to form stable duplexes. Indeed, when we observed that LC phases of six-base-long oligomers were pushed at large DNA concentration (cDNA) and low T , we assumed that four-base long oligomers would not order, being that their duplexes are unstable at all T above freezing at "ordinary" (less than micromolar) concentrations. Moreover, shorter oligomers imply more flexibility of the aggregates, which is a destabilizing factor for LC ordering. *N.B This phase formation is highly dependant on the base pair specific interaction potentials at this resolution.*

This also has implication for research on the origins of life through the role of supramolecular structuring in the first appearance of nucleic acid polymers in the early Earth. However the availability of long enough nucleic acid chains, sufficiently homogeneous in the main chain and carrying a small set of weakly polymorphic side groups capable of pairing, is yet to be understood.

Thermotropic liquid crystals from biomacromolecules - Liu et al (2014)

Abstract:

Complexation of biomacromolecules (e.g., nucleic acids, proteins, or viruses) with surfactants containing flexible alkyl tails, followed by dehydration, is shown to be a simple generic method for the production of thermotropic liquid crystals. The anhydrous smectic phases that result exhibit biomacromolecular sublayers intercalated between aliphatic hydrocarbon sublayers at or near room temperature. Both this and low transition temperatures to other phases enable the study and application of thermotropic liquid crystal phase behaviour without thermal degradation of the biomolecular components.

Motivation:

Liquid crystals (LCs) found in biology are usually dispersed in a solvent, typically water, and are therefore classified as lyotropic. However, from a technological perspective, thermotropic LCs (TLCs), typically based on small rod- or disc-shaped organic molecules, have been of much greater importance. In this contribution, we show that thermotropic liquid crystal phases and materials can

also be made from biomolecules, demonstrating a simple generic method to form thermotropic phases from biosystems ranging from nucleic acids and proteins to even whole viruses, spanning a size from only a few nanometers to 1 μ m.

Results

We demonstrate that biological TLCs (thermotropic liquid crystals) can be made from a remarkable range of biomolecules and bio-inspired molecules, including nucleic acids, polypeptides, fusion proteins, and viruses. TLC materials typically combine rigid or semirigid anisometric units, which introduce orientational anisotropy, with flexible alkyl chains, which suppress crystallization. In the present experiments, negatively charged biomolecules and bio-inspired molecules act as rigid parts, and cationic surfactants make up the flexible units to produce TLC phases with remarkably low LC-isotropic clearing temperatures, which is another TLC signature. Electrostatic interactions couple these rigid and flexible components into hybrid assemblies, which then order into lamellar phases of alternating rigid and flexible layers stabilized by the tendency in TLCs for rigid and flexible to spatially segregate.

Multiple liquid crystal phases of DNA at high concentrations - Strzeleck et al. (1988)

Details the chiral phases of DNA observed experimentally, and logistics of such measurements

Abstract

DNA packaging in vivo is very tight, with volume concentrations approaching 70% w/v in sperm heads, virus capsids and bacterial nucleoids. The packaging mechanisms adopted may be related to the natural tendency of semi-rigid polymers to form liquid crystalline phases in concentrated solutions. We find that DNA forms at least three distinct liquid crystalline phases at concentrations comparable to those in vivo, with phase transitions occurring over relatively narrow ranges of DNA concentration. A weakly birefringent, dynamic, 'precholesteric' mesophase with microscopic textures intermediate between those of a nematic and a true cholesteric phase forms at the lowest concentrations required for phase separation. At slightly higher DNA concentrations, a second mesophase forms which is a strongly birefringent, well-ordered cholesteric phase with a concentration-dependent pitch varying from 2 to 10 micrometres. At the highest DNA concentrations, a phase forms which is two-dimensionally ordered and resembles smectic phases of thermotropic liquid crystals observed with small molecules.

Theoretical Background

Ordering of semi-rigid polymers at high concentrations occurs spontaneously to minimize the macromolecular excluded volume. Semi-rigid polyelectrolyte behaviour is complicated by charge-shielding requirements. A strong polyelectrolyte is surrounded by a counterion layer which determines the effective axial ratio and excluded volume. Because polymer phase behaviour depends on the effective polymer dimensions, the critical concentration for DNA ordering is a sensitive function of ionic strength and counterion type.

Refusing to Twist: Demonstration of a Line Hexatic Phase in DNA Liquid Crystals - Strey et al. (2000)

Abstract

We report conclusive high resolution small angle x-ray scattering evidence that long DNA fragments form an untwisted line hexatic phase between the cholesteric and the crystalline phases. The line hexatic phase is a liquid-crystalline phase with long-range hexagonal bond-orientational order, long-range nematic order, but liquidlike, i.e., short-range, positional order. So far, it has not been seen in any other three dimensional system. By line-shape analysis of x-ray scattering data we found that positional order decreases when the line hexatic phase is compressed. We suggest that such anomalous behaviour is a result of the chiral nature of DNA molecules.

Experimental Detail

Oriented DNA sheets were prepared from calf thymus DNA (Pharmacia) with an average molecular weight (MW) of 10^7 (corresponding to a contour length of 5 micrometres or some 100 persistence lengths of 50 nm) by wet-spinning and then drying. Preliminary x-ray scattering measurements were performed on a rotating anode x-ray generator. The synchrotron x-ray scattering reported here was performed at the National Synchrotron Light Source (NSLS) on Exxon's beam line X10A.

Liquid Crystalline Phases of DNA - (Peng thesis)

Provides a basic but useful summary of the physical properties of DNA

Abstract

The DNA molecule is the support of the genetic information. It is a right-handed double helix, 22 angstrom in diameter, and 50 nm in the persistence length. The two strands of the helix are complementary in their nucleotide sequence with about 10 nucleotide pairs per helical turn. DNA is a long and strongly charged heteropolymer. It bears on average one elementary negative charge per each 0.17 nm of the double helix. In the late 1940s, the ability of duplex DNA to form liquid crystal (LC) phases when hydrated was known. Since that time, the LC phases of solutions of duplex B-form DNA (B-DNA) have been extensively characterized. The chain length N of DNA ranges from mega-base pair (bp) semiflexible polymers down to approximately 100 bp rigid rodlike segments. These studies of long DNA (lDNA) have revealed cholesteric, columnar hexagonal and blue liquid crystalline phases. In 2007, Michi Nakata and his collaborators found nematic and columnar liquid crystal phases in the short complementary B-form DNA oligomers with 6 to 20 base pairs in length. Structural study shows that these phases are produced by the end-to-end adhesion and consequent stacking of the duplex oligomers into polydisperse anisotropic rod-shaped aggregates, which order into liquid crystals.

Features of the DNA Double Helix

DNA is a normally double stranded macromolecule. Two polynucleotide chains, held together by weak thermodynamic forces, form a DNA molecule.

- Two DNA strands form a helical spiral, winding around a helix axis in a right-handed spiral
- The two polynucleotide chains run in opposite directions
- The sugar-phosphate backbones of the two DNA strands wind around the helix axis like the railing of a spiral staircase
- The bases of the individual nucleotides are on the inside of the helix, stacked on top of each other like the steps of a spiral staircase

Liquid crystal phases of long DNA

The ability of duplex DNA to form liquid crystals (LC) phases was found in the late 1940s. Since that time, the LC phases of solution of duplex B-form DNA (B-DNA) have been extensively characterized optical, X-ray, and magnetic resonance methods. These studies have revealed an isotropic phase (I),

chiral nematic (N^*), blue and hexagonal liquid crystal phases with increasing DNA concentration. Linear DNA fragments in aqueous solution form multiple liquid crystal phases whose nature depends on the polymer concentration. By polarizing and electron microscopy and both methods, even X-ray diffraction method, when increasing the polymer concentration, the phases sequence is described quite precisely, as schematically presented here: DNA concentration. When increasing the DNA concentration, the isotropic solution transforms into either blue phase or pre-cholesteric stage and then into a cholesteric phase which turns itself into columnar hexagonal. More concentrated systems give a true crystalline phase.

(Then gives further details of the cholesteric, blue and hexagonal columnar phases)

Liquid crystal phases of short DNA

As mentioned above, there are various liquid crystal phases in the long DNA with chain length N ranging from mega-base pair (bp) semiflexible polymers down to approximately 100 bp rigid rodlike segments, comparable in size to the B-DNA persistence length (about 50 nm). For a long time, it has been confirmed that there should be no LC phase for $L/D < 4.7$ ($N < 28$). In 2007, however, Michi Nakata and co-workers found the nematic and columnar liquid crystal phases in short complementary B-form DNA oligomers with 6-20 base pairs in length.

Computation Resources

27 February 2021

15:57

The primary resource here is "Computer Simulations of Phase Transitions in Liquid Crystals" by Daan Frenkel - Chapter 5 of the book "Phase Transitions in Liquid Crystals", edited by S. Martellucci and A. N. Chester.

- Introduction and Comparison of Monte Carlo and MD approaches
- Measurement and error in thermodynamic properties
- Phase transition theory (focus on isotropic-nematic transition discovery)

He also considers other phases, however further analysis of these is limited by the absence of an equivalent analytic theory for such systems, compared to Onsager's theory for nematic ordered phases.

However, he does suggest that a system of parallel hard spherocylinders does form a smectic phase for length-to-width ratios $L/D > 0.5$. It is unclear though whether this is maintained once rotations are allowed.

Density-functional theories for hard spherocylinder systems have been proposed by Holyst and Poniewiersk and by Somoza and Tarazona. Both theories predict the presence of a stable smectic phase if the length-to-width ratio L/D exceeds a minimum value of 3. However, the two theories differ in their estimate of the point where the nematic-smectic transition has its tri-critical point.

Molecular simulation of liquid crystals - Allen (2019)

Abstract

This article reviews recent progress in the computer simulation of liquid crystals at the molecular level. It covers the use of simple rigid-body models of the constituent molecules, and more detailed modelling via atomistic force fields. Bulk mesophases, inhomogeneous systems, and interfaces are discussed. Recent progress in calculating elastic properties and dynamics is summarised. As well as presenting an overview, some specific topics of recent interest are highlighted: the biaxial nematic phase, chiral phases, ionic liquid crystals, and charge-transfer systems.

Structure

Sections 2–4 introduce the most commonly used molecular models in increasing order of complexity: simple rigid particles, rigid and semiflexible chains, and atomistic force fields. In each case, references will be made to the corresponding mesophases. Sections 5 and 6 highlight two areas in which significant recent progress has been made: investigating the features which stabilise the biaxial nematic phase, and simulating chiral phases, respectively. Section 7 covers simulations of liquid crystals at interfaces, and confined in different geometries, including the case of embedded nanoparticles. The use of simulations to investigate elastic and dynamical properties of mesophases is covered in Section 8. Finally, Sections 9 and 10 outline two topics which seem to have grown significantly in importance over the last few years: ionic liquid crystals and charge transport.

A very useful review article on the topic; covers the basics for simulation

- *Introduces early work on rods composed of fused hard spheres*
- *"as a rough guideline, simulations of order 50 ns are now thought necessary to check mesophase stability"*

Also has an earlier review article: [Full article: Progress in computer simulations of liquid crystals \(cam.ac.uk\)](#) <https://doi-org.ezp.lib.cam.ac.uk/10.1080/01442350500361244>

Computational design of probes to detect bacterial genomes by multivalent binding - Curk

Not directly relevant, but gives an academic description of the use of LAMMPS simulation, and particularly interpreting natural units

Other Resources

28 February 2021

18:44

Interview with Daan Frenkel, Boltzmann Medallist 2016 : Simulating soft matter through the lens of statistical mechanics

<https://pubmed.ncbi.nlm.nih.gov/27349557/>

Daan Frenkel has been awarded the most important prize in the field of statistical mechanics, the 2016 Boltzmann Medal, named after the Austrian physicist and philosopher Ludwig Boltzmann. The award recognises Frenkel's seminal contributions to the statistical-mechanical understanding of the kinetics, self-assembly and phase behaviour of soft matter. The honour recognises Frenkel's highly creative large-scale simulations of soft matter capable of explaining the self-assembly of complex macromolecular systems, colloidal and biomolecular systems. In this interview with Sabine Louët, Frenkel gives his views on statistical physics, which has become more relevant than ever for interdisciplinary research. He also offers some pearls of wisdom for the next generation Statistical Mechanics experts.

*"Being a scientist is not a profession, it is an attitude.
It is my attitude. Hence, I find it hard to imagine working
outside a scientific discipline. But it does not have to
be physics. If I had to start now, I would probably apply
statistical physics thinking to understand the relation
between the microbiome and its host."*

*"Choose any topic that you find really interesting! Plan
as if you'll live forever and live as if you'll die tomorrow,
to use a rather "New Age" quote. The topic you choose
does not need to be a hot or fashionable topic, as there is
always a risk you may be given the leftovers of the field.
The skills that you acquire can be applied in all branches
of science and beyond."*

It is worth noting that the interview with Yves Pomeau, the other Boltzmann Medallist of 2016, is rather more depressing and highlights the issues in funding allocation facing modern physics (and particularly statistical physics)!

Simulations: The Dark Side - Daan Frenkel

[1211.4440.pdf \(arxiv.org\)](https://arxiv.org/pdf/1211.4440.pdf)

This paper discusses the Monte Carlo and Molecular Dynamics methods. Both methods are, in principle, simple. However, simple does not mean risk-free. In the literature, many of the pitfalls in the field are mentioned, but usually as a footnote – and these footnotes are scattered over many papers. The present paper focuses on the ‘dark side’ of simulation: it is one big footnote. I should stress that ‘dark’, in this context, has no negative moral implication. It just means: under-exposed.

I will discuss three types of issues:

1. Computer simulation methods that seem simple . . . yet require great care
2. Computer simulation methods that seem reasonable . . . but are not
3. Myths and misconceptions

Increasingly, simulations are used to complement experiment or, more precisely, to guide experiments in such a way that they can focus on the promising compounds or materials. This is the core of the rapidly growing field of computational materials science and computational ‘molecular’ design. Using computer simulations we can pre-screen candidate substances to minimise the amount of experimental work needed to find a substance that meets our requirements. In addition, simulations are very useful to predict the properties of materials under conditions that are difficult to achieve in controlled experiments (e.g. very high temperatures or pressures).

There is much further discussion in this paper of many interesting aspects to molecular dynamics simulations, and while I am reassured that I am avoiding the primary ‘common sins’ it will continue to be a useful reference!

LAMMPS

Chapter Introduction

16 October 2020

19:30

This (rather short) chapter documents my attempts to get to grips with LAMMPS - the primary simulation software used in this project. It acts as a record of the processes required to download and set up this software, so that this process may be replicated in the future. A pre-built windows package was used for this.

It also contains a guide on the basic details of running and writing scripts on LAMMPS; this is not meant to be comprehensive and (quite naturally) only covers concepts applied in my own primary scripts.

It is worth noting that some of the material contained here is a result of advice from Jiaming/Erika, and so may be duplicated from the Meetings Summary chapter. Similarly other sections may be copied from the LAMMPS documentation - I make no claim that all the words here are my own.

Software Introduction

16 October 2020

21:14

LAMMPS stands for Large-scale Atomic/ Molecular Massively Parallel Simulator. LAMMPS is a classical molecular dynamics simulation code with a focus on materials modeling. It was designed to run efficiently on parallel computers. It was developed originally at Sandia National Laboratories, a US Department of Energy facility. The majority of funding for LAMMPS has come from the US Department of Energy (DOE). LAMMPS is an open-source code, distributed freely under the terms of the GNU Public License (GPL).

The Manual

The content for this manual is part of the LAMMPS distribution. You can build a local copy of the Manual as HTML pages or a PDF file, by following the steps on the Build the LAMMPS documentation page. The manual is organized in two parts: 1) the User documentation for how to install and use LAMMPS and 2) the Programmer documentation for how to write programs using the LAMMPS library from different programming languages and how to modify and extend LAMMPS.

This is available at <https://lammps.sandia.gov/doc/Manual.html>

Overview

LAMMPS is a classical molecular dynamics (MD) code that models ensembles of particles in a liquid, solid, or gaseous state. It can model atomic, polymeric, biological, solid-state (metals, ceramics, oxides), granular, coarse-grained, or macroscopic systems using a variety of interatomic potentials (force fields) and boundary conditions. It can model 2d or 3d systems with only a few particles up to millions or billions.

LAMMPS can be built and run on a laptop or desktop machine, but is designed for parallel computers. It will run on any parallel machine that supports the MPI message-passing library. This includes shared-memory boxes and distributed-memory clusters and supercomputers.

LAMMPS is written in C++. Earlier versions were written in F77 and F90. See the History page of the website for details. All versions can be downloaded from the LAMMPS website.

LAMMPS is designed to be easy to modify or extend with new capabilities, such as new force fields, atom types, boundary conditions, or diagnostics. See the Modify doc page for more details.

In the most general sense, LAMMPS integrates Newton's equations of motion for a collection of interacting particles. A single particle can be an atom or molecule or electron, a coarse-grained cluster of atoms, or a mesoscopic or macroscopic clump of material. The interaction models that LAMMPS includes are mostly short-range in nature; some long-range models are included as well.

LAMMPS uses neighbor lists to keep track of nearby particles. The lists are optimized for systems with particles that are repulsive at short distances, so that the local density of particles never becomes too large. This is in contrast to methods used for modeling plasma or gravitational bodies (e.g. galaxy formation).

On parallel machines, LAMMPS uses spatial-decomposition techniques to partition the simulation domain into small sub-domains of equal computational cost, one of which is assigned to each processor. Processors communicate and store "ghost" atom information for atoms that border their sub-domain.

Features

LAMMPS is a classical molecular dynamics (MD) code with these general classes of functionality:

- General features
- Particle and model types
- Interatomic potentials (force fields)
- Atom creation
- Ensembles, constraints, and boundary conditions
- Integrators
- Diagnostics

- Output
- Multi-replica models
- Pre- and post-processing
- Specialized features (beyond MD itself)

General features

- runs on a single processor or in parallel
- distributed-memory message-passing parallelism (MPI)
- spatial-decomposition of simulation domain for parallelism
- open-source distribution
- highly portable C++
- optional libraries used: MPI and single-processor FFT
- GPU (CUDA and OpenCL), Intel Xeon Phi, and OpenMP support for many code features
- easy to extend with new features and functionality
- runs from an input script
- syntax for defining and using variables and formulas
- syntax for looping over runs and breaking out of loops
- run one or multiple simulations simultaneously (in parallel) from one script
- build as library, invoke LAMMPS through library interface or provided Python wrapper
- couple with other codes: LAMMPS calls other code, other code calls LAMMPS, umbrella code calls both

Particle and model types

(atom style command)

- coarse-grained particles (e.g. bead-spring polymers)
- united-atom polymers or organic molecules
- all-atom polymers, organic molecules, proteins, DNA
- Metals
- granular materials
- coarse-grained mesoscale models
- finite-size spherical and ellipsoidal particles
- finite-size line segment (2d) and triangle (3d) particles
- point dipole particles
- rigid collections of particles
- hybrid combinations of these coarse-grained

Interatomic potentials

(force fields)(pair style, bond style, angle style, dihedral style, improper style, kspace style commands)

Ensembles, constraints, and boundary conditions

(fix command)

- 2d or 3d systems
- orthogonal or non-orthogonal (triclinic symmetry) simulation domains
- constant NVE, NVT, NPT, NPH, Parrinello/Rahman integrators
- thermostating options for groups and geometric regions of atoms
- pressure control via Nose/Hoover or Berendsen barostatting in 1 to 3 dimensions

- simulation box deformation (tensile and shear)harmonic (umbrella) constraint forces
- rigid body constraints
- SHAKE bond and angle constraints
- Monte Carlo bond breaking, formation, swapping
- atom/molecule insertion and deletion
- walls of various kinds
- non-equilibrium molecular dynamics (NEMD)
- variety of additional boundary conditions and constraints

Output

(dump, restart commands)

- log file of thermodynamic info
- text dump files of atom coords, velocities, other per-atom quantities
- binary restart files
- parallel I/O of dump and restart files
- per-atom quantities (energy, stress, centro-symmetry parameter, CNA, etc)
- user-defined system-wide (log file) or per-atom (dump file) calculations
- spatial and time averaging of per-atom quantities
- time averaging of system-wide quantities
- atom snapshots in native, XYZ, XTC, DCD, CFG formats

Pre- and post-processing

A handful of pre- and post-processing tools are packaged with LAMMPS, some of which can convert input and output files to/from formats used by other codes; see the Tools doc page.

Our group has also written and released a separate toolkit called Pizza.py which provides tools for doing setup, analysis, plotting, and visualization for LAMMPS simulations.

Pizza.py is written in Python and is available for download from the Pizza.py WWW site.

Software Summary

13 October 2020

20:52

This contains a list of useful features I will likely want to apply in my project, as well as a summary of the software.

Summary

LAMMPS stands for Large-scale Atomic/ Molecular Massively Parallel Simulator. LAMMPS is a classical molecular dynamics simulation code with a focus on materials modeling. It was designed to run efficiently on parallel computers.

It can model atomic, polymeric, biological, granular, coarse-grained, or macroscopic systems using a variety of interatomic potentials (force fields) and boundary conditions. It can model 2d or 3d systems with only a few particles up to millions or billions. LAMMPS can be built and run on a laptop or desktop machine, but is designed for parallel computers.

In the most general sense, LAMMPS integrates Newton's equations of motion for a collection of interacting particles. A single particle can be an atom or molecule or electron, a coarse-grained cluster of atoms, or a mesoscopic or macroscopic clump of material. The interaction models that LAMMPS includes are mostly short-range in nature; some long-range models are included as well.

LAMMPS uses neighbor lists to keep track of nearby particles. The lists are optimized for systems with particles that are repulsive at short distances, so that the local density of particles never becomes too large. On parallel machines, LAMMPS uses spatial-decomposition techniques to partition the simulation domain into small sub-domains of equal computational cost, one of which is assigned to each processor. Processors communicate and store “ghost” atom information for atoms that border their sub-domain.

Features

The particle type I will be using is likely coarse-grained particles (e.g. bead-spring polymers), although it specifically mentions implementations for organic molecules, proteins and DNA as well.

For interatomic potentials, there is a particularly useful angle potential, for use between three particles, which I may use easily in the Nun-chucks simulation based on the OxDNA data. LAMMPS is also optimised for repulsive short distance potentials, to avoid particle overlap.

In terms of ensemble constraints, as well as multiple wall types, there are also thermosetting and pressure control options to maintain the thermodynamic properties of the system.

It will output thermodynamic info, as well as a text dump files of atom coordinates, velocities, other per-atom quantities. User-defined system-wide (log file) or per-atom (dump file) calculations are also possible, with spatial and time averaging of per-atom quantities, and time averaging of system-wide quantities.

Our group has also written and released a separate toolkit called Pizza.py which provides tools for doing setup, analysis, plotting, and visualization for LAMMPS simulations. The python doc page also provides examples of plotting LAMMPS output: https://lammps.sandia.gov/doc/Python_head.html.

The windows version also has the LAMMPS Shell, *lammps-shell*, a program that functions very similar to the regular LAMMPS executable but has several modifications and additions that make it more powerful for interactive sessions, i.e. where you type LAMMPS commands from the prompt instead of reading them from a file.

LAMMPS shell tips & tricks: Use history create input file.

When experimenting with commands to interactively to figure out a suitable choice of settings or simply the correct syntax, you may want to record part of your commands to a file for later use. This can be done with the `save_history` command, which allows to selectively write a section of the command history to a file (Example: '`save_history 25-30 in.run`'). This file can be further edited (Example: '`/vim in.run`') and then the file read back in and tried out (Example: '`source in.run`'). If the input also creates a system box, you first need to use the '`clear command`' command.

Limitations

LAMMPS is designed to be a fast, parallel engine for molecular dynamics (MD) simulations. It provides only a modest amount of functionality for setting up simulations and analyzing their output.

Specifically, LAMMPS was not conceived and designed for:

- being run through a GUI

- building molecular systems, or building molecular topologies
- assign force-field coefficients automagically
- perform sophisticated analysis of your MD simulation
- visualize your MD simulation interactively
- plot your output data

How to Run LAMMPS

18 October 2020

11:32

Basics

LAMMPS is run from the command line, reading commands from a file via the `-in` command line flag, or from standard input. Using the “`-in in.file`” variant is recommended:

```
$ lmp_serial -in in.file
$ lmp_serial < in.file
$ /path/to/Lammps/src/lmp_serial -i in.file
$ mpirun -np 4 lmp_mpi -in in.file
$ mpirun -np 8 /path/to/Lammps/src/lmp_mpi -in in.file
$ mpirun -np 6 /usr/Local/bin/lmp -in in.file
```

You normally run the LAMMPS command in the directory where your input script is located. That is also where output files are produced by default, unless you provide specific other paths in your input script or on the command line. As in some of the examples above, the LAMMPS executable itself can be placed elsewhere.

As LAMMPS runs it prints info to the screen and a logfile named `log.lammps`.

You can experiment with running LAMMPS using any of the input scripts provided in the examples or bench directory. Input scripts are named `in.*` and sample outputs are named `log.*.P` where P is the number of processors it was run on.

Some of the examples or benchmarks require LAMMPS to be built with optional packages.

Running LAMMPS on Windows

To run a serial (non-MPI) executable, follow these steps:

1. Get a command prompt by going to Start->Run... , then typing “cmd”.

2. Move to the directory where you have your input script, (e.g. by typing: cd "Documents").
3. At the command prompt, type "Lmp_serial -in in.file", where in.file is the name of your LAMMPS input script.

Note that the serial executable includes support for multi-threading parallelization from the styles in the USER-OMP packages. To run with 4 threads, you can type this:

```
Lmp_serial -in in.Lj -pk omp 4 -sf omp
```

How to Write LAMMPS scripts

25 October 2020

21:52

LAMMPS input scripts

LAMMPS executes by reading commands from a input script (text file), one line at a time. When the input script ends, LAMMPS exits. Each command causes LAMMPS to take some action. It may set an internal variable, read in a file, or run a simulation. Most commands have default settings, which means you only need to use the command if you wish to change the default.

In many cases, the ordering of commands in an input script is not important. However LAMMPS does not read your entire input script and then perform a simulation with all the settings. Rather, the input script is read one line at a time and each command takes effect when it is read. This means where a 'run' command is placed affects what parameters it will run with.

Input script structure

This page describes the structure of a typical LAMMPS input script. The examples directory in the LAMMPS distribution contains many sample input scripts; it is discussed on the Examples doc page.

A LAMMPS input script typically has 4 parts:

- Initialization
- System definition
- Simulation settings
- Run a simulation

The last 2 parts can be repeated as many times as desired. I.e. run a simulation, change some settings, run some more, etc. Each of the 4 parts is now described in more detail. Remember that almost all commands need only be used if a non-default value is desired.

Initialization

Set parameters that need to be defined before atoms are created or read-in from a file.

The relevant commands are units, dimension, newton, processors, boundary, atom_style, atom_modify.

If force-field parameters appear in the files that will be read, these commands tell LAMMPS what kinds of force fields are being used: pair_style, bond_style, angle_style, dihedral_style, improper_style.

System definition

There are 3 ways to define the simulation cell and reserve space for force field info and fill it with atoms in LAMMPS. Read them in from (1) a data file or (2) a restart file via the read_data or read_restart commands, respectively. These files can also contain molecular topology information. Or (3) create a simulation cell and fill it with atoms on a lattice (with no molecular topology), using these commands: lattice, region, create_box, create_atoms or read_dump.

The entire set of atoms can be duplicated to make a larger simulation using the replicate command.

Simulation settings

Once atoms and molecular topology are defined, a variety of settings can be specified: force field coefficients, simulation parameters, output options, and more.

Force field coefficients are set by these commands (they can also be set in the read-in files): pair_coeff, bond_coeff, angle_coeff, dihedral_coeff, improper_coeff, kspace_style, dielectric, special_bonds.

Various simulation parameters are set by these commands: neighbor, neigh_modify, group, timestep, reset_timestep, run_style, min_style, min_modify.

Fixes impose a variety of boundary conditions, time integration, and diagnostic options. The fix command comes in many flavors.

Various computations can be specified for execution during a simulation using the compute, compute_modify, and variable commands.

Output options are set by the thermo, dump, and restart commands.

Run a simulation

A molecular dynamics simulation is run using the run command. Energy minimization (molecular statics) is performed using the minimize command. A parallel tempering (replica-exchange) simulation can be run using the temper command.

Record of Installation & Testing

13 October 2020
20:13

Installation

- Installation completed on 18/10/2020
- 64-bit 3-Mar 2020 version installed (latest stable version)
- Installation completed with administrator privileges

- MPI package (needed for running in parallel) not installed*
- File location: `C:\Program Files\LAMMPS 64-bit 3Mar2020`

* I installed the regular multi-threaded LAMMPS executable called `lmp_serial`, which is more stable. The alternative is the multi-threaded LAMMPS executable, which also supports parallel execution via MPI message passing. This executable is called `lmp_mpi` and requires installation of a suitable MPICH2 package to work.

Testing

Colloids Script - 23/10/20

Running

Test Script: "colloid: big colloid particles in a small particle solvent, 2d system"

- Started in `C:\Program Files\LAMMPS 64-bit 3Mar2020\Examples`
- Ran the following code in command line:

```
cd colloid
```

```
lmp_serial -in in.colloid
```

In the README for the examples directory, it is suggested to first copy the LAMMPS executable to this directory using "`cp ../../src/lmp_mpi`", however this appears to use linux notation, and not be necessary on windows.

Use "`type in.colloid`" to view the file in command line, and "`notepad in.colloid`" to edit it in the notepad app. Notepad is used as Windows doesn't have a command-line editor built in*. Note that there may be better ways of doing this; this may also require changing the permissions of the "`in.colloid`" file so that system users can edit the file.

* To replicate the vi experience, it is possible to get Vim for windows, which runs in command line:
<https://www.vim.org/download.php#pc>

Analysis

Most of the example input scripts have commented-out lines that produce dump snapshots of the running simulation in any of 3 formats:

- If you uncomment the dump command in the input script, a text dump file will be produced, which can be animated by various visualization programs (see <http://lammps.sandia.gov/viz.html>).
- If you uncomment the dump image command in the input script, JPG snapshot images will be produced when the simulation runs. They can be quickly post-processed into a movie using commands described on the dump image doc page.

- If you uncomment the dump movie command in the input script, an MPG movie will be produced when the simulation runs. The movie file can be played using VLC player, if the default windows player struggles.

2D Hard Spheres - 25/10/20

This script was developed by modifying (and commenting) the basic colloids script. It is saved as in.run under 2d_hard_spheres_test.

Initialisation

- The default system of natural units based on the Lenard-Jones potential are used, for ease of computation.
- A system of spherical particles is initialised in 2 dimensions.

System Definition

- A 2D square lattice is created, with points every 0.01 unit length.
- This is then bound by a rectangular region (originally called 'box', but renamed to 'mybox' to avoid confusion, with given x,y and z bounds).
- This region is turned into a simulation region, set up for 2 particle types within the region previously defined (with ID = 'mybox')
- Atoms of type one are generated, filling the entire simulation box with particles on the lattice. Note that the use of 'box' is correct in this line; it is a keyword specifying placement on lattice points. The change to 'mybox' above were to avoid confusion with this keyword.

Simulation Settings

- 96% of atoms (from the group all) are selected at random to be assigned to type 2.
- Different masses are allocated to type 1 and type 2
- We then generate an ensemble of velocities using a random number generator with the specified seed (87287) at the specified temperature.
- The settings for building nearest-neighbour lists are left unchanged
- Pairwise interactions are implemented with a standard 12/6 Lennard-Jones potential, where the cut-off is defined, as well as units of energy and distance for each particle type pairing.
- Fixes impose a variety of boundary conditions, time integration, and diagnostic options. Here, we undergo isothermal and isobaric change to type 1 particles, to compress the system. A drag term is added to these changes, to prevent unwanted oscillations in these values. We then zero out z-dimension velocities and forces for type 2 particles.

Output

- Dump text file of simulation parameters, and video of animated motion
- Output thermodynamic variables of: timestep, temperature, pairwise energy, total energy, pressure, volume

It would be worth asking how to best express the numerical data; do they write code to extract the values manually from the dump file, or have they got tools to do that for them? (I.e. to plot temperature over time, as a simple example)

Rigid Rods

Molecule file - 01/11/2020

This was my main issue when transferring from the hard sphere model to the rigid rod model. While the sphere class was used previously, this did not support the formation of new bonds (the capabilities of each class are listed here: https://lammps.sandia.gov/doc/atom_style.html)

My initial approach was to use the 'molecule' file to initialise the properties of the rod. However using the molecular class seems to struggle with this approach, not recognising many of the keyword commands such as 'types' or 'coords' in the molecule file, despite these both being allowed in the documentation, and appearing as allowed keywords in the github repo code.

I have since attempted to use the broader 'bond' class, however this has also been unsuccessful, primarily due to an 'invalid bond type in the Bonds section' - although no bond types have yet been defined. I will continue to work on this, although it may be beneficial to switch to the broader, but better tested, approach of the read_data command instead of the molecule command, as used in the previous nun-chucks code.

Read_data file - 04/11/202

The documentation for the format of this file is found at

https://lammps.sandia.gov/doc/read_data.html

This was used as an alternative to the molecule format of specifying molecular properties to build the simulation molecules. The code is based on the Lammps_demo_rigidrods directory from Jiaming, adapted for the purpose of this code.

The primary changes are listed below:

- Change shell commands for windows compatibility
- Change fix to hold volume constant over simulation
- Extend simulation region
- Set central bond as rigid, and ensure all bonds are uniform
- Remove extra bond, angle and atom types for clarity

Nunchuck Testing & Documentation - 09/11/20

Input files have the form input_data_nunchucks_\${N}_\${box}.file, for N particles in an initial box size of box

This then shrinks until the run (under the npt fix) ends, or the box density is at the maximum packing efficiency.

Run of 1000 particles in 100 size box for 50,000 steps takes 228 seconds (~4min). *This is the size of system we wish to consider, but a much shorter timescale than we will use.*

Python Integration

18 October 2020

15:31

Overview

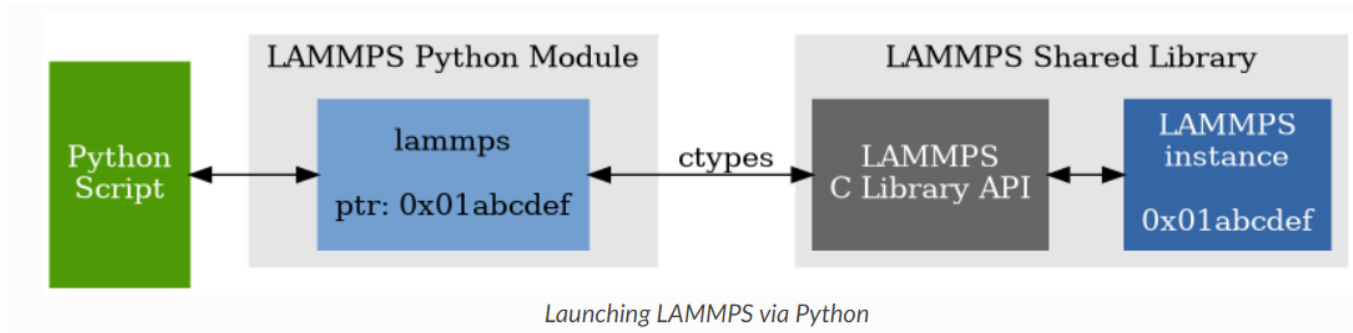
The LAMMPS distribution includes a python directory with the Python code needed to run LAMMPS from Python. The python/lammps.py contains the “lammps” Python that wraps the LAMMPS C-library interface. This file makes it is possible to do the following either from a Python script, or interactively from a Python prompt:

- create one or more instances of LAMMPS
- invoke LAMMPS commands or read them from an input script
- run LAMMPS incrementally
- extract LAMMPS results
- and modify internal LAMMPS data structures.

From a Python script you can do this in serial or in parallel. Running Python interactively in parallel does not generally work, unless you have a version of Python that extends Python to enable multiple instances of Python to read what you type.

To do all of this, you must build LAMMPS in “shared” mode and make certain that your Python interpreter can find the lammps.py file and the LAMMPS shared library file.

LAMMPS can work together with Python in three ways. Primarily, Python can wrap LAMMPS through its library interface, so that a Python script can create one or more instances of LAMMPS and launch one or more simulations. In Python terms, this is referred to as “extending” Python with a LAMMPS module.



Furthermore, the lower-level Python interface in the lammps Python class can be used indirectly through the provided PyLammps and IPyLammps wrapper classes, also written in Python. These wrappers try to simplify the usage of LAMMPS in Python, and reduce the amount of code necessary to parameterize LAMMPS scripts through Python by making variables and computes directly accessible. LAMMPS can also use the Python interpreter, so that a LAMMPS input script or styles can invoke Python code directly, and pass information back-and-forth between the input script and Python functions you write.

Energy_plot.py

Python program written 02/11/2020 to extract the thermodynamic data output to the terminal (and saved in the command line) and plot chosen thermodynamic variables. This can be used to consider energy conservation during the simulation run.

Nunchuck.py

Code to generate input file. Needs more looking at

LAMMPS Units

21 November 2020

11:56

Background

LAMMPS allows the style of units used for a simulation to be defined in a simulation. It determines the units of all quantities specified in the input script and data file, as well as quantities output to the screen, log file, and dump files. Typically, this command is used at the very beginning of an input script.

For all units except `lj`, LAMMPS uses physical constants from www.physics.nist.gov. For the definition of Kcal in real units, LAMMPS uses the thermochemical calorie = 4.184 J.

The choice you make for units simply sets some internal conversion factors within LAMMPS. This means that any simulation you perform for one choice of units can be duplicated with any other unit setting LAMMPS supports. In this context “duplicate” means the particles will have identical trajectories and all output generated by the simulation will be identical. This will be the case for some number of timesteps until round-off effects accumulate, since the conversion factors for two different unit systems are not identical to infinite precision.

More details on the use of reduced units are available at [The Art of Molecular Dynamics Simulation - D. C. Rapaport, Rapaport, Dennis C. Rapaport - Google Books](#), which handily uses the same conventions as this.

LJ Units

For style `lj`, all quantities are unitless. Without loss of generality, LAMMPS sets the fundamental quantities `mass`, `sigma`, `epsilon`, and the Boltzmann constant as unity. The masses, distances, energies you specify are multiples of these fundamental values. The formulas relating the reduced or unitless quantity (with an asterisk) to the same quantity with units is also given. Thus you can use the `mass`, `sigma`, and `epsilon` values for a specific material and convert the results from a unitless LJ simulation into physical quantities.

~~ie relative permittivity (take as unity so system has permittivity of free space as we are not considering charged interactions?) and poissons ratio (take as a third?)~~

- mass = mass or m , where $M^* = \frac{M}{m}$
- distance = σ , where $x^* = \frac{x}{\sigma}$
- time = τ , where $\tau^* = \tau \sqrt{\frac{\epsilon}{m\sigma^2}}$
- energy = ϵ , where $E^* = \frac{E}{\epsilon}$
- velocity = $\frac{\sigma}{\tau}$, where $v^* = v \frac{\tau}{\sigma}$
- force = $\frac{\epsilon}{\sigma}$, where $f^* = f \frac{\sigma}{\epsilon}$
- torque = ϵ , where $t^* = \frac{t}{\epsilon}$
- temperature = reduced LJ temperature, where $T^* = \frac{T k_B}{\epsilon}$
- pressure = reduced LJ pressure, where $p^* = p \frac{\sigma^3}{\epsilon}$
- dynamic viscosity = reduced LJ viscosity, where $\eta^* = \eta \frac{\sigma^3}{\epsilon \tau}$
- charge = reduced LJ charge, where $q^* = q \frac{1}{\sqrt{4\pi\epsilon_0\sigma\epsilon}}$
- dipole = reduced LJ dipole, moment where $\mu^* = \mu \frac{1}{\sqrt{4\pi\epsilon_0\sigma^3\epsilon}}$
- electric field = force/charge, where $E^* = E \frac{\sqrt{4\pi\epsilon_0\sigma\epsilon}}{\epsilon}$
- density = mass/volume, where $\rho^* = \rho \sigma^{dim}$

Mass of a ball in the simulation is therefore set as 1. This corresponds to about 2nm of DNA, or 6 base pairs.

Relative formula mass per base pair is 650 daltons on average (referenced in [Evaluating droplet digital PCR for the quantification of human genomic DNA: converting copies per nanoliter to nanograms nuclear DNA per microliter | SpringerLink \(cam.ac.uk\) / https://doi-org.ezp.lib.cam.ac.uk/10.1007/s00216-018-0982-1](#)

This gives $m = (6*650)/(N_A * 1000) = 6.48 \times 10^{-24} \text{ kg}$ (each ball is one mass unit in the simulation)

We have also defined that the lengthscale sigma (each ball has diameter of 2nm, equal to the unit length).

The energy-scale is defined by the magnitude of repulsive forces. Once this is known, then the relevant timescale for these simulations (ie the timescale that the simulated behaviour occurs over, so particles of this size and mass) here is easily calculated. This should be defined by room temperature, ie $298k_B$

The energy scale also defines the temperature of the system, specified in the code as 0.5
Note for $T^ = 0.5$, we get total energy in simulation (per particle) tending to 1.4 not 0.5, as there are three degrees of freedom. Furthermore we know $T^* = 0.5$ but not T or epsilon.*

Using $\epsilon = 298k_B$ gives a timescale of $\tau = \sqrt{m^2 \sigma^2 / \epsilon} = 79 \text{ ps}$.
 ie 1 million steps will last 79 microseconds. Most of my simulations are on the order of 12 million, ie about 1ms.

Implementing Fixes

03 November 2020
19:39

Fixes

In LAMMPS, a “fix” is any operation that is applied to the system during time-stepping or minimization. Examples include updating of atom positions and velocities due to time integration, controlling temperature, applying constraint forces to atoms, enforcing boundary conditions, computing diagnostics, etc.

- I have used an npt fix (constant number of particles, constant pressure and constant temperature) for my 2D spheres simulation. However, despite temperature being fixed, energy drifts over time during this process.
- Jiaming advises using an nph fix (combined with a Langevin fix), during the shrinking process which seems to work better
- For volume conservation when reaching equilibrium, nve is used instead (typically with the Langevin fix in case).
- A recentre command stops all particles being continually offset, by fixing the centre of mass of the system

N.B Only the nvt fixes perform time integration, meaning they update the velocities and positions of particles due to forces and velocities respectively. The other thermostat fixes only adjust velocities; they do NOT perform time integration updates. Thus they should be used in conjunction with a constant NVE integration fix such as these:

Parameter Values

In LAMMPS, temperature is relative, and expressed by a relative value, with only relative changes being relevant. Conversion to physical values may only be through experiment - i.e. matching values at a known phase transition. Variation in temperature parameters tends to have minimal effect on the simulation output. The absolute values used, as well as their physical conversions, will be detailed in the final project report.

Code Structure

11 December 2020
18:30

In my code, I wish to run a continuous simulation, switching between two different fixes; one where the system shrinks (so the volume fraction may be increased), and one where the system is held at a constant volume (so that the system may reach equilibrium. Ideally, I would run this over multiple mixing steps, or (potentially) different lengths. This method of how to do this is described below.

Loop variable

This method has been developed over a number of iterations, but is used to avoiding resetting the particle configuration after each run, but rather record the equilibrium positions and then compress further from this state. This method cannot use the 'jump' command, as it closes the current file, and (re-)opens the named file. Even if these files are the same, the current configuration is lost. The

label command (which determines where LAMMPS should begin executing in the new file) does not avoid this issue, as the old configuration is still not preserved.

The commands 'write_restart' and 'read_restart' allow the current configuration to be saved and reloaded at each point. In this way we may loop over multiple (different) mixing steps in one file. The full methodology for this approach is given in the next section.

Code Structure

In.run_setup

This file imports the input_data file (which is generated by nunchucks.py and contains the initial positions of each particle within the simulation box). It sets up the potential interactions, bond properties and general simulation parameters, then writes the initial positions to a restart file.

In.run_loop

Initially, all previous restart files are deleted, and then in.run_setup is run.

This file then loops over the mix_steps given at the start of the file. It loads the restart file, contracts over the given number of mix steps and then lets equilibrate over the given number of run steps. Thermodynamic variables are output to the command line, and saved in the log file, while an output file can save the particle trajectories at each timestep to be visualised in Ovito. The current implementation uses the same number of equilibration steps (under the nve fix) in each iteration, however this may be changed if desired.

Running in Parallel

23 February 2021

19:20

Put simply, this is complicated, and I don't understand all of it! In short, the lmp_mpi executable would likely be ideal. However this is difficult to setup on windows, and not compatible with lmp_serial. lmp_serial does however support multi-threading, which speeds up the computation times slightly.

MPI Running

"Only the lmp_mpi executable supports parallel execution via MPI (which can be combined with OpenMPI multi-threading). For that you also need to install a specific version of MPICH2 from Argonne lab linked above. The installer does not contain it and does not check for it. Please note, that you need to download a very specific (and rather old) version of the MPICH package, as this is what LAMMPS was compiled with and the latest available Windows binary version compatible with the GNU compilers used to compile LAMMPS."

Multi_Threading

"All LAMMPS binaries from this repository support multi-threading via OpenMP, however by default only one thread is enabled. To enable more threads, e.g. four, you need to either set it at the command line prompt via set OMP_NUM_THREADS=4, via the -pk omp 4 command line flag, or via the package omp 4 command in your input script."

lmp_serial -pk omp 8 -sf omp -in in.run_loop - Run in command line - uses 8 threads

Also added the line 'package omp 8' at the start of the setup file, which may(?) be necessary.

This enables us to set 8 (max) OpenMP thread(s) per MPI task (which remain limited to 1), and use multi-threaded neighbor list subroutines (speeding up specific sections of the code).

Miscellaneous

Chapter Introduction

10 May 2021

15:22

This section is simply as an appendix to the lab report, for miscellaneous information that I hadn't saved anywhere else.

Useful Links

13 October 2020

20:21

Dropbox for Literature:

https://www.dropbox.com/home/Nunchucks_DNA

LAMMPS Repo:

<https://github.com/lammps/lammps>

My Project Repo:

https://github.com/KCGallagher/LC_Project

Deadlines

13 October 2020

20:22

Date	Deadline	Completion?
16/10/20	Earliest Date for Project Allocation by Supervisor	Y
28/10/20	Deadline for Acceptance of Project by Student	Y
06/11/20	Deadline for Risk Assessment Forms	Y
04/12/20	Initial Report Deadline (4-6 pages)	Y
10/02/21	Secondary Progress Form (Tickbox form)	Y
10/05/21	Presentation Date	Y
17/05/21	Final Report Deadlines	Y

Using Ovito

23 November 2020

16:03

Basics

- Load file (select relevant dump file)
- Do not keep pre-existing objects
- Space to play animation

Full documentation available at [OVITO User Manual – Scientific visualization and analysis software for atomistic simulation data](#)

OVITO Introduction

Based on description in paper [OVITO---the Open Visualization Tool \(cam.ac.uk\)](#)

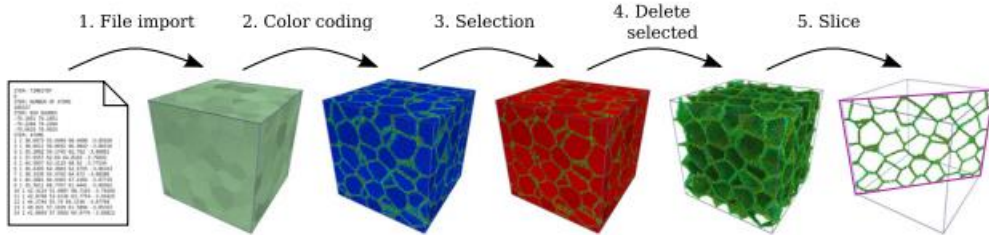


Figure 1. Illustration of the processing pipeline architecture of the OVITO visualization software. The labeled arrows denote the individual processing steps that are applied to the atomic data ‘flowing’ through the processing pipeline. The images depict the intermediate states. The final data state is shown on screen, exported to a new data file or fed into an external renderer such as POV-Ray [5] for publication-quality image output.

OVITO provides functions for the following tasks:

- Colouring atoms based on their type, selection state or any other per-atom value stored in the input file or computed in the processing pipeline
- Transformation of atoms and the simulation cell
- Calculation and visualization of displacement vectors from the differences between two states of the system
- Interactive slicing and cutting of atomic structures
- Display of periodic images and wrapping of atoms at periodic boundaries
- Selection of atoms based on user-definable criteria
- Calculation and display of atomic bonds
- Ambient lighting calculation and shading of atoms for better visualization of three-dimensional atomic structures
- Sophisticated analysis functions including common neighbour analysis, cluster analysis and the calculation of intrinsic and extrinsic atomic-level strain tensors

For my project, the spatial correlation function may be most relevant: This modifier calculates the spatial correlation function between two particle properties, $C(r) = \langle P_1(0), P_2(r) \rangle$ where P_1 and P_2 are the two properties.

Display Properties

Molecule Colours

- Ovito automatically sets colours by atom type to differentiate between different atoms.
- I have added a pre-set mapping to particle properties, which reverses the molecule ID and atom type identifiers, so that colouring is done on a per-molecule basis instead.

Modifier (Proper Method)

- Add modification / Colour coding
- Input property: Molecule Identifier
- Start Value: 0 ; End Value: N (number of particles) - Can extend this to only use part of spectrum
- Colour Gradient: Viridis (my preference)

Write-Up Lecture

22 March 2021

21:50

Notes from a lecture given by Prof Smith on writing a Part III Project

First and foremost the handin deadline is 4pm on the third monday of Easter full term (17th May 2021)

Assessment Process

Assessed by supervisor, and assessor (who marks 10 other projects)

Assessment criteria:

- Research Skills - assessment is partly based on lab book
- Scientific Content - link to previous years (mainly assesed by supervisor)
- Communication Skills (report)
- Communication Skills (viva) (with be in may/june)

Lab notebook is also handed in. Used to assess the planning of the project, effort spent on different parts of the project and how problems were overcome.

This should include your project plan - to give timeline etc for project progress etc! (A Gantt chart may also be useful here!)

Write Up

- Plan write up - try to keep different results chapters fairly balanced (in length/content etc)
- It may be beneficial to have a table of contents at the start to guide the reader!
- It is worth remembering that figure captions may give sufficient detail to understand the figure; it may well duplicate material covered in the text
 - And make sure font size in figure is similar to the rest of the text!

- While academic writing is often done in the passive voice, don't just stick to this! It can be useful to specify *which* experiments/work you personally did.
- Signpost throughout, shouldn't hint at what you did and only do a 'grand reveal' at the end. More like prosecuting a court case than writing a detective novel!

Other Notes

Some ideas of the errors present in the simulation would be ideal! Even just on the location of phase transitions for example!